Solid-State Electrochemistry

Fundamentals, Fuel Cells, Batteries

Truls Norby and Ola Nilsen

Version 2019-02-08

Abstract

This article provides an introduction and overview of solid-state electrochemistry, defined by electrochemical processes and devices comprising ionic transport in a solid phase such as an electrolyte, mixed conducting membrane, or electrode. It is intended for audiences with general, physical, and inorganic chemistry backgrounds as well as basic knowledge of electrochemistry. The text focuses on thermodynamics and transport of defects in crystalline solids, thermodynamics and kinetics of electrochemical cells, and on fuel cells and batteries, but treats also more briefly other processes and devices.

Contents

1 Introduction

1.1 Reduction, oxidation, and electrochemistry

A well-known reduction and oxidation (redox) reaction is that between hydrogen and oxygen to form water:

$$2H_2 + O_2 = 2H_2O$$

Eq. 1

Herein, hydrogen is formally oxidised to protons and oxygen reduced to oxide ions:

$$\begin{aligned} &\tfrac{1}{2}H_2 = H^+ + e^- && |\,4 \\ &\tfrac{1}{2}O_2 + 2e^- = O^{2-} && |\,2 \\ &2H_2 + O_2 = 4H^+ + 2O^{2-} = 2H_2O \end{aligned}$$

Eq. 2

Many such reactions involving combustion of a fuel with oxygen in air evolve a lot of energy in the form of heat – the enthalpy of the reaction at constant pressure. The reaction happens locally on molecular and atomic scale by collisions, breaking bonds, exchanging electrons, and remaking new bonds. The heat can be utilised for driving combustion engines, gas turbines, and more. In principle we can also drive the reaction backwards and split water, but the temperature needed is prohibitive.

What distinguishes and defines *electrochemistry* from redox chemistry is that the *reduction and oxidation take place at different locations*. From that we understand that electrochemistry requires transport of electrons from the location of oxidation to the location of reduction, and charge compensating currents of ions; it needs ionic conduction (an electrolyte) and electronic conduction (typically metallic electrodes and an external metallic circuit). In order to describe the transport of ions, the reduction and oxidation reactions are in electrochemistry written using the same ion. If we have a proton conducting electrolyte, the reactions above are

$$\begin{aligned} &\tfrac{1}{2}H_2 = H^+ + e^- && |\,4 \\ &\tfrac{1}{2}O_2 + 2H^+ + 2e^- = H_2O && |\,2 \\ &2H_2 + O_2 = 2H_2O \end{aligned}$$

Eq. 3

These reactions – taking place in an electrochemical cell – a fuel cell – with a solid proton conducting electrolyte is depicted in Figure 1-1 (left). It shows also how it is done with an oxide ion conducting electrolyte (right). An important part of electrochemistry and of the solid-state materials chemistry is the design of the chemistry of various electrolytes and electrodes to make them conductive of ions – of the right kind, preferably – and/or electrons.

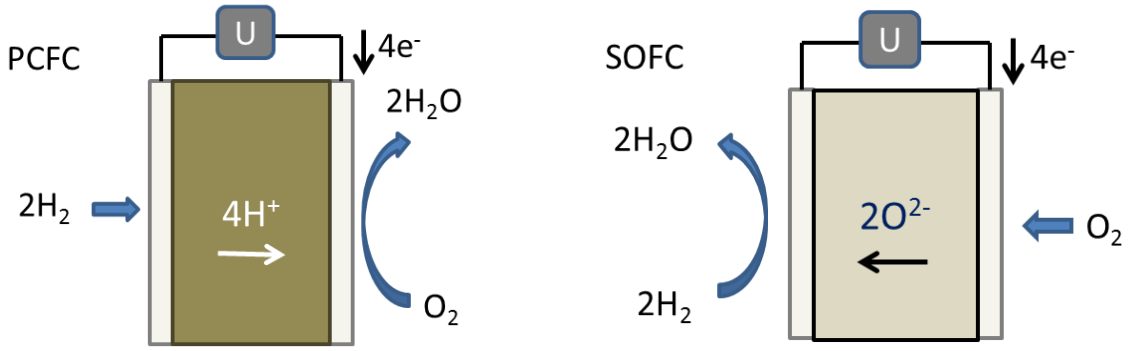

Figure 1-1. Proton conducting and oxide ion conducting electrolytes in proton ceramic fuel cell (PCFC) and solid-oxide fuel cell (SOFC) in both cases reacting hydrogen and oxygen to form water (vapour).

Electrochemistry using an electrolyte and electrodes applies to fuel cells, electrolysers, batteries, and electrochemical sensors. The electrode, or half-cell, where oxidation takes place is called the anode. The electrode where reduction takes place is called the cathode:

Anode *Oxidation* (both start with vowels)

Cathode *Reduction* (both start with consonants)

The definition of anode and cathode is thus in general *not* defined by the sign of the voltage of the electrode, but on whether the process releases or consumes electrons. (This will become confusing when we later deal with batteries where the correct terminology is commonly only applied during discharge.)

Current may pass in the ionic and electronic pathways – driven by electrical or chemical gradients. 200 years ago, Michael Faraday found the relation between the magnitude of the current and the amount of chemical entities reacting. He established the constant we today call *Faraday's constant*, namely the amount of charge per mole of electrons: F = 96485 C/mol, where C is the coulomb, the charge carried by one ampere in one second (1 C = 1 A·s).

In comparison with redox reactions in homogeneous media, the electrochemical cells allow us to take out the energy released as electrical work via the electrons passing the electrodes. This work is proportional to the Gibbs energy change, and fuel cells therefore do not suffer the loss of the entropy in the Carnot cycle of combustion engines. Similarly, the reverse reaction – splitting of water – can now be done with applying a mere 1.5 V (using e.g. a penlight battery). Many other non-spontaneous reactions can be done in other types of electrochemical cells, e.g., metallurgical electrolysis for production of metals and anodization of metals for corrosion protection.

In many cases, both ions and electrons can be transported in the same component (mixed conductor), which is at play in gas separation membranes, battery electrodes and other chemical storage materials, and during oxidation of metals and many other corrosion processes.

1.2 Solid-state electrochemistry

Early on, electrochemistry was devoted to systems with solid-state electrolytes, covering examples from near ambient temperatures such as silver halides and other inorganic salts to high temperatures such as Y-substituted ZrO_2. Moreover, solids with mixed ionic electronic conduction share many of the same fundamental properties and challenges as solid electrolytes. Secondary (rechargeable) batteries (accumulators) comprise mostly solid-state electrodes in which there must also be mixed ionic-electronic conduction, so also these should be well described in solid-state electrochemistry. Hence, we choose to define solid-state electrochemistry as electrochemistry involving ionic conduction in a solid phase.

Polymer electrolytes such as Nafion® are often taken as solid, but the ionic transport takes place in physisorbed liquid-like water inside. Similarly, many porous inorganic materials exhibit protonic surface conduction in physisorbed liquid-like water. Hence, it is unavoidable that there will be overlap between solid-state and "regular" (liquid, including aqueous) electrochemistry. In this short treatment we will try to stay with simple clear-cut cases and not make much discussion about borderline cases.

1.3 Solid-state vs aqueous and other liquid-state electrochemistry

Despite the fact that solid-state electrolytes were discovered early and much of the early electrochemistry and even chemistry were explored using such electrolytes, solid-state electrochemistry is much less developed than aqueous and other liquid-state electrochemistry. This can be attributed to the lack of important applications utilising solid-state electrolytes. In comparison, many industrial processes utilise molten salt electrolytes, e.g. for metallurgical production of metals by electrolysis, and molten carbonate fuel cells are well commercialised. And of course the applications of aqueous electrochemistry are countless in metallurgy and other electrolysis, batteries, sensors, and many scientific methods. Corrosion in aqueous environments is of serious impact. The immense accumulated knowledge and experience and number of textbooks for aqueous electrochemistry in all of this is only for one single electrolytic medium; water, H_2O. Yet, one may say that while the technological importance has enforced all this communicated knowledge and experience for aqueous systems, the atomistic understanding of ionic transport and electrochemical reactions at electrodes and interfaces is far from complete.

In comparison, solid-state electrochemistry deals with a large number of different electrolytes and mixed conductors, with different structures, chemistries, redox-stabilities, operating temperatures, and properties, and must be said to be its infancy. In consequence, the number of textbooks in these fields is relatively limited. Among the more recent ones we mention some edited by Gellings and Bouwmeester 1997,[1] Bruce 1994,[2] and Kharton,[3] all collections of chapters or articles by various contributors, and Maier.[4]

[1] P. J. Gellings, H. J. Bouwmeester (eds.), "Handbook of Solid State Electrochemistry", 1997 CRC Press.
[2] P.G. Bruce (ed.), «Solid State Electrochemistry», 1994, Cambridge University Press.
[3] V.V. Kharton (ed.), «Solid State Electrochemistry», 2011, Wiley.
[4] J. Maier, «Physical Chemistry of Ionic Materials: Ions and Electrons in Solids», 2004, Wiley.

A few factual differences between solid-state and aqueous and other liquid systems can be pointed out, and are important to know when one can and when one cannot transfer theory, principles and experience from one to the other. Firstly, liquid systems have usually faster mobility of ions, and moreover similar transport of both cations and anions. Both chemical and electrical gradients may lead to opposite driving forces for the two, adding up the net current, while net material transport is cancelled by liquid counter-flow. Solids have ionic current usually dominated by only one charge carrier – transport of the other may lead to materials creep or so-called kinetic demixing or phase separation. Secondly, liquid electrolytes such as molten salts, ionic liquids, and strong aqueous solutions and are often more concentrated in terms of charge carriers. This decreases the Debye-length, i.e., the extension of space charge layers from charged interfaces or point charges. Solid electrolytes may thus experience stronger effects on electrode and surface kinetics, and also along and across grain boundaries and dislocations, which are obviously not present in liquids. Thirdly, many liquid electrolytes are very redox stable, exhibit no electronic conductivity, and can be used in e.g. Li-ion batteries. In contrast, very redox-stable solids rarely exhibit good ionic conductivity, and most good solid electrolytes exhibit detrimental electronic conductivity in large gradients of chemical potential, i.e., under reducing and/or oxidising conditions.

There are review articles and conference proceedings devoted to differences between liquid- and solid-state electrochemistry.[5]

1.3.1 Exercise in introductory electrochemistry

1. Write half-cell reactions for Eq. 3 in the case that the electrolyte is an O^{2-} conductor. Do the same for the cases that the electrolyte is an H_3O^+ or OH^- conductor. Draw also the simplified schematic diagrams for each of the two latter, similar to Figure 1-1.

2 Fundamentals

Electrochemical processes are the result of all charged species responding to gradients in their chemical and electrical potentials. In the bulk of condensed phases, the rate of the response is governed by the electrical conductivity of each charged species. The conductivity of a particular species is the product of its charge, its concentration (how many there are), and its charge mobility (how easily they move). In order to move, the species has to be a defect, or it must move by interacting with a defect – nothing moves in a perfect crystal. The two solid-state electrolytes in Figure 1-1 conduct proton or oxide ions (and not electrons) because of their different compositions, structures, and resulting defects. Before we look at how the ionic transport takes place, we will thus introduce defects and the defect chemistry that allows us to use thermodynamics to make accurate analyses of defect concentrations.

[5] E.g., I. Riess, "Comparison Between Liquid State and Solid State Electrochemistry. Encyclopedia of Electrochemistry", 2007, Wiley-VCH.

2.1 Defect chemistry

2.1.1 Ionic compounds and formal oxidation numbers

In order to have ionic transport in a solid, it must have some degree of ionicity, i.e., it must be a compound of at least two elements with significantly different electronegativities. In such compounds, chemists assign formal oxidation numbers to the elements as if they were fully ionic, i.e., each element fully takes up or yields the number of electrons required to fulfil the octet rule as far as possible. This is not quite true – all compounds have only a partial ionicity (take or yield electrons) and hence a partial covalency (share electrons). However, the fully ionic model satisfactorily applies to the fact that when an ion moves, it has to bring along an integer charge – the electrons cannot split in half – they stay or go. And it turns out that they bring the full charge we assign to them in the ionic model. This all means that the full charge is at the ion, it is just spreads more or less on the neighbouring ions. But when the ion moves it takes all that charge with it. In order to handle the forthcoming defect chemistry, it is necessary to know or learn some formal oxidation numbers – the charge an ion has in the fully ionic model. This will allow us to assign charges to ions and to understand the effective charge we get on defects, such as vacancies, interstitial ions, and foreign ions. As an example, titanium is in group 4 and has 4 valence electrons, and prefers to yield them all and make Ti^{4+} ions. It hence forms the oxide TiO_2, where Ti has formal oxidation number +4 and oxygen has -2. It is recommendable to try to know the valences and preferred oxidation states of the top element in each group of the periodic table.

2.1.2 Type of defects

In crystalline materials certain atoms (or ions) are expected to occupy certain sites in the structure, because this configuration gives the lowest total energy. We attribute this energy lowering to bonding energy. At $T = 0$ K, there are ideally no defects in the perfect crystalline material. As temperature increases the entropy gain leads to formation of defects in order to minimize Gibbs energy and hence reach new equilibrium. Defects can also be introduced by doping or as a result of synthesis or fabrication. Many defects will in reality be present not because they have reached an equilibrium, but because they have had no practical possibility to escape or annihilate – they are ”frozen in”.

Defects can be zero-dimensional (e.g. point defects), one-dimensional (a row of defects such as a dislocation), two-dimensional (a plane of defects such as a grain boundary – a row of dislocations) and three-dimensional (a foreign phase). As a rule of thumb one may say that high-dimensional defects give relatively little disorder, and they do not form spontaneously. However, they remain present at low temperatures once formed during fabrication. Low-dimensional defects – point defects – give high disorder and form spontaneously and are stable at high temperatures.

One-dimensional defects comprise primarily dislocations, of primary importance for mechanical properties. Two-dimensional defects comprise grain boundaries and surfaces. When objects or grains become nanoscopic these interfaces come very close to each other, start to dominate the materials properties, and we enter the area of nanotechnology.

We shall here focus on zero-dimensional defects, which comprise three types:

Point defects, which are atomic defects limited to one structural position:

vacancies; empty positions where the structure predicts the occupancy of a regular atom,

interstitials; atoms on interstitial position, where the structure predicts that there should be no occupancy, and

substitution; presence of one type of atom on a position predicted to be occupied by another type of ion.

Electronic defects, which may be subdivided into two types:

delocalised or itinerant electronic defects, comprising defect electrons (or conduction electrons; in the conduction band) and *electron holes* (in the valence band),

localised or valence defects; atoms or ions with a different formal charge than the structure predicts; the extra or lacking electrons are here considered localised at the atom.

Cluster defects; two or more defects associated into a pair or larger cluster.

2.1.3 Rules for writing defect chemical reactions

The formation of defects and other reactions involving defects follow two criteria in common with other chemical reactions; *conservation of mass* and *conservation of charge*, maintaining mass and charge balance. In addition, specific for defect chemistry, we must have *conservation of the structure*. This means that if structural positions are formed or annihilated, this must be done in the ratio of the host structure, so that the ratio of positions is maintained. This implies that defect chemical reactions apply only to one and the same crystalline phase - no exchanges between phases, and no phase transitions.

2.1.4 Nomenclature; Kröger-Vink notation

In modern defect chemistry we use so-called *Kröger-Vink notation*, A_s^c, where A is the chemical species (or v for vacancy) and s denotes a lattice position (or i for interstitial).[6] c denotes the *effective charge*, which is the real charge of the defect minus the charge the same position would have in the perfect structure. Positive effective charge is denoted $^{\cdot}$ and negative effective charge is denoted $^{/}$. Neutral effective charge can be denoted with ^{x} (but is often omitted).

2.1.5 Electronic defects

Let us first review electronic defects in a semiconductor in terms of defect chemical nomenclature and formalism. A non-metallic material has an electronic band gap between the energy band of the valence electrons (the valence band) and next available energy band (the conduction band). An electron in the valence band can be excited to an available state (hole)

[6] Kröger and Vink used V for vacancy and I for interstitial position, probably because such nouns in German would be written with capital first letters. However, to avoid confusion with the chemical element vanadium (V) or an iodine (I) site, I introduce the lower-case v and i for vacancy and interstitial position, respectively.

in the conduction band, leaving a hole in the valence band. If we describe a valence electron and empty conduction band state as effectively neutral, we have

$$e_v^x + h_c^x = e_c^/ + h_v^\bullet \qquad \text{or more simply} \qquad e^x = e^/ + h^\bullet$$

Eq. 4

The equation is most often written also without the valence band electron, since it is effectively neutral and we neglect the mass and mass balance of electronic species:[7]

$$0 = e^/ + h^\bullet$$

Eq. 5

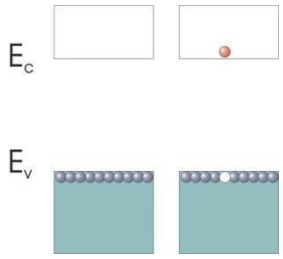

Figure 2-1. Schematic representation of the valence and conduction band of a semiconductor, and intrinsic ionisation.

Foreign atoms or native point defects make local energy levels in the band gap. A defect which contains an easily ionised electron is a *donor* and is placed high in the band gap (the electron has a relatively high energy compared to the other valence electrons). A phosphorus atom in silicon, P_{Si}, has 5 valence electrons, but donates one to the crystal in order to fit better into electronic structure of the Si host atoms with four valence electrons:

$$P_{Si}^x = P_{Si}^\bullet + e^/$$

Eq. 6

Phosphorus is thus a donor dopant in silicon and makes it an n-type conductor.

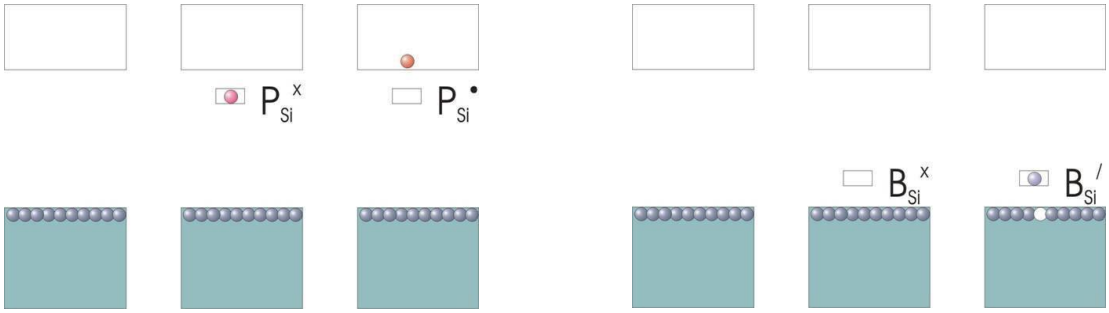

Figure 2-2. Band gap of Si. Donor doping with phosphorous (P) (left) and acceptor-doping with boron (B) (right).

A defect that easily accepts an extra electron from the crystal (low in the band gap) is called an *acceptor*. Boron has only three valence electrons and readily takes up an extra in order to dissolve in silicon, making boron-doped silicon a p-type conductor.

[7] In semiconductor physics, this is expressed $0 = e^- + h^+$, i.e., the $^+$ there expresses effective positive charge.

$$B_{Si}^{x} = B_{Si}^{/} + h^{\bullet}$$

Eq. 7

In electrochemical devices we use also ionic compounds with small band gaps which therefore become electronic conductors by intrinsic ionization or donor or acceptor doping in a similar manner. An example is Sr-substituted $LaMnO_3$ (LSM) where the Sr^{2+} takes La^{3+} positions, and the effectively negative charge of the Sr acceptors is compensated by electron holes: $[h^{\bullet}]=[Sr_{La}^{/}]$. The holes can be seen as Mn^{3+} ions being oxidised to Mn^{4+}. The material is used as cathode in solid-oxide fuel cells. A similar example is $LaCrO_3$, also substituted with Sr^{2+} for La^{3+}, a p-type conductor used as interconnect in SOFCs. NiO becomes a good p-type conductor when acceptor-doped with Li and is used as cathode in molten carbonate fuel cells.

2.1.6 Point defects in stoichiometric and non-stoichiometric binary ionic oxides

In order to now move on to point defects, let us use again nickel oxide, NiO. Here, a metal ion vacancy will be denoted $v_{Ni}^{//}$, while an interstitial nickel ion is denoted $Ni_i^{\bullet\bullet}$. An oxide ion vacancy is denoted $v_O^{\bullet\bullet}$. Heating an ionic compound will create disorder in the form of charge compensating defect pairs. In the case of NiO these may be so-called Frenkel pairs (vacancies and interstitials) on the cation sublattice;

$$Ni_{Ni}^{x} + v_i^{x} = v_{Ni}^{//} + Ni_i^{\bullet\bullet}$$

Eq. 8

or Schottky pairs (vacancies of both cations and anions):

$$Ni_{Ni}^{x} + O_O^{x} = v_{Ni}^{//} + v_O^{\bullet\bullet} + Ni_{Ni}^{x} + O_O^{x} \quad \text{or simply, by elimination:} \quad 0 = v_{Ni}^{//} + v_O^{\bullet\bullet}$$

Eq. 9

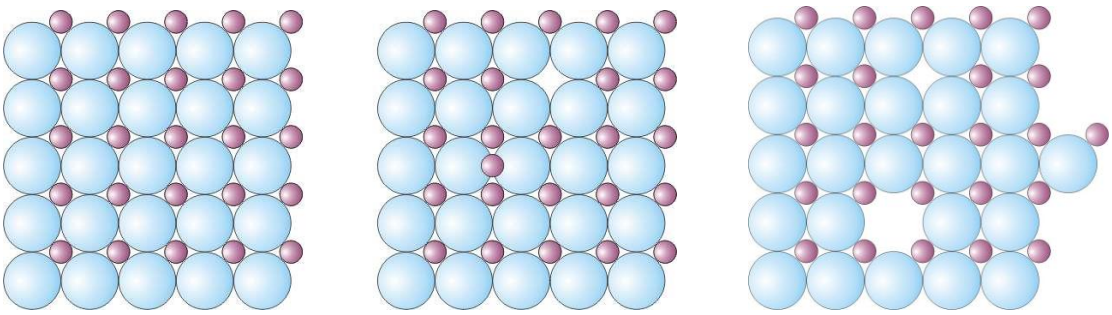

Figure 2-3. Left: Schematic perfect MO structure. Middle: Frenkel defect pair. Right: Schottky defect pair.

We have in both cases formed two defects and maintained electroneutrality, conserved mass, and maintained the ratio between the types of positions.

The reactions we have considered do not change the ratio between cations and anions, and the oxide thus remains *stoichiometric*.

ZrO_2 is an oxide that has a tendency to become reduced and oxygen deficient at low oxygen activities, thus being represented as ZrO_{2-y}:

$$O_O^x = v_O^{\bullet\bullet} + 2e^{/} + \tfrac{1}{2}O_2(g)$$

Eq. 10

We may use this latter reaction to illustrate that point defects such as the cation vacancies in $Ni_{1-x}O$ and oxygen vacancies in ZrO_{2-y} are in fact acceptors and donors. Figure 2-4 visualises how an oxygen vacancy can be formed with the two electrons left localised at the vacancy. They are then placed at high donor levels in the band gap and are easily ionised in two steps until all electrons are delocalised in the conduction band according to

$$v_O^x = v_O^{\bullet} + e^{/} = v_O^{\bullet\bullet} + 2e^{/}$$

Eq. 11

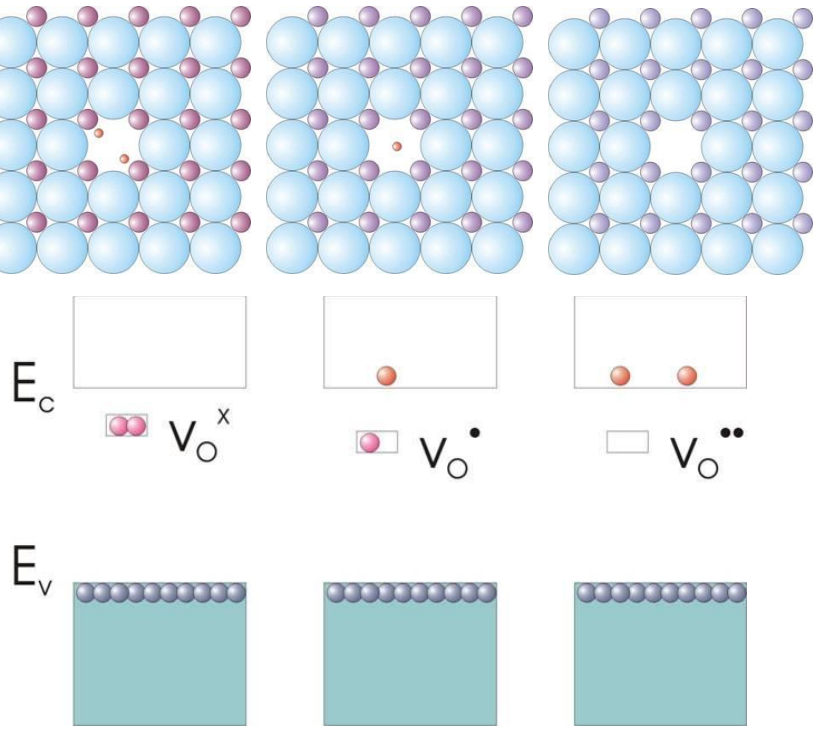

Figure 2-4. Schematic representation of the ionization of oxygen vacancy donors in two steps to the fully ionized defect, in which small spheres in the top figures represent electrons.

2.1.7 Foreign ions; substituents, dopants, impurities

We may affect the concentration of native defects in ionic compounds by adding aliovalent dopants. Electron-poor dopants act as electron acceptors, and the negative charge thus obtained is charge compensated by increasing the concentration of positive defects. Donors correspondingly increase the concentration of negative defects.

Nickel oxide is under ambient conditions overstoichiometric, it contains Ni vacancies compensated by electron holes (representing Ni^{3+} states); $Ni_{1-x}O$. It can be acceptor-doped with lithium: Li^+ dissolves on Ni^{2+} sites to form $Li_{Ni}^{/}$. This is compensated by an increase in the major positive defect – electron holes – and in this way Li-doped NiO becomes a good p-type electronic conductor that can be used as electrode on the air-side (cathode) of certain types of fuel cells. The doping reaction by which the Li in the form of Li_2O enters the lattice of the NiO host structure can be written:

$$Li_2O(s) + \tfrac{1}{2}O_2(g) \rightarrow 2Li'_{Ni} + 2O_O^x + 2h^\bullet$$

Eq. 12

One may note that the reaction forms two new Ni^{2+} sites (and fills them with Li^+ ions) and two new oxide ion sites, as well as two electron holes. The 1:1 ratio of sites conserves the host NiO structure. (Li_2O is the dopant oxide, not the host oxide.) The right arrow is used to indicate that the reaction is not necessarily at equilibrium – we dissolve all the Li_2O and it stays there, either because it is frozen in or because the amount present is below the solubility limit. We also note that the formation of holes is an oxidation reaction – the reaction consumes oxygen gas.

In zirconia ZrO_{2-y} we have oxygen vacancies compensated by electrons. An acceptor dopant - typically yttrium, Y^{3+} or some other rare earth substituting the Zr^{4+} will be compensated by forming more oxygen vacancies:

$$Y_2O_3(s) \rightarrow 2Y'_{Zr} + 3O_O^x + v_O^{\bullet\bullet}$$

Eq. 13

The concentration of electrons is correspondingly suppressed, such that the material becomes an oxide ion conductor – a solid state electrolyte.

Defects have a tendency of association to each other. This may be due to electrostatic attraction between defects of opposite charge, e.g. defect-dopant pairs. But it may also be due to reduction of total elastic strain and comprise defects of the same charge. In the latter case defects (e.g. oxygen vacancies) order in lines or planes and form new structure polymorphs where the former defects are no longer defects but parts of the new structure. Formation of defect associates and ordered structures involve gain in enthalpy but loss of entropy. It is thus typical of low temperatures while dissociated separate defects are typical of high temperatures. An important consequence of defect association is suppression of mobility.

Of particular importance for solid electrolytes is the association between the mobile charge carrying defect and the dopant added for enhancing the concentration of that defect. In Y substituted ZrO_2 electrolytes the oxygen vacancies are associated with the Y dopants in nearest or next-nearest neighbour position according to

$$Y'_M + v_O^{\bullet\bullet} = \left(Y_M v_O\right)^\bullet$$

Eq. 14

whereby the associated vacancies are immobilised. The ionic conductivity increases with dopant content, but eventually goes through a maximum and decreases as the free oxygen vacancies are effectively trapped.

We have considered foreign cations, but also anions can be substituted. In oxides, homovalent foreign anions comprise S^{2-}, while common aliovalent foreign anions comprise F^- and N^{3-}. They can enter as impurities during synthesis, or dissolve from gaseous species under reducing atmospheres, e.g.,

$$O_O^x + H_2S(g) = S_O^x + H_2O(g)$$

Eq. 15

$$3O_O^x + 2NH_3(g) = 2N_O^{/} + v_O^{\bullet\bullet} + 3H_2O(g)$$

Eq. 16

2.1.8 Protons in oxides

When metal oxides are exposed to gas atmospheres containing water vapour or other hydrogen containing gases, hydrogen will dissolve in the oxides. Under oxidizing or mildly reducing conditions, the hydrogen atoms ionise to protons and associate with oxygen atoms on normal structure sites and thereby form hydroxide ions on normal oxygen sites, $OH_O^{\bullet}$. We may thus for instance write the hydrogenation as

$$H_2 + 2O_O^x = 2H_i^x + 2O_O^x = 2OH_O^{\bullet} + 2e^{/}$$

Eq. 17

(see Figure 2-1) in which case the protons dissolved are charge compensated by the formation of defect electrons. In terms of defect chemistry the dissolved proton, located on a normal oxide ion as hydroxide, may also be considered to constitute an interstitial hydrogen ion, and as such it is also in the literature alternatively written $H_i^{\bullet}$. One just has to bear in mind that the protons do not occupy regular interstitial positions (voids).

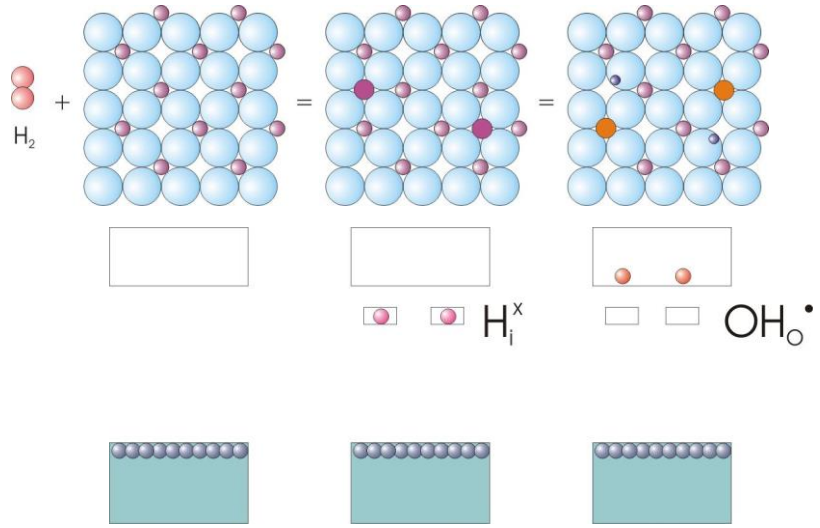

Figure 2-1. Schematic hydrogenation of an oxide MO_2 and ionisation of the hydrogen interstitial atoms into protons in OH groups and electrons.

The electrons may interact with other defects in the oxide so that the protons in effect are compensated by formation of other negative defects or by the annihilation of positive defects. From the dissolution reaction and through the interaction with native defects in the oxide it is clear that the dissolution of hydrogen in metal oxides is dependent both on the partial pressure of the hydrogen source (e.g. water vapour or hydrogen) and of oxygen. These aspects will be described in more detail in a later chapter.

Under reducing conditions, where hydrogen is stable in oxidation state 0 (as H_2 in the gas phase) we may foresee neutral hydrogen atoms dissolved in oxides, probably interstitially, as H_i^x, as mentioned above. Under even more reducing conditions could also hydride ions be

expected to become stable, e.g. as dissolved substitutionally for oxide ions, as the defect $H_O^{\bullet}$.

Protons may also dissolve from water vapour as a source. The dissolution of hydrogen from its oxide, H_2O, is in principle similar to dissolution of other foreign cations. However, the possibility of a controlled water vapour pressure and the fast diffusion of protons makes it much easier to attain and vary (and more difficult to completely avoid) an equilibrium content of protons in the oxide. Of particular interest is the reaction between water vapour and oxygen vacancies, by which an acceptor-doped oxide compensated by oxygen vacancies in the absence of water (dry state) becomes dominated by protons when hydrated:

$$H_2O(g) + v_O^{\bullet\bullet} + O_O^x = 2OH_O^{\bullet}$$

Eq. 18

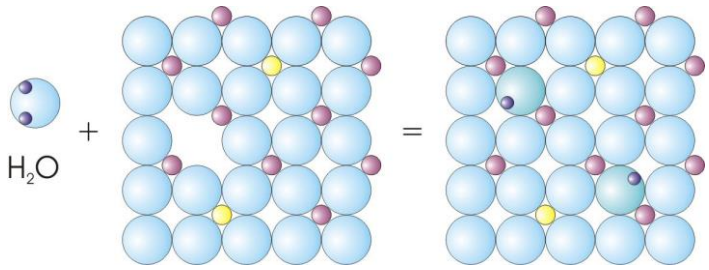

Figure 2-2. Hydration of oxygen vacancies in acceptor-doped MO_2.

2.1.9 Ternary and higher compounds

We have so far concentrated on elementary solids (for electronic defects) and binary oxides for charged point defects. Ternary and higher compounds fall, however, under exactly the same rules of writing and using defect reactions.

A typical ternary compound is a ternary oxide such as perovskite, $CaTiO_3$. As an example of defect reactions for this case, we consider first the formation of Schottky defects. When we form new structure sites in this reaction, we need to form vacancies on both Ca and Ti sites to maintain the ratio between them, in addition to the appropriate number of oxygen vacancies:

$$0 = v_{Ca}^{//} + v_{Ti}^{////} + 3v_O^{\bullet\bullet}$$

Eq. 19

If we further consider the uptake of oxygen by formation of cation vacancies and electron holes, we again have to balance the cation sites:

$$\tfrac{3}{2}O_2(g) = v_{Ca}^{//} + v_{Ti}^{////} + 3O_O^x + 6h^{\bullet}$$

Eq. 20

Similar principles should be applied also in cases where one and the same element is distributed on different crystallographic sites. For instance, Y_2O_3 has a structure where all oxide ions are not strictly equal. Similarly, distorted perovskites may have unequal oxygen sites. In the pyrochlore structure, $A_2B_2O_7$, there are 6 oxygen sites of one type and 1 of slightly different coordination and energy (and one which is structurally empty and thus to be

regarded as an interstitial site). In principle the formation or annihilation of crystal units has to maintain the ratio between those different sites in all such cases. However, this is so far hardly ever practiced in defect chemistry.

Contrary to binary oxides, ternary and higher oxides can have non-stoichiometry not only in terms of the oxygen-to-metal ratio, but also internally between the various cations. This is in practice often a result of synthesis. For instance, it may be difficult to weigh in exactly equal numbers of moles of Ca and Ti precursors when synthesizing $CaTiO_3$, so that the synthesized material has a permanent number of vacancies on one of the cation sites. Such non-stoichiometry may also be a result of equilibria. For instance, if A-site deficiency is energetically favourable over B-site deficiency in the compound ABO_3, we may at very high temperatures (e.g., during sintering) see a preferential evaporation of the A component. For a perovskite $A^{2+}B^{4+}O_3$ we can for this case write:

$$A_A^x + O_O^x = v_A'' + v_O^{\bullet\bullet} + AO(g)$$

Eq. 21

During oxidation we might similarly see a preferential incorporation of A-site vacancies, resulting in a precipitation of an A-rich phase:

$$A_A^x + \tfrac{1}{2}O_2(g) = v_A'' + 2h^{\bullet} + AO(s)$$

Eq. 22

It may be noted that these reaction equations do not violate the site ratio conservation requirement of the ternary oxide.

When we earlier doped elementary or binary compounds the reaction was fairly straightforward. When we dope a ternary or higher compound, however, the reaction may be less obvious – we have some choices. It is quite common, however, to do the synthesis and write the equation in such a way that one takes out a corresponding amount of the host element that is substituted. If we, for instance, want to dope $LaScO_3$ with Ca substituting for La, we go for a composition $La_{1-x}Ca_xScO_3$. In order to see how we write the doping reaction in this case we first just look at the trivial normal synthesis:

$$\tfrac{1}{2}La_2O_3 + \tfrac{1}{2}Sc_2O_2 = La_{La}^x + Sc_{Sc}^x + 3O_O^x$$

Eq. 23

Accordingly, we then write the defect reaction for the doping in the way that we let there be Sc_2O_3 reserved for the CaO:

$$CaO + \tfrac{1}{2}Sc_2O_3 = Ca_{La}' + Sc_{Sc}^x + \tfrac{5}{2}O_O^x + \tfrac{1}{2}v_O^{\bullet\bullet}$$

Eq. 24

2.1.10 Defect structure; solving equilibrium coefficients and electroneutralities

The identities and concentrations of all defects is called the defect structure (even if it has no resemblance with the periodic crystal structure). In order to find the concentrations we use approaches equivalent to those used in aqueous solutions. This comprises expressions for the equilibrium constant and the electroneutrality, and in some cases mass balances. In crystalline compounds we may also employ site balances.

The energetics and thermodynamics of the Frenkel pair formation Eq. 8 is simple: No lattice positions are formed or lost, the crystal remains of the same size, and the energy change of the reaction is simply that of the defective crystal minus that of the perfect crystal. We can apply mass action law thermodynamics to express equilibrium:

$$K_F = \frac{a_{v''_{Ni}} a_{Ni_i^{\bullet\bullet}}}{a_{Ni_{Ni}^x} a_{v_i^x}} = \frac{X_{v''_{Ni}} X_{Ni_i^{\bullet\bullet}}}{X_{Ni_{Ni}^x} X_{Ni_{Ni}^x}} = \frac{\frac{[v''_{Ni}]}{[Ni]}\frac{[Ni_i^{\bullet\bullet}]}{[i]}}{\frac{[Ni_{Ni}^x]}{[Ni]}\frac{[v_i^x]}{[i]}} = \frac{[v''_{Ni}][Ni_i^{\bullet\bullet}]}{[Ni_{Ni}^x][v_i^x]} = e^{\frac{-\Delta G_F^0}{RT}} = e^{\frac{\Delta S_F^0}{R}} e^{\frac{-\Delta H_F^0}{RT}} \approx [v''_{Ni}][Ni_i^{\bullet\bullet}]$$

Eq. 25

This expression contains all essential steps of such treatments for all defect chemical equilibrium considerations, and it is imperative to understand each and every of these steps. First, the equilibrium coefficient is given by the ratio of activities (*a*) of products over those of the reactants according to normal mass action law for chemical reactions. Next, if the concentration of defects is small and hence activity coefficients unity, the activity of defects (and native species) in a lattice is defined as their site fraction (*X*). A site fraction is defined as the concentration of the species over the concentration of the site itself (here Nickel sites and interstitial sites). In the present case we see that we can eliminate these. This equilibrium coefficient is related to the standard Gibbs energy change and the standard entropy and enthalpy changes in the normal manner.

The concentrations of native species are often considered constant if defect concentrations are small. As the rightmost term in Eq. 25 suggests, the concentrations of native species can then in our case be set equal to unity and be omitted if concentrations are expressed as formula unit or mole fractions. This is analogous to simplified situations such as ”weak acid”, ”pure ampholyte”, ”buffer”, etc. in aqueous acid-base-chemistry.

The *electroneutrality condition* states that the crystal must be electrically neutral. This can be expressed by summing up the volume concentrations of all positive and negative charges and requiring the sum to be zero. It can however be done in terms of effective charges, which is more convenient and useful to us. If the Frenkel defects in the case above are the dominating defects, the simplified electroneutrality condition can be written

$$2[Ni_i^{\bullet\bullet}] - 2[v''_{Ni}] = 0 \quad \text{or} \quad 2[Ni_i^{\bullet\bullet}] = 2[v''_{Ni}] \quad \text{or} \quad [Ni_i^{\bullet\bullet}] = [v''_{Ni}]$$

Eq. 26

Here, the factor 2 comes from the two charges contributing per defect. We now have two equations and can solve the system of two unknown defect concentrations, by inserting Eq. 26 into Eq. 25 to obtain

$$[v''_{Ni}] = [Ni_i^{\bullet\bullet}] = K_F^{\frac{1}{2}} = e^{\frac{\Delta S_F^0}{2R}} e^{\frac{-\Delta H_F^0}{2RT}}$$

Eq. 27

From this, we see that the defect concentrations will follow a van ‘t Hoff type of temperature dependency, with $\Delta H_F^0 / 2$ as the apparent enthalpy. (The systematics fan will see that the factor ½ here comes from the two defects formed.)

Here it may be useful to note the following: This (and any) equilibrium coefficient expression in the material is *always true* (at equilibrium), regardless of dominating defects. Similarly, the electroneutrality condition taking all defects into account is also necessarily true. However, the simplified limiting electroneutrality expression we used is *a choice*.

Let us next consider electronic defects and think of Eq. 5 in terms of a chemical equilibrium. The equilibrium constant can then be expressed as

$$K_g = a_{e'} a_{h^\bullet} = \frac{[e']}{N_C}\frac{[h^\bullet]}{N_V} = \frac{n}{N_C}\frac{p}{N_V} = K_{g,0}\exp(\frac{-E_g}{RT})$$

Eq. 28

By tradition, we use the notation n and p for the volume concentrations of electrons and holes, respectively. Here, we have chosen the density of states of the conduction and valence bands, N_C and N_V, as the standard states for electrons and holes, respectively, and the activities represented by the ratios between the concentrations of defects and these densities of states. E_g is the band gap, expressing the enthalpy change of the reaction (here per mole of electrons, since we use the gas constant R instead of Boltzmann's constant k). The band gap generally exhibits a small temperature dependency mostly attributable to thermal lattice expansion.

In semiconductor physics it is common to express instead

$$K_g^{/} = [e'][h^\bullet] = np = N_C N_V K_{g,0}\exp(\frac{-E_g}{RT}) = K_{g,0}^{/}\exp(\frac{-E_g}{RT})$$

Eq. 29

where we exclude the density of states. Instead they are therefore multiplied into the pre-exponential term. The new equilibrium constant therefore does not relate to standard conditions for the electronic defects in the same way as normal chemical equilibria do, hence are not expressed in terms of standard entropy changes in the same way, and we thus here denote it with a prime "$^{/}$".)

If we now choose that intrinsic electronic excitation dominates, the simplified limiting electroneutrality can be expressed $n=p$, and insertion of this into the equilibrium coefficient Eq. 29 yields

$$n = p = (K_g^{/})^{1/2} = (N_C N_V K_{g,0})^{1/2}\exp(\frac{-E_g}{2RT})$$

Eq. 30

We see that we obtain the familiar half the bandgap as enthalpy of the concentration of mobile charge carrying electrons and holes in an intrinsic semiconductor. We moreover see that the pre-exponential contains the density of states, which are usually considered somewhat temperature dependent, typically each with $T^{3/2}$ dependencies.

Now, let us do the same treatment for the formation of oxygen vacancies, Eq. 10. The equilibrium coefficient should be

$$K_{vO} = \frac{a_{v_O^{\bullet\bullet}} a_{e'}^2 a_{O_2(g)}^{1/2}}{a_{O_O^x}} = \frac{\frac{[v_O^{\bullet\bullet}]}{[O]}\left(\frac{n}{N_C}\right)^2\left(\frac{p_{O_2}}{p_{O_2}^0}\right)^{1/2}}{\frac{[O_O^x]}{[O]}} = \frac{[v_O^{\bullet\bullet}]}{[O_O^x]}\left(\frac{n}{N_C}\right)^2\left(\frac{p_{O_2}}{p_{O_2}^0}\right)^{1/2}$$

Eq. 31

It is common for most purposes to neglect the division by N_C, to assume $[O_O^x] = 1$, and to remove $p_{O_2}^0 = 1$ bar, so that we get

$$K_{vO}^{/} = [v_O^{\bullet\bullet}] n^2 p_{O_2}^{1/2}$$

Eq. 32

This means that $K_{vO}^{/} = N_C^2 K_{vO}$ and that the expression is valid for small concentrations of defects. If these oxygen vacancies and the compensating electrons are the predominating defects in the oxygen deficient oxide, the principle of electroneutrality requires that

$$2[v_O^{\bullet\bullet}] = n$$

Eq. 33

By insertion we then obtain:

$$2[v_O^{\bullet\bullet}] = n = (2K_{vO}^{/})^{1/3} p_{O_2}^{-1/6} = (2K_{0,vO}^{/})^{1/3} \exp\left(\frac{-\Delta H_{vO}^0}{3RT}\right) p_{O_2}^{-1/6}$$

Eq. 34

and deliberately use a pre-exponential $K_0^{/}$ instead of an entropy change. The enthalpy ends up divided by 3, the number of defects.

A plot of log *n* or log $[v_O^{\bullet\bullet}]$ vs log p_{O_2} (at constant temperature) will give straight lines with a slope of –1/6. Such plots are called *Brouwer diagrams*,[8] and they are commonly used to illustrate schematically the behaviour of defect concentrations under simplified limiting cases of dominating defects.

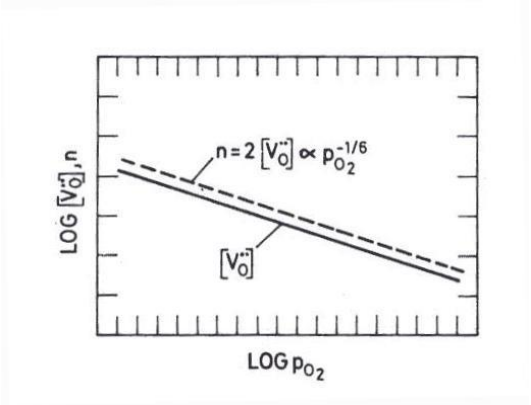

Figure 2-5. Brouwer diagram for $n = 2[v_O^{\bullet\bullet}]$ as the simplified limiting electroneutrality condition.

[8] G. Brouwer, *Philips Research Reports* 1954, 9, 366–376

As we have seen earlier, ZrO_2 can be acceptor-doped with Y^{3+} from Y_2O_3, Eq. 13. This introduces one more defect, and the new electroneutrality condition would be

$$2[v_O^{\bullet\bullet}] = [Y_{Zr}^{/}] + n$$

Eq. 35

If we want to solve now the situation for all three defects simultaneously, we could use the equilibrium coefficient of Eq. 13, but this is not common for doping reactions, because they are rarely at equilibrium. Instead we assume that the amount of dopant and hence $[Y_{Zr}^{/}]$ is fixed because all dopant is dissolved (below the solubility limit) or frozen in. In any case, the combination of equations for three or more defects is most often not solvable analytically, one must use numerical solutions. It is common and instructive to therefore divide the problem into simplified ones, and compute and plot each simplified electroneutrality condition with sharp transitions, although we know that the transitions in reality are smooth.

If $2[v_O^{\bullet\bullet}] \approx n >> [Y_{Zr}^{/}]$, the foreign cations do not affect the native defect equilibrium, and the electron and oxygen vacancy concentrations are given by their own equilibrium, and they are proportional to $p_{O_2}^{-1/6}$ as we have shown above. This will occur at relatively low oxygen activities, where these concentrations are relatively large.

If $2[v_O^{\bullet\bullet}] \approx [Y_{Zr}^{/}] >> n$, the oxygen vacancy concentration is determined and fixed by the dopant content (extrinsic region).

Figure 2-6 shows the two situations plotted in a Brouwer diagram (for the general case of a lower valent dopant Ml substituting a host metal M).

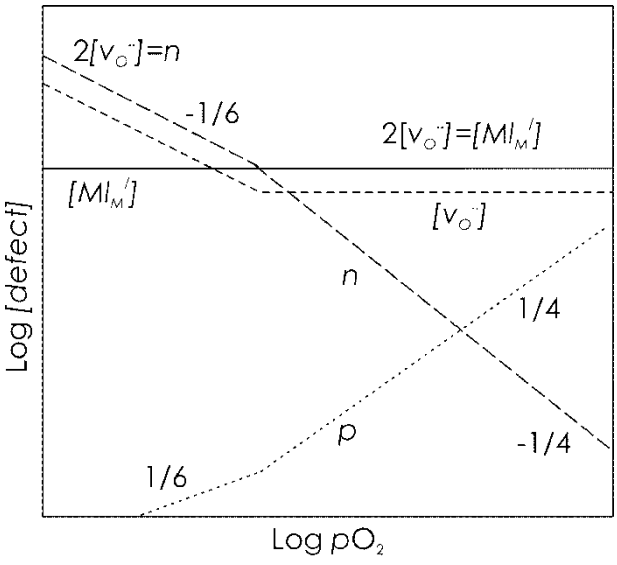

Figure 2-6. Brouwer plot of the concentrations of defects as a function of oxygen partial pressure in an oxygen deficient oxide predominantly containing doubly charged oxygen vacancies, showing the effects of a constant concentration of lower valent cation dopants, $[Ml_M^{/}]$.

When we explore defect structures like this, it is useful to find the behaviour of the minority defects. In the situation that $2[v_O^{\bullet\bullet}] = [Y_{Zr}^{/}]$, the concentration of minority electrons, *n*, can be found by inserting this into the (always valid) equilibrium constant relating oxygen vacancies and electrons, Eq. 32, to obtain

$$n = (2K_{vO}^{/})^{1/2}[Y_{Zr}^{/}]^{-1/2} p_{O_2}^{-1/4}$$

Eq. 36

This and the corresponding line for minority electrons in Figure 2-6 shows that the concentration of electrons now decreases with a different dependency on p_{O_2} than in the former case where they were in majority compensated by oxygen vacancies. As the concentration of electrons and minority electron holes are related through the equilibrium $K_i = np$, the electron hole concentration in this extrinsic region correspondingly increases with increasing oxygen activity. Electron holes will remain a minority defect, but depending on the impurity content, oxygen activity and temperature, *p* may become larger than *n*, as seen in in Figure 2-6.

A useful type of Brouwer diagram, although not so commonly seen, is a double-logarithmic plot of defect concentrations vs the concentration of the dopant, see Figure 2-7.

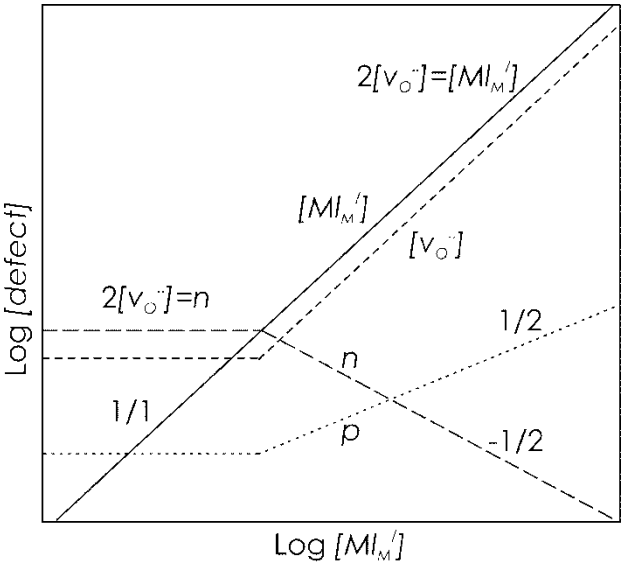

Figure 2-7. Brouwer plot of the concentrations of defects as a function of the concentration of lower valent dopants, $[Ml_M^{/}]$, for an oxygen deficient oxide intrinsically dominated by doubly charged oxygen vacancies and electrons, showing the transition from the intrinsic to the extrinsic region.

2.1.11 Defects in battery materials

Defect chemistry has not been much developed or used to understand battery materials, because crystalline solid-state electrolytes have not been in commercial use till now, and electrodes have very large changes in composition during use, which is considered challenging to describe in terms of defect chemistry. We will still look at an example of application of defect chemistry for a cathode material, $LiFePO_4$, following mainly a treatment

by Maier and Amin.[9] $LiFePO_4$ represents the low-energy, fully reduced case, with Fe in the +2 state. Many indications point at Li vacancies as the predominant point defect, charge compensated by electron holes (representing Fe^{3+} states), such that the general formula is $Li_{1-\delta}FePO_4$. If we were not in a closed battery, such defects might be formed in equilibrium with the oxide Li_2O as a separate phase:

$$Li_{Li}^{x} + \tfrac{1}{4}O_2(g) = v_{Li}^{/} + h^{\bullet} + \tfrac{1}{2}Li_2O(s)$$

Eq. 37

In a Li-ion battery, the Li ions are exchanged with the anode where the Li may considered to be in a metallic state, so we might alternatively write the formation of the defect couple:

$$Li_{Li}^{x} = v_{Li}^{/} + h^{\bullet} + Li(s)$$

Eq. 38

In a battery, the charging of the cathode does however take place by extracting Li through the electrolyte, and electrons through the external circuit. The reaction above may therefore be written:

$$Li_{Li}^{x} = v_{Li}^{/} + h^{\bullet} + Li^{+} + e^{-}$$

Eq. 39

Here, it must be emphasised that the Li^+ ions are not in the electrode phase, but in the electrolyte, and that the electrons may be taken to be in the current collector of the electrode. In this way, we may mix defect chemistry (for the cathode material, and with effective charges) with species in other phases (with real charges). Note that the effective and real charges are conserved separately.

At high Li activities, donor dopants or impurities may dominate and increase the concentration of Li vacancies and supress the hole concentration. These may be for instance Al^{3+} or Mg^{2+} substituting Li^+, the latter forming $Mg_{Li}^{\bullet}$ defects. The electroneutrality condition including donors will be

$$[D^{\bullet}] + [h^{\bullet}] = [v_{Li}^{/}]$$

Eq. 40

Figure 2-8 (left) illustrates the changeover from donor-doped dominance at high Li activities ("D regime"), to intrinsic defect dominance at low Li activities ("P-regime"). The electroneutrality shows how an increase in the donor concentration will increase the Li vacancy concentration and decrease the hole concentration. When the donor concentration exceeds the hole concentration, these changes become substantial, as illustrated in Figure 2-8 (right).

[9] J. Maier and R. Amin, "The defect chemistry of $LiFePO_4$", *J. Electrochem. Soc.*, **155** (2008) A339-A344.

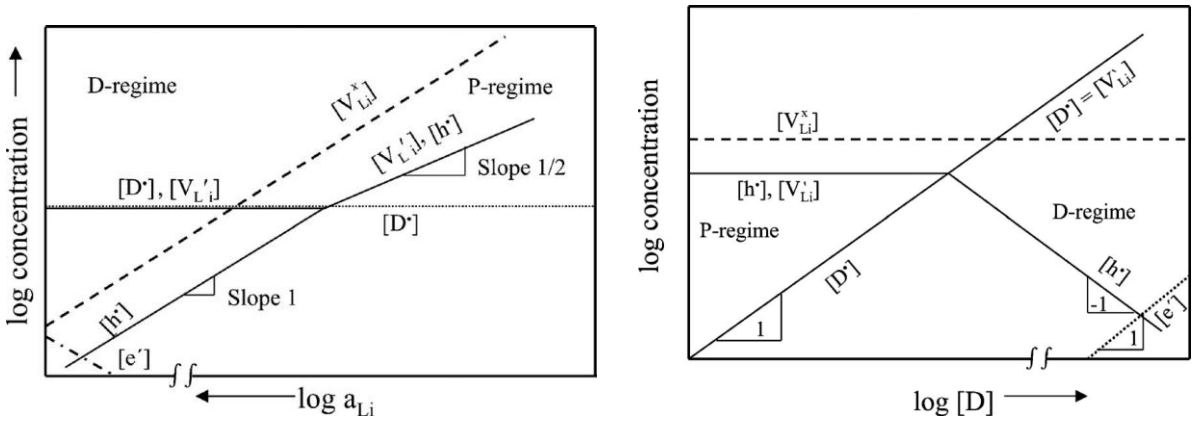

Figure 2-8. Left: Brouwer diagram of defect concentrations in $LiFePO_4$ vs Li activity.[9] Right: Brouwer diagram of log defect concentrations in $LiFePO_4$ vs log donor dopant concentration.[9]

Figure 2-9 shows a plot of the concentration of electron holes vs 1/T – at two different regimes of Li activity and donor doping. In both regimes, the temperature dependencies are given by the defect equilibrium forming Li vacancies and electron holes (Eq. 38) but under different dominating electroneutrality conditions.

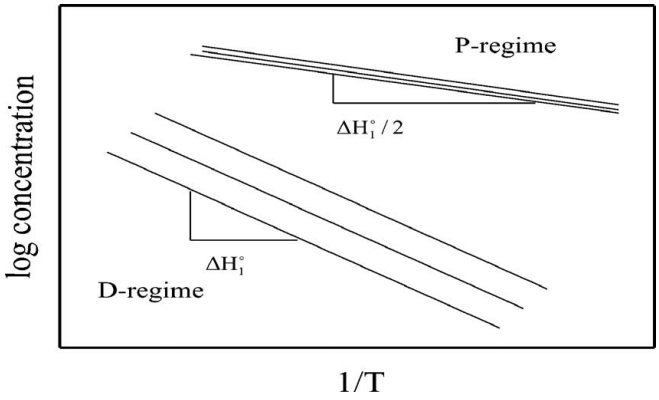

Figure 2-9. Schematic plot of log concentration of electron holes for different Li activities in the P- and D-regimes vs 1/T for $LiFePO_4$.[9] ΔH_i^0 is the standard enthalpy change for the reaction in Eq. 38. The concentration lines will be representative also for conductivity lines.

As the cathode is charged, the concentrations of Li vacancies and holes grow large. The effect of this is first that the diffusivity of Li^+ and electronic (p-type) conductivity both increase. But the effect is moderated by trapping between the Li vacancies and the holes:

$$v_{Li}^{/} + h^{\bullet} = (v_{Li}^{/}h^{\bullet})^{x}$$

Eq. 41

The associated defect is neutral and will not contribute to electronic (or ionic conductivity). Figure 2-8 (right) shows how the concentration of these neutral defects may be higher than that of the charged vacancies, and that it varies independently of dominating electroneutrality, since they are neutral.

At high concentrations, a defect like the neutral vacancies will start to resemble a new structure and eventually order, whereby the new structure is formed. In simple terms, the new

structure may be simply $FePO_4$. When it forms, it will still have a content of Li, but these will be interstitials in the new structure, $Li_\varepsilon FePO_4$. They may be compensated by electrons, and if this phase is dominated by these two defects, the electrode materials changes in principle from a p- to an n-type material upon charging.

2.1.12 Computational methods in defect chemistry

Defect formation reactions including the ones we have mentioned above may be modelled using a range of computational methods. These are in principle the same as would be used to calculate structures of crystalline solids. They vary in accuracy and computer requirements from simple classical electrostatic models to density functional theory (DFT)-based (so called *ab initio*) approximations of quantum mechanics for the bonding electrons. For defect formation reactions, one calculates the energy of the structure with and without the defect, $E^{\mathrm{tot}}_{\mathrm{defect}}$ and $E^{\mathrm{tot}}_{\mathrm{bulk}}$, and takes the energy (or chemical potentials) of external reactants or products also into account. The energy of electrons get terms given by the Fermi level. The energy (enthalpy) at 0 K for formation of a charged defect by formation or annihilation of electrons and exchange with neutral species (e.g. gases) is then:

$$\Delta E^{\mathrm{f}}_{\mathrm{defect}} = E^{\mathrm{tot}}_{\mathrm{defect}} - E^{\mathrm{tot}}_{\mathrm{bulk}} + \sum_i \mu_{\mathrm{i}} + q\mu_{\mathrm{e}}$$

Eq. 42

In modern computational defect chemistry, one furthermore estimates or calculates the entropy of the reactions. Together with the computational energy, one then obtains Gibbs energies. From the Gibbs energy, we have an expression for the ratio of the defect concentration over the concentration of the perfect occupied site:

$$[\mathrm{defect}] = N_{\mathrm{sites}} \exp\left(\frac{-\Delta G^{\mathrm{f}}_{\mathrm{defect}}(P,T)}{\mathrm{k_b}T}\right)$$

Eq. 43

Now, the Fermi level that enters Eq. 42 is unknown. But by combining Eq. 45 these for the relevant defects with the electroneutrality condition, one may numerically solve the entire defect structure at any given (and as a function of) temperature and activities of components or doping level. The Fermi level becomes a result of the calculations.

One may also simulate and parametrise transport of defects by various computational methods, comprising molecular dynamics with classical or more or less quantum mechanical interactions, or by calculating energies of a number of positions along a chosen path for a jump between two sites (nudged elastic band method).

2.1.13 Exercises in defect chemistry

1. List the main types of 0-, 1-, 2-, and 3-dimensional defects in crystalline solids
2. Write the Kröger-Vink notation for the following fully charged species in MgO: Cation and anion on their normal sites, oxygen vacancy, magnesium vacancy, interstitial magnesium ion.
3. Write a defect chemical reaction for formation of Frenkel defects in ZrO_2. Do the same for anti-Frenkel (anion Frenkel) defects in ZrO_2. Write expressions for the equilibrium constants.

4. Write a defect chemical reaction for formation of Schottky defects in ZrO_2. Write the expression for the mass action law equilibrium coefficient, combine it with the limiting electroneutrality condition, and solve it with respect to the concentration of defects. What is the temperature dependency of Schottky defects in ZrO_2? (Use e.g. a schematic van 't Hoff plot)
5. ZrO_{2-y} has – as the formula indicates here – oxygen deficiency under normal conditions. Write the formation reaction for the defects involved and solve the defect structure if these defects predominate. What is the pO_2 dependency for the concentration of the different defects?
6. We dope ZrO_{2-y} with Y_2O_3 to increase the concentration of oxygen vacancies and decrease the concentration of electrons. This stabilises its tetragonal and – at high temperatures and high Y contents – its cubic fluorite structure (CaF_2-type). We thus call it yttria-stabilised zirconia (YSZ). Write a reaction for the doping. Write the total electroneutrality condition. Write the simplified limiting electroneutrality condition at high Y contents.
7. ZrO_2 is commonly doped with 8 mol% Y_2O_3. What is then the mole fraction of Y and the mole and site fraction of oxygen vacancies?
8. Write a defect chemical reaction for the substitution of Li for Ni in NiO.
9. Write a defect chemical reaction for the substitution of Sr for Ca in $CaTiO_3$.
10. Write a defect chemical reaction for the substitution of Sr for La in $LaMnO_3$.
11. Write the electroneutrality condition for defects in boron-doped silicon. Write the electroneutrality condition for defects in phosphorous-doped silicon. Write the electroneutrality condition for pure (undoped) silicon and for boron-doped silicon.
12. Write an electroneutrality condition for MO_{1-x} (hint: includes an oxygen defect type and an electronic defect type).
13. Write an electroneutrality condition for MO_{1+x}.
14. Write an electroneutrality condition for $M_{1-x}O$.
15. Write an electroneutrality condition for $M_{1+x}O$.
16. For Figure 2-8 (right), deduce the different slopes for the hole concentration vs Li activity.

2.2 Random diffusion and ionic conductivity in crystalline ionic solids

In order to make solid-state electrochemical devices we need ionic transport in the normally crystalline solid electrolyte. Most efficient devices, not least rechargeable batteries, need also mass transport in the electrodes. In crystalline phases, this transport takes place by defects. We have seen what defects are and how they are formed by equilibration at elevated temperatures or by doing. Now we are therefore ready to look a bit more into the atomic processes that give rise to mobility of defects.

Ionic conductivity originates from *random diffusion* of ions resulting from thermal vibrations – in crystalline solids by help of defects, so that we may equally well call it random diffusion of defects. Random diffusion for a constituent of the lattice (e.g. metal cations or oxide ions of an oxide) is also referred to as *self-diffusion*.

Mechanistically, atoms and ions can move in crystalline solids in many ways. The simplest and most important are the vacancy mechanism and the interstitial mechanism, see Figure 2-10.

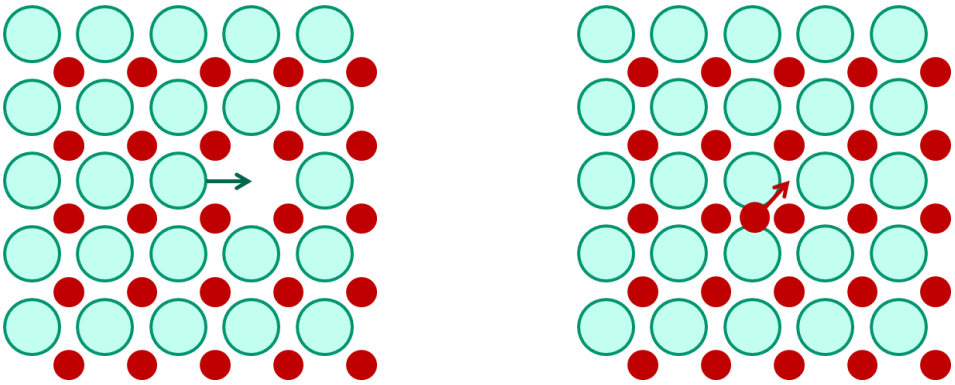

Figure 2-10. Simple diffusion mechanisms in crystalline solids, illustrated for an ionic compound MX, where M cations are small and X anions are larger: Vacancy mechanism for anions (left) and interstitial mechanism for cations (right).

Once a vacancy is formed in the lattice, it may move by another ion jumping into it. Once an interstitial ion is formed, it may move into another interstitial position. Both these defects will have an energy barrier to overcome to enable the jump: Bonds have to be broken and neighbouring ions in the jump path must be pushed out of their equilibrium position to make way. Hence, the random diffusivity (or random diffusion coefficient) is exponentially dependent on the thermal energy kT (or RT per mol) compared to the energy barrier Q_D of the diffusional jump, and has the general form:

$$D_r = D_r^0 \exp(-\frac{Q_D}{kT})$$

Eq. 44

Diffusion and the diffusion coefficients are considered difficult to comprehend. One of the reasons is that few experimental methods give direct measure of the simplest process, namely the random diffusion coefficient. In fact, ionic conductivity is the only one – we shall see why later. There are other diffusion coefficients defined so as to fit empirically and more intuitively to various experiments, notably the chemical diffusion coefficient, which expresses the net flux of matter in a concentration gradient (according to Fick's law) and the tracer diffusion coefficient D_t, which expresses the flux of an isotope of an element in a gradient of isotopic composition.

In order to understand better the concept of random diffusion and the random diffusion coefficient, we shall look at a few relationships and models. We shall restrict ourselves to cubic materials (isotropic behaviour) where transport coefficients are the same in all directions. Firstly, the random diffusion coefficient is simply given as a product of the individual jump distance squared and the frequency of successful jumps in any direction, divided by the number of directions, which is 6 in an orthogonal axis system:

$$D_r = \tfrac{1}{6} s^2 \Gamma = \tfrac{1}{6} s^2 \frac{n}{t}$$

Eq. 45

Here, s is the jump distance, Γ is the jump rate – namely the number of jumps n per time t. This equation allows calculations of e.g. total jump distance over a time t if D_r is known. Figure 2-11 shows schematically how a diffusing atom - or vacancy – travels far, but because of the randomness ends up getting not very far from the starting point, statistically speaking.

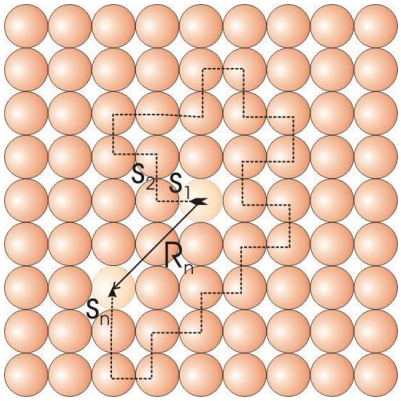

Figure 2-11. Schematic illustration of *n* individual jumps each of distance *s*, resulting in a total travelled distance *ns*, but on average getting nowhere, at a modest radius (or sphere in the 3D case) out of the starting point.

The jump frequency is the product of the vibrational frequency ν^0, the number of neighbouring sites Z to jump to, the fraction X of these that are available, and the probability that the thermal energy overcomes the energy barrier. For random diffusion of ions by a vacancy mechanism this would be

$$D_r = \tfrac{1}{6} s^2 \Gamma = \tfrac{1}{6} s^2 Z \nu^0 \exp(-\frac{\Delta G_D}{kT}) X_v = \alpha a_0^2 \nu^0 \exp(-\frac{\Delta H_D}{kT}) X_v$$

Eq. 46

Here, ΔG_D is the Gibbs energy barrier for the diffusional jump and X_v is the fraction of vacancies. In the rightmost part of Eq. 46 we have split the Gibbs energy for the jump into an activation entropy (usually negligible) and enthalpy, and we have expressed the jump distance in terms of the lattice constant a_0, and finally collected the entropic part and all the other temperature independent factors in a single constant α (alpha).

Now, we will link diffusivity to conductivity. First we acknowledge (without deriving it) that the random diffusion coefficient is proportional to how easy it is to move a species – the mechanical mobility – in a way the inverse of friction. This mobility is termed B (after German "Beweglichkeit"). The diffusivity is driven by and thus also proportional to the thermal energy kT:

$$D = kTB \quad \text{or} \quad B = \frac{D}{kT}$$

Eq. 47

This is called the Nernst-Einstein relationship. One of its consequences is that mobility (ease of movement) and other properties related to this, like ionic conductivity, has a somewhat different temperature dependency than random diffusivity.

Let us now expose our mobile ions A^z with charge *ze* to an electrical field *E*, which may for instance arise in a conductivity measurement, or by applying a voltage to a charging battery or electrolyser. This imposes a force $F = -zeE$ on the ions. Even if they predominantly move randomly by thermal energy, there will be a small net drift velocity *v* in the direction of the field. This is given by the product of force and mobility:

$$v = BF = -BzeE$$

Eq. 48

The process is called migration. The flux density *j* is given by the velocity multiplied with the density (volume concentration) of mobile ions:

$$j = cv = cBF = -cBzeE$$

Eq. 49

The current density *i* is given by the flux density multiplied with the charge:

$$i = zecv = zecBF = -cB(ze)^2 E$$

Eq. 50

We now define charge mobility $u = |ze|B$ and get

$$i = -|ze|cuE$$

Eq. 51

This is a form of Ohm's law, and it is evident that $|ze|cu$ is electrical conductivity: $\sigma = |ze|cu$. By back-insertion, we obtain

$$\sigma = |ze|cu = (ze)^2 cB = \frac{(ze)^2 c}{kT} D_r$$

Eq. 52

These are essentially again Nernst-Einstein relationships, linking conductivity, mobility terms, and random diffusivity. The two first expressions are valid for all charged species, while the last is only relevant for charged species which move by (hopping) diffusion.

2.2.1 Defects and constituent ions

In the previous section we considered diffusivity of constituent ions by a vacancy mechanism. We saw that the diffusivity was proportional to the concentration of available sites to jump to, namely vacancies. We can deduce that then also the mobility and hence conductivity of ions are proportional to the concentration of vacancies. The vacancies on their part will have much higher probabilities of finding a site to jump to, namely an occupied site. Hence, the diffusivities of vacancies v and constituent atoms C have diffusivity ratios given by the ratio of occupied over vacant sites:

$$\frac{D_{r,v}}{D_{r,C}} = \frac{X_C}{X_v} = \frac{1 - X_v}{X_v} \approx \frac{1}{X_v}$$

Eq. 53

The defect is much faster than the constituent atoms. The same holds for interstitial diffusion, where the interstitial always can jump, but the constituent atom must be interstitial to jump and hence its diffusivity is is proportional to the concentration of defects – interstitials.

We conclude this part by stating again that defects have in general higher diffusivity and hence mobilities than constituent atoms. But the conductivity – where the concentration enters as a factor - obviously ends up the same whether one considers the defect or the constituent.

When the ions of interest are foreign to the compound, and diffuse by an interstitial mechanism, there is no difference between the interstitial defect and the species itself; there is only one diffusivity and mobility to consider. This applies for instance to protons diffusing by the so-called free proton – or Grotthuss – mechanism.

2.3 Electronic conductivity

It is important to understand also how electrons move, since their transport may partly short-circuit electrolytes, facilitate transport in mixed conducting membranes, battery electrodes, and storage materials, determine corrosion processes, and be essential in catalysis and electrode processes.

2.3.1 Mobility of electrons in non-polar solids – itinerant electron model

The charge carrier mobility and its temperature dependency is dependent on the electronic structure of the solid. For a pure non-polar solid - as in an ideal and pure covalent semiconductor - the electrons in the conduction band and the electron holes in the valence band can be considered as quasi-free (itinerant) particles. If accelerated by an electrical field they move until they collide with a lattice imperfection. In an ideally pure and perfect crystal the mobilities of electrons and electron holes, u_n and u_p, are then determined by the thermal vibrations of the lattice in that the lattice vibrations result in electron and electron hole scattering (lattice scattering). Under these conditions the charge carrier mobilities of electrons and electron holes are both proportional to $T^{-3/2}$, e.g.

$$u_{n,latt} = u_{n,latt,0} T^{-3/2} \qquad u_{p,latt} = u_{p,latt,0} T^{-3/2}$$

Eq. 54

If, on the other hand, the scattering is mainly due to irregularities caused by impurities or other imperfections, the charge carrier mobility is proportional to $T^{3/2}$, e.g.

$$u_{n,imp} = u_{n,imp,0} T^{3/2} \qquad u_{p,imp} = u_{p,imp,0} T^{3/2}$$

Eq. 55

If both mechanisms are operative, each mobility is given by

$$u_n = \frac{1}{\frac{1}{u_{n,latt}} + \frac{1}{u_{n,imp}}} \qquad u_p = \frac{1}{\frac{1}{u_{p,latt}} + \frac{1}{u_{p,imp}}}$$

Eq. 56

and from the temperature dependencies given above it is evident that impurity scattering dominates at low temperature while lattice scattering takes over at higher temperature.

2.3.2 Polar (ionic) compounds

When electrons and electron holes move through polar compounds, such as ionic oxides, they polarise the neighbouring lattice and thereby cause a local deformation of the structure. Such an electron or electron hole with the local deformation is termed a polaron. The polaron is considered as a fictitious particle – the deformation moves along with the electron or hole.

When the interaction between the electron or electron hole and the lattice is relatively weak, the polaron is referred to as a large polaron - the deformation gives a shallow energy minimum for the location of the electron or hole. Large polarons behave much like free electronic carriers except for an increased mass caused by the fact that polarons carry their associate deformations. Large polarons still move in bands, and the expressions for the effective density of states in the valence and conduction bands are valid. The temperature dependence of the mobilities of large polarons at high temperatures* is given by

$$u_{\text{largepolarons}} = u_{\text{largepolarons},0} T^{-1/2}$$

Eq. 57

The large polaron mechanism has been suggested for highly ionic non-transition metal oxides, with large band gaps.

For other oxides it has been suggested that the interactions between the electronic defects and the surrounding lattice can be relatively strong and more localised. If the dimension of the polaron is smaller than the lattice parameter, it is called a small polaron or localised polaron, and the corresponding electronic conduction mechanism is called a small polaron mechanism.

The transport of small polarons in an ionic solid may take place by two different mechanisms. At low temperatures small polarons may tunnel between localised sites in what is referred to as a narrow band. The temperature dependence of the mobility is determined by lattice scattering and the polaron mobility decreases with increasing temperature in a manner analogous to a broad band semiconductor.

However, at high temperatures (for oxides above roughly 500 °C) the band theory provides an inadequate description of the electronic conduction mechanism. The energy levels of electrons and electron holes do not form bands, but are localised on specific atoms of the crystal structure (valence defects). It is assumed that an electron or electron hole is self-trapped at a given lattice site, and that the electron (or electron hole) can only move to an adjacent site by an activated hopping process similar to that of ionic conduction. Consequently it has been suggested that the mobility of a small polaron can be described by a classical diffusion theory as described in a preceding chapter and that the Nernst -Einstein can be used to relate the activation energy of hopping, E_u, with the temperature dependence of the mobility, u, of an electron or electron hole:

* "High temperatures" are temperatures above the optical Debye temperature, θ. For oxides $\theta \sim (h\omega)/2\pi k$, where h is the Planck constant, k the Boltzmann constant and ω the longitudinal optical frequency which for an oxide is $\sim 10^{14}$ s^{-1}.

$$u = \frac{e}{kT} D = u_0 T^{-1} \exp\left(\frac{-E_u}{kT}\right)$$

Eq. 58

where E_u is the activation energy for the jump.

At high temperatures, the exponential temperature dependence of small polaron mobilities can thus in principle be used to distinguish it from the other mechanisms.

The different mechanisms can also be roughly classified according to the magnitude of the mobilities; the lattice and impurity scattering mobilities of metals and non-polar solids are higher than large-polaron mobilities which in turn are larger than small-polaron mobilities. Large polaron mobilities are generally of the order of 1-10 $cm^2/V^{-1}s^{-1}$, and it can be shown that a lower limit is approximately 0.5 $cm^2V^{-1}s^{-1}$. Small polaron mobilities generally have values in the range 10^{-4}-10^{-2} $cm^2V^{-1}s^{-1}$. For small polarons in the regime of activated hopping the mobility increases with increasing temperature and the upper limit is reported to be approximately 0.1 $cm^2V^{-1}s^{-1}$.

2.3.3 Exercises – transport in solids

1. In this section we have discussed *intensive* and *extensive* electrical materials properties, like *conductivity* and *resistance*, respectively. Review them; what do the terms mean, and which are which? We have omitted several: Derive the ones missing (mathematics, name, suggested symbol).
2. A compound has a random diffusion coefficient of 10^{-8} cm^2/s and a jump distance of 3 Å for one of its constituents. What is the jump frequency? If the vibrational frequency is 10^{13} Hz (s^{-1}), what is the fraction of vibrations that end in a successful jump? How many jumps does the atom (or ion) make in an hour? What is the total jump distance?
3. The value α (alpha) in Eq. 46 often takes values of the order of unity. Try to derive it for a cubic structure. Discuss and make choices where needed.
4. Eq. 48 - Eq. 51 describe a process named migration. Discuss its driving force as compared to the driving force for diffusion. (Diffusion may mean different things; try to be clear on which one you refer to, and if possible include more than one.)
5. What is Ohm's law? Show that Eq. 51 is equivalent to Ohm's law.
6. Consider Eq. 52. What is the one most essential difference (or factor if you will) between conductivity on the one hand side and the mobility and random diffusivity terms on the other?

2.4 Thermodynamics of electrochemical cells

2.4.1 Electrons as reactants or products

Now we will address what happens at electrodes. As example, we will consider an oxide ion conducting electrolyte, like Y-substituted ZrO_2 (YSZ), with an inert electrode like platinum, Pt, in oxygen gas, O_2(g).

The overall half-cell electrode reaction is

$$O_2(g) + 4e^- = 2O^{2-}$$ Eq. 59

When the reaction runs forward, electrons taken from the metal electrode are reactants. reducing oxygen gas to oxide ions in the electrolyte. If it runs backward, electrons are products. If we put the electrode at a more negative electrical potential compared to the electrolyte, the electrochemical potential of the left hand side becomes higher and that on the right hand side lower, relative to each other, and the reaction is driven more to the right. If we increase the partial pressure of oxygen, pO_2, the reaction is also driven more to the right. For a given pO_2, there is a certain voltage at which the reaction is at equilibrium, i.e., there is no net reaction or current running. By having electrons as reactants or products, the reaction and equilibrium becomes affected by the half-cell electrode voltage.

Before we move on, we dwell on a couple of things that seems to confuse many in solid-state electrochemistry: Firstly, the electrode reaction Eq. 59 is not a defect chemical reaction; it is not the reaction that changes the content of the species (here oxygen, Eq. 10) and it is not the reaction that introduces the charge carrier through doping (here, Eq. 13). Electrode reactions exchange electrons with the electrode which is a separate phase. Therefore, we don't use effective charges when we write electrode reactions – we don't balance effective charges in one phase with effective charges in another.

2.4.2 Half-cell potential. Standard reduction potentials. Cell voltage

The problem with an electrode reaction is that we cannot measure the voltage of a half cell – we need a second electrode. When we measure the voltage between two electrodes, we know the difference between them, but cannot know the voltage of each of them. In aqueous electrochemistry, we have defined that a standard hydrogen electrode (SHE) , namely an inert Pt electrode in contact with 1 M H^+ and pH_2 = 1 bar, to have 0 V. We can then measure other electrodes vs this electrode and construct a table of reduction potentials with the SHE as reference.

A similar system could in principle be established for each solid-state electrolyte. For instance we can define an electrode to have a zero open circuit voltage when in equilibrium with the standard state of the element(s) corresponding to the charge carrier. Hence we could define the standard voltage of the electrode in Eq. 59 to be 0 when pO_2 = 1 bar. It is however simply common to operate only with full cell voltages. A practical exception for this is when referring to the chemistries in Li-ion batteries where the potentials are reported towards the Li/Li^+ reduction pair.

2.4.3 Cell voltage and Gibbs energy

In an electrode or an entire electrochemical cell we can do electrical work, w_{el}. *The electrical work we do reversibly on an electrolytic cell is equal to the increase in Gibbs energy of the cell system* (strictly speaking at constant pressure and temperature). Similarly, *the electrical work a galvanic cell does on the surroundings equals the reduction in the cell system's Gibbs energy*. Thus, generally, we have

$$\Delta G = w_{el}$$

Eq. 60

The electrical work for each electron taking part in the reaction is given by its elementary charge *e* times the electrical potential difference between positive and negative electrode, i.e., the cell voltage *E*. The electrical work for the reaction is thus obtained by multiplication by the number of electrons. The work for a mole of reactions is similarly obtained by further multiplying with Avogadro's number:

$$w_{el} = \Delta G = -neU \qquad \text{(for a reaction with } n \text{ electrons)}$$

Eq. 61

$$w_{el} = \Delta G = -nN_A eU = -nFU \qquad \text{(for } n \text{ mol electrons)}$$

Eq. 62

From this, the cell voltage *U* will, like $-\Delta G$, express how much the reaction tends to go forward:

$$\Delta G = -nFU \quad \text{or} \quad U = \frac{-\Delta G}{nF}$$

Eq. 63

The *standard* Gibbs energy change, ΔG^0, corresponding to the change in Gibbs energy when all reactants and products are present in standard state (unit activity, e.g. at 1 bar pressure or 1 M concentration, or as a pure condensed phase) has a corresponding standard cell voltage E^0:

$$\Delta G^0 = -nFU^0$$

Eq. 64

A total red-ox reaction does not indicate electron transfer, it does not specify the number *n* of electrons exchanged and can be done without an electrochemical cell. Nevertheless, we can still represent its thermodynamics by a cell voltage. The relation between Gibbs energy and the cell voltage then requires knowledge of the number of electrons *n* transferred in the reaction.

Gibbs energy change for a total reaction is the sum of the change for each half cell reaction:

$$\Delta G_{total} = y\Delta G_{red} + x\Delta G_{ox}$$

Eq. 65

or, if we use reduction data for both reactions:

$$\Delta G_{total} = y\Delta G_{red1} - x\Delta G_{red2}$$

Eq. 66

We see from this that

$$U_{total} = \frac{\Delta G_{total}}{-nF} = \frac{\Delta G_{total}}{-xyF} = \frac{y(-xFU_{red}) + x(-yFU_{ox})}{-xyF} = U_{red} + U_{ox}$$

Eq. 67

or

$$U_{total} = U_{red1} - U_{red2}$$

Eq. 68

The reaction between hydrogen and oxygen:

$$H_2(g) + ½\ O_2(g) = H_2O(g)$$

Eq. 69

has standard Gibbs energy change of –228.7 kJ/mol at ambient temperature. We can utilise this in a fuel cell, but what is the standard cell voltage? We may assume that the process involves O^{2-} or H^+ as ionic charge carrier in the electrolyte, and thus that we get two electrons (n = 2) per reaction unit (i.e. per hydrogen or water molecule):

$$U^0 = \frac{\Delta_r G^0}{-2F} = +1.185\ \mathrm{V}$$

Eq. 70

Gibbs energy change is an *extensive* property. If we consider the double of the reaction above,

$$2H_2(g) + O_2(g) = 2H_2O(g)$$

Eq. 71

then Gibbs energy is twice as large; 2*-228.7 = -457.4 kJ/mol. But the number of electrons is also doubled, so the cell voltage remains constant, it is an *intensive* property:

$$U^0 = \frac{-457400}{-4F} = +1.185\ \mathrm{V}$$

Eq. 72

There are two ways to define equilibrium in electrochemistry: For an electrode or electrochemical cell, we may state that we have equilibrium if the current is zero. Then there is no reaction and no losses. We refer to the voltage in these cases as the open circuit voltage (OCV), and since there are no losses, it corresponds to the voltage given by thermodynamics as discussed above. We may refer to this potential also as the reversible potential, and we may refer to the equilibrium as being a kinetic equilibrium: No current passes because we don't allow any electrical current – we keep the cell open circuit.

However, in thermodynamics of reactions, we have also learned that we have equilibrium when $\Delta G = 0$. We can hence say, for a full cell like a battery, that the cell is at equilibrium only when $\Delta G = 0$ and hence $U = 0$. This represents a fully discharged battery – there is no driving force in any direction left – it has reached the minimum in energy. This is a thermodynamic equilibrium.

It is worth noting that the above reaction and associated standard cell voltage refer to formation of water vapour (steam). Often – especially for processes at room temperature and up to 100 °C – it is more relevant to consider formation of liquid water,

$$2H_2(g) + O_2(g) = 2H_2O(l)$$

Eq. 73

which has the familiar standard potential of 1.23 V.

2.4.4 The Nernst equation

When the activities of reactants and products change from the standard activities, the Gibbs energy change from the standard value, and the voltage of the electrode or cell changes

correspondingly from the standard voltage. From the relation between the Gibbs energy change and the reaction quotient Q

$$\Delta G = \Delta G^0 + RT \ln Q$$

Eq. 74

and the relations between Gibbs energies and voltages, Eq. 63 and Eq. 64, we obtain

$$U = U^0 - \frac{RT}{nF} \ln Q \qquad \text{(Nernst equation for reduction (cathodes) and full cells)}$$

Eq. 75

This important and widely applied equation is called the *Nernst equation*. It can be applied to both half cells and full cells.

The minus sign in Eq. 75 applies to reduction half-cell reactions, i.e., cathodes, and to full cells. For oxidation (anodes) the sign reverses to plus, because, while the reaction reverses, the voltage is still measured at the electrode vs the electrolyte (or reference):

$$U = U^0 + \frac{RT}{nF} \ln Q \qquad \text{(Nernst equation for oxidation (anodes))}$$

Eq. 76

Equilibrium means that the Gibbs energy sum of the products and that of the reactants are equal. At equilibrium we thus have $\Delta G = 0$, so that also $U = 0$:

$$U = U^0 - \frac{RT}{nF} \ln Q_{equilibrium} = 0$$

Eq. 77

, i.e.,

$$U^0 = \frac{RT}{nF} \ln Q_{equilibrium} = \frac{RT}{nF} \ln K$$

Eq. 78

All in all, we can give the standard data for a reaction in terms of ΔG^0, U^0, or K:

$$\Delta G^0 = -nFU^0 = -RT \ln K$$

Eq. 79

The importance of the Nernst equation (Eq. 75 and Eq. 76) is that it allows us to calculate any cell voltages – whether for a half cell or a full cell - different from the standard voltage if the reactants or products take on any activities different from unity.

Consider again the hydrogen-oxygen cell, Eq. 71, but now with varying partial pressures of the gases. If we use an oxide ion conducting electrolyte, the O_2/O^{2-} half-cell potential for Eq. 59 will according to the Nernst equation Eq. 75 be

$$U_{O_2(g)/O^{2-}} = U^0_{O_2(g)/O^{2-}} - \frac{RT}{nF} \ln Q_{O_2(g)/O^{2-}} = U^0_{O_2(g)/O^{2-}} - \frac{RT}{4F} \ln \frac{a^2_{O^{2-}}}{a_{O_2(g)}} = U^0_{O_2(g)/O^{2-}} - \frac{RT}{2F} \ln \frac{a_{O^{2-}}}{a^{1/2}_{O_2(g)}}$$

Eq. 80

From physical chemistry we repeat that the activity is related to a standard state. For gases, the standard state is 1 bar. For ideal gases, the activity coefficient is unity, and we have therefore $a_{O_2(g)} = p_{O_2}/1\,\text{bar}$, which for convenience usually is simplified to $a_{O_2(g)} = p_{O_2}/\text{bar}$.

A similar expression can be written for the $H_2(g)+O^{2-}/H_2O(g)$ half-cell using the Nernst equation for oxidation, Eq. 76:

$$U_{H_2(g),O^{2-}/H_2O(g)} = U^0_{H_2(g),O^{2-}/H_2O(g)} + \frac{RT}{nF}\ln Q_{H_2(g),O^{2-}/H_2O(g)} = U^0_{H_2(g),O^{2-}/H_2O(g)} + \frac{RT}{2F}\ln\frac{a_{H_2O(g)}}{a_{H_2(g)}a_{O^{2-}}}$$

Eq. 81

The overall cell voltage of the H_2/O_2 cell then becomes

$$U_{H_2(g),O_2(g)/H_2O(g)} = U_{O_2(g)/O^{2-}} - U_{H_2(g),O^{2-}/H_2O(g)} = U^0_{H_2(g),O_2(g)/H_2O(g)} - \frac{RT}{2F}\ln\frac{a_{H_2O(g)}}{a_{H_2(g)}a^{1/2}_{O_2(g)}}$$

Eq. 82

If we transform from natural logarithm ($\ln_e$) to $\log_{10}$-based logarithm, and collect the three constants with T = 298.15 K (room temperature), we obtain a more familiar version of a Nernst equation:

$$U_{H_2(g),O_2(g)/H_2O(g)} = 1.185\,\text{V} - \frac{0.059\ \text{V}}{2}\log\frac{a_{H_2O(g)}}{a_{H_2(g)}a^{1/2}_{O_2(g)}} == 1.185\,\text{V} - \frac{0.059\ \text{V}}{2}\log\frac{p_{H_2O(g)}}{p_{H_2(g)}p^{1/2}_{O_2(g)}}$$

Eq. 83

However, it must be stressed that the commonly seen number 0.059 V (divided by the number of electrons) is only valid if one uses log (not ln) and for room temperature (298 K), and that the partial pressures must be given in bar, or more correctly divided by the standard pressure 1 bar to become unit-less.

Eq. 83 lets us see how the cell voltage changes with changing concentrations of reactants and products. For instance, each decade (order of magnitude) changes the cell potential by 0.059/2 V, i.e., approximately 30 mV. Hence a 10-fold increase in e.g. $p\text{H}_2$ would increase the open circuit voltage of a fuel cell by merely 30 mV. On the other hand, a steam electrolyser could produce directly hydrogen at e.g. 100 bar at merely 60 mV extra voltage. This is hence typical of 2-electron reactions at room temperature. 1-electron reactions change for the same reason approximately by 60 mV per decade change in reactant or product activities. Obviously, temperatures other than room temperature change both the standard voltage and the factor RT/F in front of the logarithm of the activity coefficient.

2.4.5 Exercises in thermodynamics of electrochemical reactions

1. Review the definition of electrochemical potential of a given species.
2. Review the relationships between the units for gas pressure: Pa, bar, atm, torr. Which is the SI unit? What is the standard state for gases? What is meant by an ideal gas? When are gases ideal and when are they not?

3. The reaction $H_2(g) + ½ O_2(g) = H_2O(l)$ often utilised in fuel cells has $U^0 = 1.23$ V at room temperature. Write the Nernst equation for the reaction, and use it to calculate what the cell voltage is if it is operated with 1 atm $H_2(g)$ and 1 atm air.
4. For the same reaction as in the previous exercise, use the Nernst equation to estimate (or calculate if necessary) how much the cell voltage would increase if it was operated with 10 atm of $H_2(g)$ instead of 1 atm.

2.5 Electrochemical cells

2.5.1 Open circuit voltage (OCV) and overpotential losses

Till now we have dealt with the Nernst voltage of electrochemical cells. This is the voltage thermodynamics tells us we will get from a discharging battery or a fuel cell, or the voltage we need to supply to charge a battery or run an electrolyser. But it will only be the Nernst voltage as long as there is no current; The Nernst voltage is therefore also called the open circuit voltage (OCV). All devices where current is running will have losses in the form of transport and reactions happening at finite rates, giving rise to what we observe as resistance R and, when current flow through those resistances, overvoltages η. By tradition, overvoltages are most often referred to as overpotentials, and we shall in the following also do that for the most part, but the two terms mean the same. The current I through the device and the resistance and overpotential of a process step s are in a first approach naturally related through ohm's law: $\eta_s = I R_s$. The resistance can be constant (a linear property), as it is for the electrolyte ion transport resistance, or it can vary with current, as it may do for the electrochemical redox-processes at the electrodes (a typical non-linear property).

The power dissipated over any resistance is the product of the voltage and the current, i.e., $P_s = \eta_s I$ for overpotential power losses in the cell, and $P_{external} = U_{cell} I$ for the power delivered or supplied over the external load. This means that each power term is proportional to the square of the current: $P_s = R_s I^2$ and $P_{external} = R_{load} I^2$, so losses increase and efficiencies decrease strongly with the current.

In the simplest case, the voltages in the circuit following the direction of the current must sum up to zero:

$$U_N + \eta_{electrolyte} + \eta_{anode} + \eta_{cathode} + U_{cell} = 0$$

Eq. 84

The external voltage U_{cell} is the voltage over the load to a battery or fuel cell, or the voltage applied by a charger to a battery or a power source to an electrolyser.

Figure 2-12 shows example situations. Firstly, note that the Nernst potential arbitrarily is placed on one of the half-cell electrodes. Overpotentials are drawn as gradients in potential at each electrode and in the electrolyte. In the fuel cell the current runs from the O_2 electrode to the H_2 electrode in the external load, while the ionic current flows from the H_2 side to the O_2 side in the electrolyte. In the electrolyser, the currents flow the opposite way. The most important thing to note is that the overpotentials in the case of the fuel cell act opposite and have opposite signs of the Nernst potential, such that the cell provides a smaller cell voltage than predicted thermodynamically. In the electrolyser cell the overpotentials act the same way

as the Nernst potential such that one must apply a higher potential than predicted thermodynamically.

One may note that the definition by Eq. 84 makes the cell voltage have the opposite sign of the Nernst voltage. If one chooses to always operate with positive Nernst and cell voltages for fuel cells and electrolysers, one may use another summation:

$$U_N + \eta_{electrolyte} + \eta_{anode} + \eta_{cathode} = U_{cell}$$

Eq. 85

This is used in the current-voltage plots in Figure 2-12.

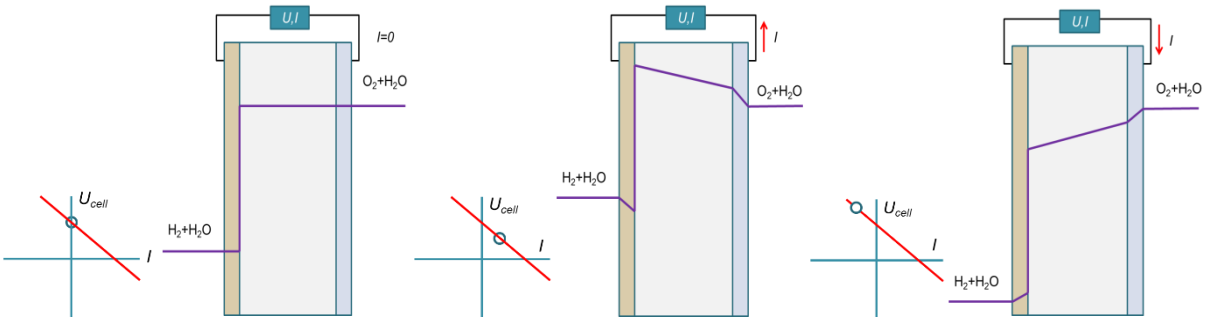

Figure 2-12. Schematic electrochemical cell with electrodes in wet hydrogen gas and wet oxygen gas. Nernst potential arbitrarily placed at the hydrogen electrode. Cell voltage measured at oxygen electrode. Left: *I*=0, Open circuit voltage, no overpotentials. Cell voltage equals Nernst voltage. Middle: *I* > 0, fuel cell operation. Overpotentials are negative and decrease the cell output voltage. Right: *I* < 0, electrolyser operation. Overpotentials are positive and increase the applied cell voltage.

2.5.2 Ionic conductivity and electrolyte ohmic (IR) overpotential losses

Ionic conductivity in the solid state facilitates solid-state electrochemistry and must in general be as high as possible. Inversely, the resistance to ionic transport gives rise to an overpotential in the electrolyte. This resistance is often called R_i, and the overpotential $\eta_{electrolyte} = I\,R_i$ is often referred to simply as the IR loss. It is an ohmic type of loss, i.e., the resistance is constant, independent of the current. It is therefore also often referred to simply as the ohmic loss.

The ionic resistance R_i is inversely proportional to the ionic conductivity σ_i. It furthermore scales with the area A and thickness d of the electrolyte:

$$R_i = \frac{d}{A}\frac{1}{\sigma_i}$$

Eq. 86

The resistance has units of ohm (or Ω) and the conductivity has units of S/m or, more commonly, S/cm. We are often interested in area specific properties, and the area specific resistance (*ASR*) is

$$ASR = R \cdot A = \frac{d}{\sigma}$$

Eq. 87

and has units of ohm m^2 or more commonly ohm cm^2.

The partial electrical conductivity of a charged species s, σ_s, can be expressed as the product of charge, $z_s e$ (unit C) or $z_s F$ (C/mol), volume concentration of charge carriers c_s (1/cm^3 or mol/cm^3) and the charge mobility u_s (cm^2/sV):

$$\sigma_s = z_s e c_s u_s = z_s F c_s u_s$$

Eq. 88

It is important to realize that only volume concentrations can enter in these formulae. Concentrations like site fractions or formula fractions typically used in solid state ionics must be converted to volume concentrations by multiplying by the site or molar density.

A number of solid-state inorganic electrolytes are under development, yet with limited commercial impact compared with liquid molten salt, ionic liquids, or aqueous ones. The main interest is related to transport of protons and oxide ions (for fuel cells and electrolysers) and Li ions (for batteries). In these, the conductivity relies on defects (vacancies or interstitials) in the crystalline lattice, and an activated process of diffusion of the defect (or of the ion via the defect). A high concentration of defects is usually obtained by doping with an appropriate charged dopant (acceptor or donor). However, a high mobility in the solid state requires an elevated temperature, in order to overcome the binding energy of the ion to the lattice or interstitial position. Solid-state conductivities thus vary much with temperature, from decent levels of around 0.01 S/cm for oxide ions in Y-substituted ZrO_2 (YSZ) at temperatures around 600°C or protons in CsH_2PO_4 at 250 °C, both relevant for fuel cells, to below 10^{-4} S/cm for solid-state Li ion conductors like $LiAlO_2$ or $La_{1-x-y}Li_yTiO_3$ at ambient temperatures relevant for Li-ion batteries.

What are the consequences of various conductivities? Most electrochemical devices for energy conversion or storage operate with current densities of the order of 1 A/cm^2. With around 1 V of Nernst and output voltage, this means around 1 W/cm^2 of power density converted. If the electrolyte has a high conductivity of 1 S/cm and a thickness of 1 mm (0.1 cm), Eq. 87 tells us that we get an *ASR* of 0.1 ohm cm^2, i.e., a voltage loss of 0.1 V over the electrolyte. This is 10% of a Nernst voltage of around 1 V, a severe loss of energy (and money!) and a considerable source of heating the device – and only for the electrolyte part of the losses!

For this reason, we strive to make electrolytes thinner, typically 100 μm, whereby the loss is only 0.01 V, or 1%, intuitively much more acceptable. With a smaller conductivity of, say, 0.1 S/cm, we must correspondingly have 100 and 10 μm thickness for, respectively, 10 and 1% loss. It is possible to conceive use of 0.01 S/cm in conductivity with electrolyte films of 1-10 μm, but it is difficult to make cheap reliable films in large areas in this thickness range.

So how do we circumvent this if we want or need to use electrolytes with conductivities of 10^{-3} S/cm or below? If we are aiming for a certain total power, we can of course simply increase the area of the cell, and run a fraction of the current density. A 10 times larger cell can operate at 1/10 of the current density, hence with 1/10 of the loss, and still give the same total power output. The problem is that the cost of manufacturing the cell will expectedly be 10 times higher, and so will the weight and footprint.

In batteries, particular developments go in the direction of thinner electrolytes and larger areas by wrapping up many thin layers of cell and/or corrugating each layer to add to the area.

From batteries, we also learn that voltage is better than current when it comes to increasing cell efficiency: A Li ion battery operates with Nernst voltages around 4 V, a fuel cell only 1 V. With the same electrolyte conductivity and thickness and the same current density, the losses in terms of voltage are the same, but the loss makes up only ¼ in the battery compared to what it does in the fuel cell. Hence: Increase the voltage if you can! But keep in mind that high voltages can induce high chemical activity gradients and unwanted electronic conduction in the electrolyte and electrochemical decomposition of the electrolyte itself.

2.5.3 Electrode kinetics

Now we will look at the origins of overpotentials at the electrodes. Let us consider a very simple solid-state reaction in which a hydrogen atom dissolved in or adsorbed on a nickel anode oxidises to a proton, like in Eq. 3. Figure 2-13 shows schematically an example of the potential Gibbs energies of reactants and products through the electrochemical reaction. The reactants diffuse in or on a solid crystalline electrode towards the interface to the electrolyte, where their energy becomes intolerably high. Instead, the products (in our example a proton and an electron) take on a more favourable energy if the proton moves into the electrolyte and the electron stays behind in the metal electrode. One may note that it appears like the x-axis represents a distance that species travel in passing the electrode interface, and this may be an acceptable "picture", but it is strictly a reaction coordinate. For instance, the electron may not take the same route as the ions.

The example could equally well be a Li atom diffusing in the graphite lattice anode of a battery, releasing an electron to the graphite electrode as it becomes a Li^+ ion in the electrolyte. Or it could reflect an oxygen atom diffusing on the surface of a fuel cell cathode, taking up two electrons as it meets the interface to the electrolyte and becomes an oxide ion.

Importantly, at the coordinate in time and space where the reaction occurs – the transition state – both the reactants and products are unfavourable, we get an extra energy barrier both forward (f) and backward (b) for forming the transition state.

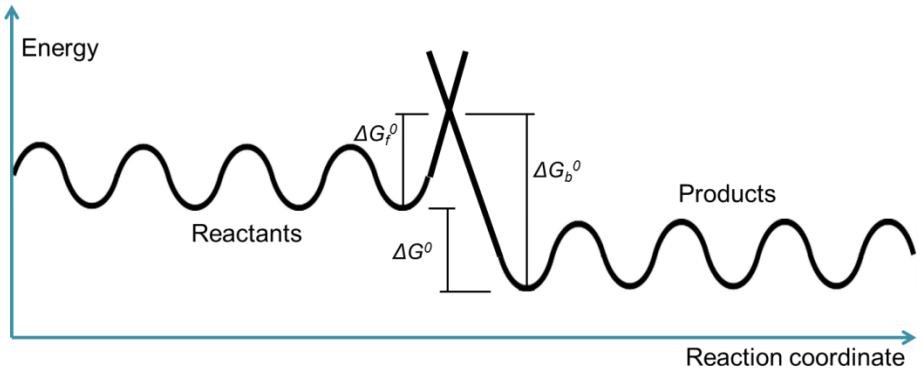

Figure 2-13. Potential Gibbs energy vs reaction coordinate (RC) for a reaction, illustrating diffusional transport to and from the reaction site, forward and backward standard Gibbs energy barriers to the transition state, and the standard Gibbs energy change of the reaction.

In the example in Figure 2-13, the products have a lower energy than the reactants, so there is a negative standard Gibbs energy change for the reaction and a positive half-cell voltage if it is a cathode (takes electrons) and negative if it is an anode (leaves electrons).

So far, this description would hold for any chemical reaction. We would have no means of affecting it. But in electrochemistry, we do. We can change the electrical potential of the electrode and thereby the electrochemical potential and Gibbs energy of the electron, and, in turn, the Gibbs energy change of the electrochemical reaction.

The forward reaction can be a general reduction, $Ox^z + ne^- = Red^{z-n}$, or an oxidation $Red^{z-n} = Ox^z + ne^-$. We will use the latter onwards and let Figure 2-13 illustrate an energy diagram of the proceeding reaction as it goes from left (reactants, reduced species) to right (products, oxidised species and electrons).

If a positive voltage is applied to the electrode (right hand side of the reaction coordinate) vs the electrolyte, the energy of the product electrons will decrease by an amount proportional to the voltage difference and the charge nF. The energy at the activated transition state also decreases, but since it is only halfway to the new location, only by half. If the transition state is not halfway, but a fraction β from the stable product position, the transition state changes by a factor (1- β). In this sense, β expresses the symmetry of the activation barrier. In the absence of information of β we commonly take it to be 0.5 (symmetrical barrier).

Now, let us consider the reaction rates, with the goal of eventually being able to express the current density that runs through an electrode as a function of the applied potential, often called the Butler-Volmer (BV) equation. In our example, the forward direction is an anodic (oxidation) reaction, and in the absence of an electrical potential, the forward (anodic) rate is simply proportional to the activity of reactants – reduced species – and is given by

$$r_a = k_a a_R = k_{a,0} a_R \exp\left(\frac{-\Delta G_a^0}{RT}\right),$$

Eq. 89

where r is the specific rate, k is the rate constant and k_0 is the pre-exponential of the rate constant, also called the frequency factor, since it contains the attempt frequency. The exponential term states the probability that the reactant(s) in the standard state have the required thermal energy to overcome the standard Gibbs energy barrier in the forward reaction.

The rate can be specific with respect to a volume, an area (of electrode or surface), or a length (e.g. of triple phase boundary), and hence have units of $cm^{-3}s^{-1}$, $cm^{-2}s^{-1}$, or $cm^{-1}s^{-1}$ or of $mol \cdot cm^{-3}s^{-1}$, $mol \cdot cm^{-2}s^{-1}$, or $mol \cdot cm^{-1}s^{-1}$. Since activities are unit-less, the rate constant and pre-exponentials correspondingly must have the same units as the specific rate itself. For electrodes we will here consider area specific rates in $mol \cdot cm^{-2}s^{-1}$.

One commonly converts activities into concentrations assuming ideal conditions where $a_i = c_i/c_{i,0}$ and that standard concentrations $c_{i,0}$ are unity (e.g. 1 M for aqueous solutions, 1 bar for gases, unity surface coverage for adsorbed species, or unity site fractions for species in

crystalline lattices). However, this would change the units of the rate constants, and we will here stay with activities for now.

The use of activities means that we express the statistical chance of having a reacting species in place for the reaction, as compared with that of the standard state, where the activity is one and the concentration the same as that in the standard state.

The backward (cathodic) rate is correspondingly

$$r_c = k_c a_O = k_{c,0} a_O \exp\left(\frac{-\Delta G_c^0}{RT}\right)$$

Eq. 90

We may note that both the forward (anodic) and backward (cathodic) rates are positive at all times, but they may be of different magnitude based on the balance between the activities of the reactants and the standard barrier height in that direction. At equilibrium, however, the rates are equal, so that the net rate is zero: $r = r_a - r_c = 0$ and $r_a = r_c$:

$$r_a = r_c \Rightarrow k_{a,0} a_R \exp\left(\frac{-\Delta G_a^0}{RT}\right) = k_{c,0} a_O \exp\left(\frac{-\Delta G_c^0}{RT}\right) \Rightarrow$$
$$\frac{a_O}{a_R}\frac{k_{c,0}}{k_{a,0}} = \exp\left(\frac{-(\Delta G_a^0 - \Delta G_c^0)}{RT}\right) = \exp\left(\frac{-\Delta G^0}{RT}\right) = K$$

Eq. 91

This connects the activities of reactants and products of the overall reaction at equilibrium with the standard Gibbs energy change, i.e., with the equilibrium coefficient *K*. Equilibrium is achieved when the ratio between the activities of the products and reactants counteracts the heights of the activation barriers for the two. It shows that equilibrium is a result of the difference in activation heights in the forward and backward (or anodic and cathodic) directions, but that the height of the barrier itself is irrelevant for the equilibrium. It also shows that our normal concept of an equilibrium coefficient related to the quotient of products over reactants contains the ratio of pre-exponentials of the rate constants (frequency factors). We may not be able to distinguish this ratio experimentally, and then tacitly take it to be unity.

Now, let us do the same for our electrode reaction, allowing us to apply and monitor a voltage $U = U_2 - U_1$ over the electrode. According to what we learned earlier, the energy change gets an electrical additional term, which affects the anodic and cathodic rates as follows:

$$r_a = k_a a_R = k_{a,0} a_R \exp\left(\frac{-(\Delta G_a^0 - (1-\beta)nFU)}{RT}\right)$$

Eq. 92

$$r_c = k_c a_O = k_{c,0} a_O \exp\left(\frac{-(\Delta G_c^0 + \beta nFU)}{RT}\right)$$

Eq. 93

and we can express the net reaction rate *r* as:

$$r = r_a - r_c = k_{a,0} a_R \exp\left(\frac{-(\Delta G_a^0 - (1-\beta)nFU)}{RT}\right) - k_{c,0} a_O \exp\left(\frac{-(\Delta G_c^0 + \beta nFU)}{RT}\right)$$

Eq. 94

At equilibrium,

$$r_a = r_c \Rightarrow k_a a_{R,e} = k_c a_{O,e}$$

Eq. 95

and if we have standard conditions, $a_{R,e} = a_{O,e} = 1$, there will be a certain cell voltage – the **standard voltage U^0** – that maintains the equilibrium. In this situation, we have standard equilibrium rate constants which also must be equal in order to get equal rates with standard activities: $k_a^0 = k_c^0 = k^0$, so that

$$k_a^0 = k_{a,0} \exp\left(\frac{-(\Delta G_a^0 - (1-\beta)nFU^0)}{RT}\right) = k_c^0 = k_{c,0} \exp\left(\frac{-(\Delta G_c^0 + \beta nFU^0)}{RT}\right) = k^0$$

Eq. 96

The **equilibrium standard rate constant k^0** is a useful quantity as it tells us how fast the reaction proceeds at equilibrium – forwards and backwards – under standard conditions.

At conditions different from standard conditions, corresponding to equilibrium activities $a_{R,e}$ and $a_{O,e}$, the open circuit voltage (OCV), U_{eq}, will be different from the standard voltage. The net current will be zero, $i = 0$ and $i_a = -i_c = \boldsymbol{i_0}$**, the exchange current density**. It may be derived that this is given by:

$$i_0 = nFk^0 a_{R,e} \exp\left(\frac{(1-\beta)nF(U_{eq} - U^0)}{RT}\right) = nFk^0 a_{O,e} \exp\left(\frac{-\beta nF(U_{eq} - U^0)}{RT}\right)$$

Eq. 97

This expresses how fast forward and backward the reaction goes in terms of current density at equilibrium, i.e. at the open circuit half-cell voltage (OCV) where there is no net external current.

By using the Nernst equation for the oxidation reaction, we can transform this to

$$i_0 = nFk^0 a_{R,e} \exp\left((1-\beta)\ln Q\right) = nFk^0 a_{O,e} \exp\left(-\beta \ln Q\right)$$

Eq. 98

which for $\beta = ½$ is

$$i_0 = nFk^0 a_{R,e} Q^{1/2} = nFk^0 a_{O,e} \frac{1}{Q^{1/2}}$$

Eq. 99

$$i_0 = nFk^0 a_{R,e} \left(\frac{a_{O,e}}{a_{R,e}}\right)^{1/2} = nFk^0 a_{O,e} \left(\frac{a_{R,e}}{a_{O,e}}\right)^{1/2} = nFk^0 (a_{O,e} a_{R,e})^{1/2}$$

Eq. 100

We notice that i_0 is proportional to the square root of the activities of both reactants and products. This reflects that the exchange current density involves reactions in both directions, even if we happened to describe it as an oxidation reaction.

As we shall soon, the charge transfer resistance R_{ct} which we can measure electrically is inversely proportional to i_0, and through these the above relationships we can use the dependence of the resistance on the activities of reactants and products to verify or discard a particular charge transfer reaction for the electrode.

Now we move on to express non-zero net current densities by changing the voltage from the open circuit equilibrium voltage. We define the overvoltage (or overpotential) $\eta = U - U_{eq}$ and it can be shown that the net current density is:

$$i = i_a + i_c = i_0 \left\{ \frac{a_R}{a_{R,e}} \exp\left(\frac{(1-\beta)nF\eta}{RT} \right) - \frac{a_O}{a_{O,e}} \exp\left(\frac{-\beta nF\eta}{RT} \right) \right\}$$

Eq. 101

If the activities of reduced and oxidised species can be assumed to remain at the equilibrium values, it simplifies into the commonly known form of the ***Butler-Volmer (BV) equation:***

$$i = i_a + i_c = i_0 \left\{ \exp\left(\frac{(1-\beta)nF\eta}{RT} \right) - \exp\left(\frac{-\beta nF\eta}{RT} \right) \right\}$$

Eq. 102

While we have dealt with the equations above in terms of current density (e.g. A/cm^2), they are easily transformed to current (A) by multiplication with the area of the electrode (or any other geometrical unit depending on how current density was defined).

Figure 2-14 shows a schematic example of the net current including anodic and cathodic components as a function of the overpotential.

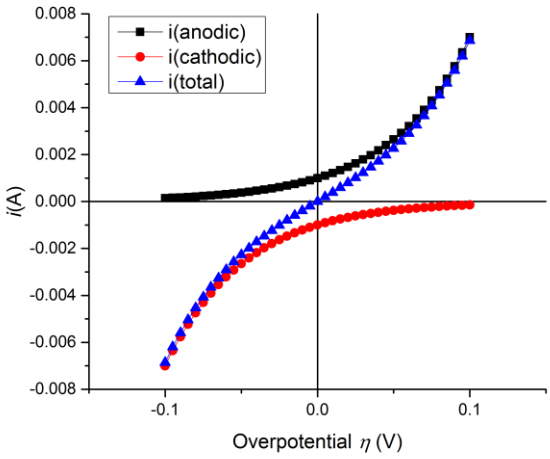

Figure 2-14. Plot of current vs overpotential, showing the anodic and cathodic components. i_0 = 0.001 A, β = 0.5, T = 299.15, n = 1.

The relationship between current density and overpotential can be simplified in certain regimes of assumptions:

For ***small overpotentials*** ($|\eta| << RT/\beta nF$), we can linearise the BV equation. From Taylor series expansion we have $e^{x} \xrightarrow{x\to 0} 1+x$ and $e^{-x} \xrightarrow{x\to 0} 1-x$. Inserting this yields

$$i \xrightarrow{\eta\to 0} i_0\left\{1+\frac{(1-\beta)nF\eta}{RT}-(1-\frac{\beta nF\eta}{RT})\right\}=i_0\frac{nF\eta}{RT}$$

Eq. 103

We note that the symmetry factor β became eliminated in the linearization. We now have the linear part of the current density, it is represented by the linear part of the total current at overpotential close to zero in Figure 2-14. The slope of overpotential over current yields the **charge transfer resistance**, $\boldsymbol{R_{ct}}$, and the overpotential over the current density yields the **charge transfer area-specific resistance (*ASR*), $\boldsymbol{R_{ct\,ASR}}$**:

$$R_{\text{ct ASR}}=\frac{\eta}{i}=\frac{RT}{i_0 nF}$$

Eq. 104

The charge transfer area-specific current density – like the exchange current density – says something about the kinetics of the half-cell reaction at equilibrium and open circuit conditions, for a given set of activities of reduced and oxidised species. We may recall that another parameter that represented the kinetics of the reaction at equilibrium – the equilibrium standard rate constant k^0 – on the other hand did so under standard conditions.

By small overpotentials we mean $|\eta| << 2RT/nF$. Insertion of n = 1 and room temperature (T = 298 K) yields $2RT/nF$ = 50 mV, suggesting that overpotentials should stay well below this to remain in the linear region. The limit is proportional to the absolute temperature, while it halves for two-electron processes (n=2). At room temperature one thus often see voltages of 5-20 mV applied in impedance spectroscopy or voltammetry to find R_{ct} or i_0, while in high temperature solid-state or molten salt electrochemistry one can increase this to e.g. 20-50 mV in order to get better signal-to-noise ratio while still being in the linear region.

We can measure R_{ct} or $R_{\text{ct ASR}}$ by voltammetry, AC impedance measurements, or impedance spectroscopy. Through the expression for i_0 (Eq. 100) we obtain:

$$\frac{1}{R_{\text{ct ASR}}}=\frac{i_0 nF}{RT}=\frac{(nF)^2 k^0}{RT}(a_{O,e}a_{R,e})^{1/2}$$

Eq. 105

More generally – still for the case of β = 0.5 – we will get

$$\frac{1}{R_{\text{ct ASR}}}=\frac{i_0 nF}{RT}=\frac{(nF)^2 k^0}{RT}(Q_O Q_R)^{1/2}$$

Eq. 106

where Q_{O} and Q_{R}, respectively, are the reaction quotients for the oxidised and reduced species taking part in the charge transfer.

By investigating $1/R_{ct}$ vs activities of potential reactants and products in the rate determining charge transfer step, we may through Eq. 110 verify whether the chosen model may be correct or not. For instance, a solid-state oxygen electrode might be assumed to have the following reaction steps:

$$O_2(g) + v_{ads} = O_{2\ ads} \quad | 1$$

$$O_{2\ ads} + v_{ads} = 2O_{ads} \quad | 1$$

$$\underline{O_{ads} + v_O + 2e^- = O^{2-} + v_{ads} \quad | 2}$$

$$O_2(g) + 2v_O + 4e^- = 2O^{2-}$$

Eq. 107

The two first steps represent surface adsorption and dissociation, while the third step is the charge transfer. By using Eq. 110, we obtain

$$\frac{1}{R_{ct\ ASR}} = \frac{i_0 2F}{RT} = \frac{(2F)^2 k^0}{RT}(a_{O_{ads}} a_{v_O} a_{O^{2-}} a_{v_{ads}})^{1/2}$$

Eq. 108

From Eq. 111 we may predict that for small coverages, the activity of O_{ads} on the electrode surface is proportional to $pO_2^{1/2}$, while the activity of empty adsorption sites v_{ads} is constant close to unity, and $1/R_{ct}$ will then be proportional to $pO_2^{1/4}$, according to Eq. 112, which would confirm that the assumption may be correct. At higher pO_2 and lower temperatures, the surface may become saturated with O_{ads}, and in this case it would be the available adsorption sites that would become limiting, and we would expect a $pO_2^{-1/4}$ dependency for $1/R_{ct}$. Intermediate dependencies could mean that one has a transition between the two, while constant independency of pO_2 or dependencies larger in magnitude than $pO_{2\pm1/4}$ would mean that the rate limiting step of the charge transfer is another than assumed.

For **large overpotentials**, either the anodic or the cathodic component will dominate and the other vanish. For large anodic overpotentials, $\eta >> RT/nF$:

$$i = i_a = i_0 \exp\left(\frac{(1-\beta)nF\eta}{RT}\right) \quad \Rightarrow \quad \ln|i| = \ln|i_a| = \ln i_0 + \frac{(1-\beta)nF}{RT}\eta$$

Eq. 109

For large cathodic overpotentials, $-\eta >> RT/nF$:

$$i = i_c = -i_0 \exp\left(\frac{-\beta nF\eta}{RT}\right) \quad \Rightarrow \quad \ln|i| = \ln|i_c| = \ln i_0 - \frac{\beta nF}{RT}\eta$$

Eq. 110

Figure 2-15 shows plots of these equations – so-called Tafel plots. Linear fits to the Tafel region part of the curves yield $\ln i_0$ (or $\log i_0$) as the intercepts at $\eta = 0$, while the slopes yield $(1-\beta)nF/RT$ and $-\beta nF/RT$, respectively, for the anodic and cathodic parts. If n is known, one may find β, or – assuming a value for β – one may determine n, the number of electrons involved in the charge transfer.

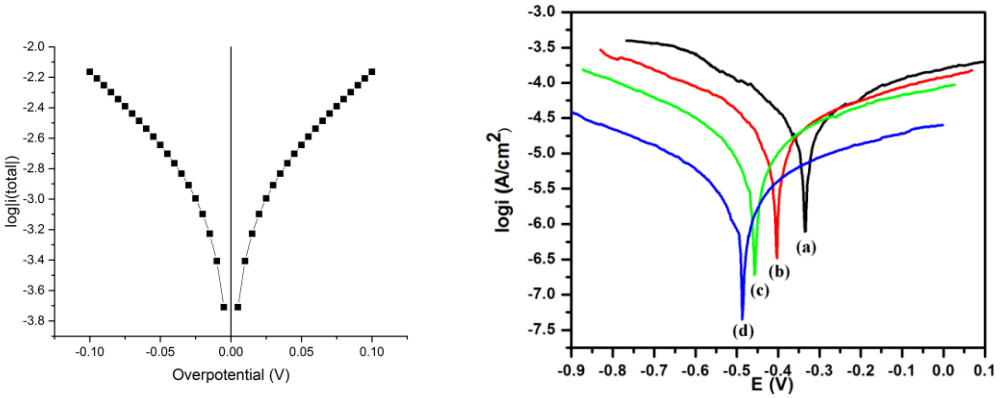

Figure 2-15. Tafel plots. Left: Schematic plot of log|*i*(total)| vs overpotential, using the same data as in Figure 2-14. Note that the linear regions extrapolate back to i_0 (0.001 A in this case). Right: Tafel plot for an electrode with different concentrations of the redox couple. Note that i_0 changes, and that the x-axis here shows electrode voltage, and that the open circuit voltage changes, giving the overpotential different starting points for each curve. Also, the slopes are different between the anodic and cathodic directions, suggesting that the barrier mat be asymmetric and β hence different from 0.5.

A third limiting case arises when the concentrations of reactants and/or products change a lot at the electrode, most commonly as a result of mass transport limitations.

2.5.4 Exercise – Losses in electrochemical cells

1. A fuel cell has a Nernst voltage of 1.1 V. It has an electrolyte with conductivity of $5x10^{-3}$ S/cm and a thickness of 20 µm. It has an electrode area of 10x10 cm^2. We draw 1 A/cm^2 from the cell. What is the total current? What is the ASR (excluding other losses than from the electrolyte)? What is the output voltage? What is the electrical power output? What is the electrical efficiency of the fuel cell?

3 Solid-oxide fuel cells and electrolysers

3.1.1 General aspects

A fuel cell is a galvanic cell in which the chemicals (fuel and oxidant) are continuously supplied to the electrodes, and products are continuously let out.

The fuel can be of fossil origin or come from renewable energy. With fossil origin we think primarily of gases produced from natural gas, oil, or coal. They comprise hydrogen, CO, methane or propane, methanol, gasoline or diesel, or mixtures such as syngas or coal gas (both mainly H_2 + CO). Fuels from renewables comprise primarily hydrogen, but also a number of what we may call hydrogen carriers; methanol, ammonia, etc. Recently, focus has been put on biofuels (alcohols, bio-diesel, etc.) from organic harvest of sunlight.

Fuel cells offer potential advantages in efficiency and environment-friendly operation for all types of fuels. The choice of fuel has nevertheless influence on which type of fuel cell it is most reasonable to use.

All fuel cells can use hydrogen as fuel, but hydrogen is not straightforward to store and transport, and there is thus a desire to use other fuels for many applications. As a general rule, the higher the operating temperature of the fuel cell, the better the cell tolerates non-hydrogen elements of the fuel. CO and many other compounds poison electrodes at low temperatures, so that organic fuels, that often contain traces of CO or form CO as intermediate combustion product, for the most part is excluded from use with low temperature fuel cells. Some poisons such as sulphur affect also high temperature cells, but the tolerance level generally gets higher the higher the temperature. Direct use of kinetically inert molecules such as CH_4 can only be imagined in high temperature cells. Water soluble fuels such as methanol can be used below 100 °C because they can then be supplied in an aqueous phase. Fossil fuels, forming the acidic product CO_2, cannot be used in alkaline fuel cells because CO_2 will react with the electrolyte. Conversely, ammonia, which is a basic gas, cannot be used in phosphoric acid fuel cells or other fuel cells with an acidic electrolyte.

The discovery of the fuel cell has been attributed to Sir William Grove, who filled small containers with hydrogen and oxygen and used sulphuric acid as electrolyte and platinum for electrodes. He described that when he connected several such cells in series, the voltage of the end terminals became increasingly painful to touch. He also showed that a number of such cells connected to two electrodes standing in sulphuric acid led to the production of hydrogen and oxygen over those two electrodes (electrolysis) (see figure below). Grove published his findings in 1839 – thus usually considered the year of the discovery of the fuel cell.

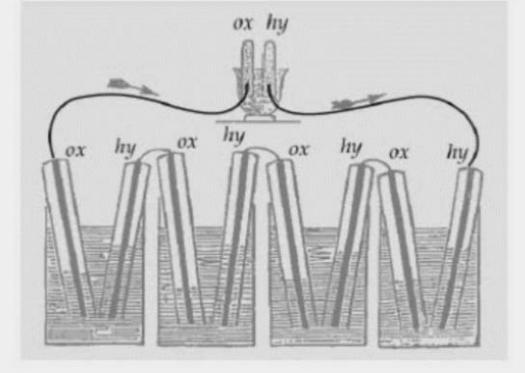

Figure 3-1. Grove's illustration of his fuel cell, consisting of four individual cells in series, each supplied with H_2 and O_2, using Pt for electrodes and sulphuric acid as proton conducting electrolyte, and using the electrical power to drive the reverse reaction – to electrolyse sulphuric acid.

3.1.1.1 General principle of operation and requirements of materials for fuel cells

A fuel cell consists of 4 central elements: Electrolyte, anode, cathode, and the interconnect that connects stacked cells. Each element has individual tasks and requirements.

The electrolyte must be an ionic conductor, being able to transport ions of fuel or oxidant elements to the opposite side. The ionic transport number (fraction of the total conductivity) should be above 0.99 to limit the loss due to short circuit by electronic conductivity. The electrolyte moreover has to be very redox-stable, i.e. withstand the oxidising conditions of the oxidant as well as the reducing conditions of the fuel. The electrolyte must furthermore not

react with the electrodes or have any degree of mutual solubility. If the electrolyte is solid, one must furthermore appreciate the chemical potential gradient it faces. This causes the fast ions to migrate, but it also puts a similar force on the stationary ions in the material; if the metal cations of a solid electrolyte have non-negligible mobilities, the whole electrolyte membrane may move. Thus, there is a requirement on small diffusivities for stationary components.

The cathode must be an electronic conductor to transport electrons from the electrochemical reaction site to the current collector. It should also be catalytic to the electron transfer and other reaction steps. The cathode stands in the oxidant and must tolerate oxidising conditions. For this reason, metals except the most noble ones such as Pt, Au, and Ag are excluded from use here. Instead one tends to use graphite at low temperatures and oxidic materials at higher temperatures. The cathode must not react with the electrolyte or with the interconnect (current collector). Finally, the cathode must be porous so as to allow the fuel medium to react the reaction site and the products to diffuse away.

The anode must similarly be an electronic conductor, stable under reducing conditions. In addition to noble metals, some additional metals may be stable here, like Ni and Cu. Like the cathode the anode must not react with the electrolyte and interconnect.

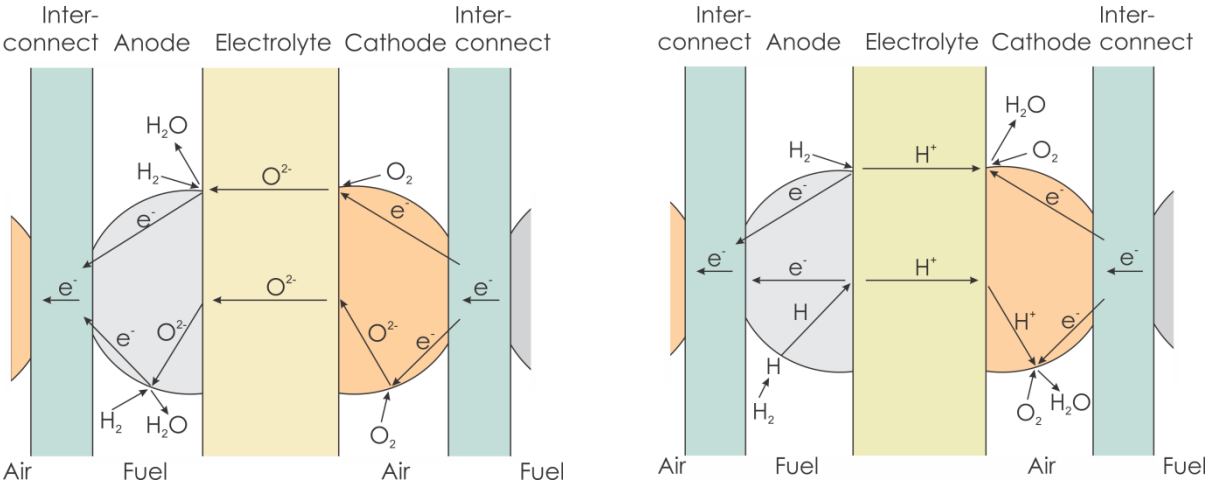

Figure 3-2. General principle of fuel cells with or O^{2-} (left) or H^{+} (right) conducting solid electrolytes, running H_2 as fuel vs O_2 (or air). For each cell is shown a schematic anode and cathode electrode grain. For each of these the electrode reaction on the top of the grain is the normal three-phase-boundary reaction, while the lower part depicts extended reaction possibilities if the electrode conducts also ions or is permeable to atomic species.

One cell is usually series connected to a next cell in order to increase the overall voltage. The material that makes this connection is called an interconnect or bipolar plate and is thus placed between one cathode and the next anode. It must thus be an electronic conductor, and in this case have no mixed conduction; any transport of ions will lead to chemical short-circuit; loss of fuel by permeation. The interconnect must obviously also not react with either of the electrodes it contacts. Moreover, the interconnect separates the oxidant of one cell from the fuel in the next. This requires that it is redox stable and gas tight (and as said above, also diffusion tight).

Especially in ceramic fuel cells, the thermal expansion coefficient must match between the various materials, or else delamination, bending, and cracking may result from start-ups, shutdowns, thermal cycling, and even load variations. This is hard, because ceramic materials usually have smaller expansion coefficients than metals. In addition to the thermal expansion, many materials also suffer from chemical expansion. One example is the swelling of polymers during water uptake. In ceramic cells, some materials similarly expand upon stoichiometry changes. Even metals may be affected: A metal serving as interconnect may for instance dissolve hydrogen and carbon at the fuel side, and dissolve oxygen or oxidise at the air side. This may lead to expansion, stresses and bending of the interconnect and eventually cracking of cells and stack.

3.1.1.2 Three-phase boundaries of electrodes and ways to expand them

Both anode and cathode are in principle rate limited by the length of the three-phase boundary, i.e. the place where electrons, ions, and reacting neutral species in gas or liquid phases can all meet. The width of the reaction zone can be increased by diffusion of adsorbed species on the surface of the electrode or electrolyte, as shown in two of the cases in Figure 3-3 (left) below.

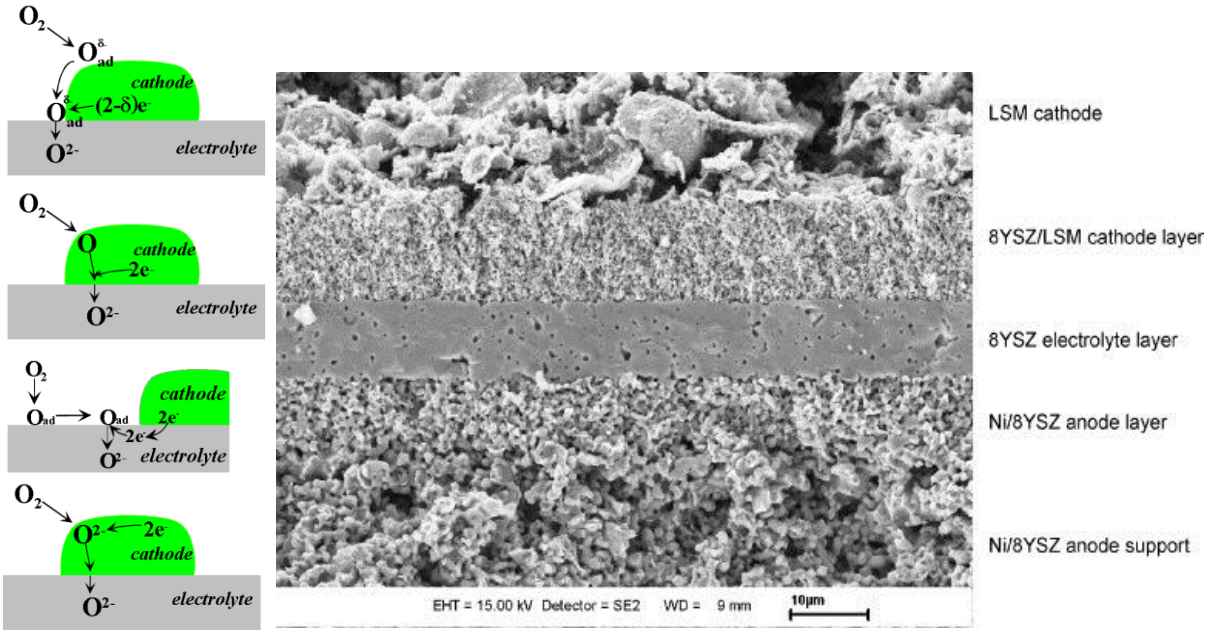

Figure 3-3. Left: Schematic showing four ways of expanding the reaction area from a pure three-phase boundary line in a solid oxide fuel cell cathode: Cathode surface diffusion of adsorbed oxide ions or atoms; cathode volume diffusion of oxygen atoms; electrolyte surface diffusion of oxygen atoms; mixed ionic-electronic conduction in the cathode. Right: Cross-section of real SOFC cell,[10] showing dense electrolyte and porous, composite electrode-electrolyte layers of cathode (top) and anode (bottom). Notice how the innermost composite layers are fine-grained to increase the number of triple-phase-boundaries, while the outermost layers are coarser to facilitate easier gas transport in the porosity.

Diffusion of reactant atoms or molecules in the volume of the electrode increases the reaction zone inwards under the electrode. Finally, one may apply electrode materials that are mixed ionic and electronic conductors. The two latter cases are also illustrated in the figure.

[10] T. Van Gestel, D. Sebold, H.P. Buchkremer, D. Stöver, *J. European Ceramic Society*, **32** [1] (2012) 9–26.

From being a one-dimensional three-phase boundary line, these extra transport paths make the reaction zone transform into an area.

3.1.1.3 Porous and composite electrodes

In order to further increase the number of reaction sites one usually makes the electrode in the form of a porous structure of the electron conductor in which a percolating ionically conducting network is embedded and the fuel or oxidant medium can flow. With liquid electrolytes, one lets the electrolyte and reactants penetrate a porous electrode. With solid electrolytes, one makes a porous composite of the electron and ion conductors. This composite must have three percolating phases: The pores, the electron conductor and the ion conductor (electrolyte).

In polymer fuel cells, these electrodes are called gas diffusion electrodes, made of a porous nano grained carbon-polymer composite.

In solid oxide fuel cell anodes, one uses a porous cermet – a porous mixture of electrolyte ceramic and Ni metal. For the cathode, one uses a porous ceramic-ceramic composite ("cercer") of the electrolyte and Sr-substituted $LaMnO_3$ (LSM), see Figure 3-3 (right).

The SOFC technology has for the most part based itself on yttrium stabilised (cubic) zirconia (YSZ) as oxide ion conducting electrolyte. The cathode is typically Sr-doped $LaMnO_3$ (lanthanum manganite) or similar perovskites. As anode, most often is used a cermet of nickel and YSZ. The cells operate typically at 700-1000 °C depending on the thickness of the electrolyte and quality of the electrodes.

The SOFC can, like other fuel cells run pure H_2 as fuel. Compared with the purely proton conducting fuel cell, the SOFC is characterised by forming water at the anode (fuel) side. The figure below shows an SOFC that uses CH_4 as fuel: CH_4 reacts (is reformed) with H_2O over the anode, whereby the H_2 is oxidised electrochemically to H_2O. This is used in its turn to reform more CH_4 and to shift CO to CO_2 + H_2. In practice we must add H_2O (steam) to the CH_4 *before* the cell, because we otherwise get too reducing conditions with too high carbon activities, giving sooting in the fuel inlet.

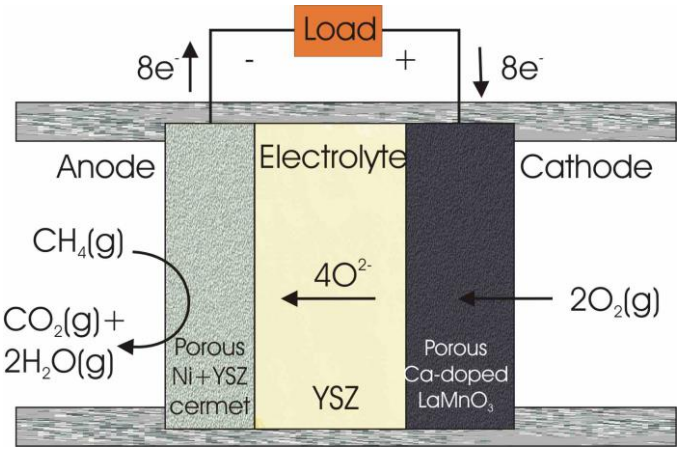

Figure 3-4. SOFC with methane as fuel and internal reforming over the anode.

SOFCs can in principle be used with all kinds of fossil fuels, because the fuel is reformed on its way to and over the anode. In reality, we have, as mentioned, some problems with sooting in the fuel inlets. Moreover, the reforming reaction is endothermic. This may cool the cells anode too much at the inlet and we may get cracks because of the thermal stresses. One may design the cell such that the cooling from the reforming just balances the heating from the ohmic losses, but one usually chooses to do the reforming in a separate reactor *before* the cell.

It has been speculated and tested whether one can oxidise the CH_4 molecule *directly* on the anode (without reforming). However, such a process from CH_4 to CO_2+$2H_2O$ is an 8-electron process – a very unlikely pathway. Thus, intermediate reforming and shift by the formed water and subsequent oxidation of H_2 and possibly CO is probably inevitably the reaction path in operation on an SOFC anode.

3.1.2 Materials for solid oxide fuel cells (SOFCs)

3.1.2.1 Oxide ion conductors

Already at the end of the 1800s, the German scientists Walther H. Nernst discovered that ZrO_2 with additions of other (lower-valent) metal oxides became well conducting at high temperatures. He developed the so-called Nernst-glower, in which a bar of Y-doped ZrO_2 was preheated and subjected to a voltage. The current through the material heated it further, making it even more conductive and ending up white-glowing. Edison's lamps based on coal and later tungsten needed vacuum or inert atmospheres in order not to burn, while Nernst's ZrO_2 was already an oxide stable in air and with very high melting point and hardly any evaporation. Nernst himself hardly realised the mechanism of conduction in ZrO_2 – only well into the 1900s did one begin to understand defects in crystalline solids and that the Nernst glower was based on lower-valent Y^{3+} ions in the ZrO_2 structure compensated by mobile oxygen vacancies. Later it was proposed that doped ZrO_2 could be used as a solid electrolyte in electrochemical energy conversion processes. Only in the last quarter of the 1900s did this begin to approach reality. Doped ZrO_2 has been and is still the dominating electrolyte in the development of solid oxide solid oxide fuel cells (SOFCs).

Undoped ZrO_2 is monoclinic. At higher temperature it expands and transforms into more symmetric tetragonal and cubic modifications (see figure). The cubic polymorph is the fluorite structure (named after fluorite, CaF_2). Lower-valent cations, like Ca^{2+} or Y^{3+} lead to charge compensation by oxygen vacancies. While the oxygen vacancies are smaller than oxide ions, the dopants are effectively larger than the Zr^{4+} ions they substitute, and the overall effect of the substitution is that the lattice expands. This stabilises the more symmetrical high temperature modifications so that 3 mol% Y_2O_3 may stabilise the tetragonal polymorph to room temperature (meta-stable), while 8-10 mol% Y_2O_3 or more can stabilise the cubic structure. The latter type of materials is abbreviated YSZ (yttria stabilized zirconia).

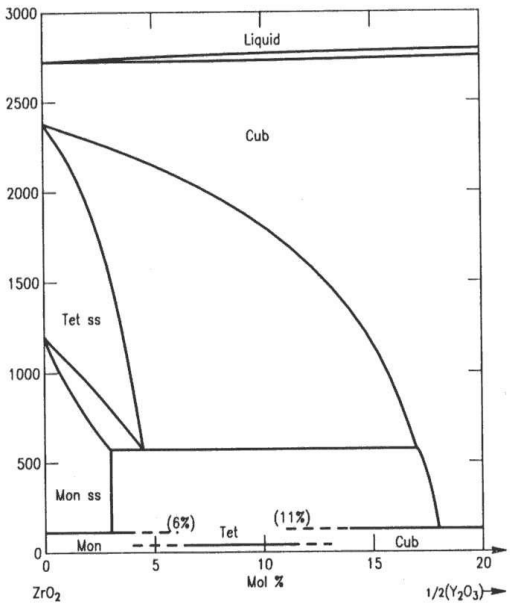

Figure 3-5. Sketch of temperature (°C) *vs* composition (mol% $YO_{1.5}$) in the ZrO_2-rich part of the ZrO_2-$YO_{1.5}$-phase diagram. ss=solid solution. Beneath a certain temperature equilibrium is in practice frozen out, and the lines near room temperature indicate the phase one gets. From Phase Diagrams for Ceramists (VI-6504), The American Ceramic Society.

The defect reaction of dissolution of Y_2O_3 in ZrO_2 can be written

$$Y_2O_3(s) = 2Y_{Zr}^{/} + v_O^{\bullet\bullet} + 3O_O^x$$

Eq. 111

and the concentration of vacancies is thus fixed by the concentration of yttrium substituents:

$$2[v_O^{\bullet\bullet}] = [Y_{Zr}^{/}] = \text{constant}$$

Eq. 112

The conductivity, given by the charge, concentration, and charge mobility, then becomes

$$\sigma_{v_O^{\bullet\bullet}} = 2e[v_O^{\bullet\bullet}]u_{v_O^{\bullet\bullet}} = e[Y_{Zr}^{/}]u_{0,v_O^{\bullet\bullet}}T^{-1}\exp\left(\frac{-\Delta H_{m,v_O^{\bullet\bullet}}}{RT}\right)$$

Eq. 113

At temperatures around 1000°C YSZ has sufficient mobility of oxygen vacancies and thereby sufficient oxide ion conductivity that we can make a working fuel cell with 100 μm thick YSZ electrolyte.

There has been considerable optimism around such cells; the high temperature enables use of fossil fuels and the heat loss is easy to heat exchange and utilise. One early on identified cathode ($LaMnO_3$-based) and anode (Ni+YSZ cermet) and the interconnect ($LaCrO_3$-based), which all had thermal expansion sufficiently similar to that of YSZ so that cells could be constructed and assembled. However, it has turned out that degradation is too fast at this temperature. The $LaCrO_3$ interconnect is expensive to buy and hard to machine. Thus, the operation temperature must be brought down so that the life time can be improved and we can

use a cheap and machineable metal as interconnect. The development of better electrolytes has therefore been going on continuously the last decades.

Firstly, one has been able to reduce the thickness of the electrolyte. Early, one used self-supported sheets of 100-200 μm thickness, made by tape-casting (in which ceramic powder is dispersed in a plastic medium, cast to a thin film on a glass plate by a doctor's blade, dried to a foil, and burned and sintered at high temperature). Today, typically 10 μm thick films supported on a porous substrate of anode or cathode material is used, so that we can have an order of magnitude lower conductivity and thus temperatures lowered to 7-800 °C.

One may in principle add more dopant to get more oxygen vacancies, but the conductivity goes through a maximum as a function of concentration. At higher concentrations, vacancy-vacancy and vacancy-dopant association becomes dominant, immobilising the vacancies. Moreover, vacancy ordering and superstructure formation set in. Computer simulations of the lattice may give insight into e.g. dopants with lower association to the vacancies. It turned out from such simulations that scandium, Sc^{3+}, should fit better in ZrO_2 than Y^{3+}, and thus give less association. Scandia-stabilised zirconia (ScSZ) was developed based on this, and has higher conductivity than YSZ by typically half an order of magnitude. The combination of thin films and use of ScSZ enables so-called intermediate temperature SOFC (ITSOFC) down towards 600°C.

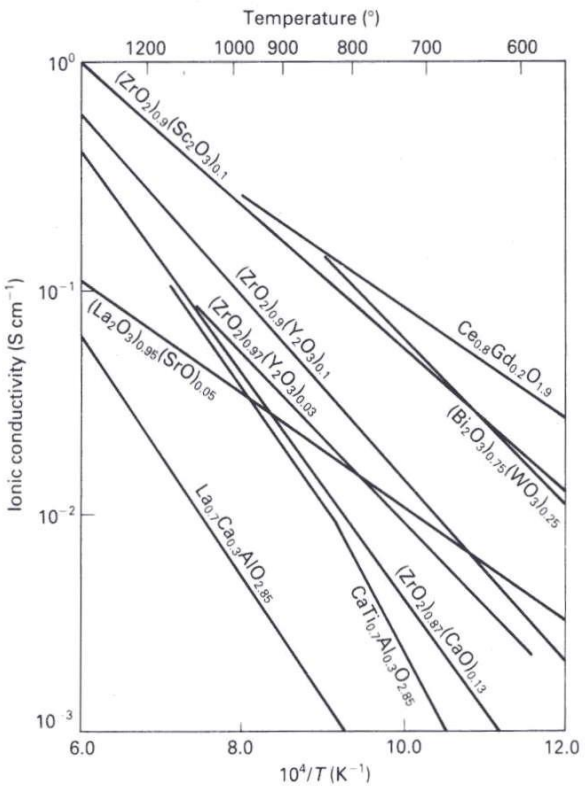

Figure 3-6. Conductivity of some oxide ion conductors. From P.G. Bruce: Solid State Electrochemistry.

A number of other oxides also exhibit high oxide ion conductivity. CeO_2 is similar to ZrO_2 and has higher ionic conductivity when acceptor doped, in this case optimally by Sm^{3+} or

Gd^{3+}. It can thus be used at lower temperatures. But it also has a higher tendency of reduction:

$$O_O^x = v_O^{\bullet\bullet} + 2e' + \tfrac{1}{2}O_2(g) \qquad K'_{red} = \left[v_O^{\bullet\bullet}\right] n^2 p_{O_2}^{1/2} \left[O_O^x\right]^{-1}$$

Eq. 114

and accordingly exhibit higher n-type electronic conductivity as well as some chemical expansion due to the extra oxygen vacancies.

Bismuth oxide, Bi_2O_3, has several structure polymorphs. One of these, δ-Bi_2O_3 has a cubic fluorite structure similar to ZrO_2. It lacks ¼ of the oxide ions, but without doping; it has inherent deficiency and disorder. It thus has a high oxide ion conductivity. However, the cubic, disordered polymorph is stable only over a limited temperature window and it reduces easily. It can thus not be used in fuel cells it seems, but has been employed in e.g. oxygen pumps for medical oxygen generators. The δ-Bi_2O_3 phase can be stabilised by certain dopants, such as WO_3 (see figure above).

New oxide ion conductors are continuously being discovered. After numerous attempts at the end of the 1990s one finally succeeded in making a good perovskite-structured oxide ion conductor based on $LaGaO_3$. A combination of Sr^{2+} and Mg^{2+} as acceptor-substituents for La^{3+} and Ga^{3+} was necessary to give mutually high solubility and a high concentration of oxygen vacancies. Sr+Mg-doped $LaGaO_3$ (LSGM) has higher conductivity than ZrO_2-based electrolytes at low temperature and are therefore promising, except for a problem with Ga evaporation under reducing conditions.

Among other new oxide ion conductors, we find materials based on $La_{10}Ge_6O_{27}$ and $La_2Mo_2O_9$, both with interstitial oxide ions as defects.

3.1.2.2 SOFC anodes

Only two non-noble metals are stable in typical fuel gas conditions; nickel (Ni) and copper (Cu). Nickel is the common choice for SOFC, because of its good catalytic properties for anode reactions involving hydrogen, and its mechanical stability at high temperatures. Ni is applied in a composite with the electrolyte, e.g. a Ni-YSZ cermet. This must be porous to allow gas access, and both the Ni and YSZ phases should percolate. It is often applied in a fine-grained microstructure close to the electrolyte (to optimise catalytic area) and in a coarser version towards the interconnect to optimise electronic conduction and current collection.

Nickel is applied during fabrication and sintering of the anode as NiO, which is subsequently reduced to Ni during the first operation when fuel is introduced.

Ni cermet anodes have the disadvantages that they are catalytic not only to the electrochemical reaction, but also to reforming

$$CH_4 + H_2O = CO + 3H_2$$

Eq. 115

This means that this endothermic reaction takes place quickly as soon as any unreformed fossil fuel and water meets at the anode inlet, and this part of the stack may get too cold. Internal reforming (by supplied water or by water from the anode reaction) may thus be

possible and advantageous to consume joule heat from the stack, but requires very difficult control of many parameters to avoid large temperature gradients and resulting cracks.

The other reaction which is catalysed by Ni is coking:

$$CH_4 = C(s) + 2H_2$$

Eq. 116

which takes place quickly unless counteracted by a supply of an oxidant, such as oxide ions or water from the anode, or steam in the fuel stream.

Finally, Ni has a problem in a cell which is running at too high current and anode overpotential: The oxygen activity may be too high, and Ni oxidises to NiO. This has a low electronic conductivity and the overpotential gets even higher, locking the cell (which may be only one detrimental cell in a whole stack) in an ”off” state.

The problems altogether with Ni anodes has led some to try to develop alternative anodes, especially to achieve direct introduction of fossil fuels, hoping to avoid coking and instead have direct oxidation on the anode, e.g.

$$CH_4 + 4O^{2-} = CO_2 + 2H_2O + 8e^-$$

Eq. 117

Formulations for such anodes are mainly either to replace Ni with Cu (troubled by Cu’s lower melting point and thus higher tendency to creep and sinter) or to have an oxide with high electronic conductivity. The latter can be achieved by donor-doping, for instance by substituting Sr^{2+} in $SrTiO_3$ with Y^{3+}, which is then compensated by conduction band electrons. Such materials do work, but are troubled by limiting electronic conductivity and catalytic activity.

3.1.2.3 SOFC cathodes

For cathodes, we cannot use any metals except the noble ones (Pt, Au, Ag). They are mainly considered too expensive. Silver, Ag, is thinkable, and it has a beneficial oxygen diffusivity that would spread out the reaction zone considerably. However, its melting point is close to the operating temperatures, and it has a considerable evaporation.

Thus, oxides is the common choice, and in particular La*M*O_3 perovskites where *M* is Mn, Fe or Co are much studied. We will here use $LaMnO_3$ as example. It has a favourable thermal expansion match with YSZ.

The first thing we need to do is to give it a high electronic conductivity. The material itself has a relatively low band gap such that the intrinsic formation of electrons $e^{/}$ and holes $h^{\cdot}$ is considerable. The states $e^{/}$ and $h^{\cdot}$ can be seen as representing Mn^{4+} and Mn^{2+}, respectively, in $LaMnO_3$ which otherwise nominally contains Mn^{3+}.

We use an acceptor dopant that will enhance the concentration of holes. A suitable dopant is Sr^{2+} substituting La^{3+} and the resulting electroneutrality becomes

$$[h^{\bullet}] = [Sr'_{La}] = \text{constant}$$

Eq. 118

We note that this oxide chooses to compensate the acceptors with holes instead of oxygen

vacancies (as in ZrO_2) – a result of the lower bandgap. The Sr-doped $LaMnO_3$ is abbreviated LSM or LSMO.

The lack of oxygen vacancies means LSMO has little mixed conduction and little spreading of the reaction three-phase boundary. Additions of Co and Fe on the B site increase the oxygen vacancy concentration and thus the reactive area and also the catalytic activity.

LSMO tends to form reaction layers of $La_2Zr_2O_7$ and $SrZrO_3$ in contact with YSZ. This is fortunately counteracted by stabilisation of the perovskite structure by the Sr dopants in LSMO. Despite these reactions, cathode performance is often increase by making porous ”cercer” composites of YSZ and LSMO.

3.1.2.4 SOFC interconnects

Finally, the SOFC interconnect presents a challenge. Early on it was common to use Sr-substituted $LaCrO_3$ (here called LSCrO). Its defect structure is much like that of LSMO, but LSCrO has a lower p-type conductivity – especially in hydrogen. Its essential advantage is that it is stable in hydrogen, contrary to LSMO. Problems of LSCrO comprise chemical expansion and some permeation due to mixed conduction from a certain concentration of oxygen vacancies.

As an alternative one can use metallic interconnects. These are alloys which form Cr_2O_3 on the surface during oxidation. This provides oxidation protection while being electronically conductive. The problem is that Fe-Cr super-alloys with sufficient Cr content to form a protective Cr_2O_3 layer at high temperature are very hard and difficult to machine and end up very expensive. There is thus a driving force to develop intermediate temperature ITSOFCs where normal chromia-forming stainless steels are protective enough. Temperatures of 600 °C or less are probably required.

Metallic interconnect have much higher electronic and thermal conductivity than ceramic ones, and give easier design of stacks and more robust stacks. However, the corrosion problem is always there, and in addition, evaporation of chromium in the form of gaseous Cr^{6+} oxohydroxides from the interconnect’s protective Cr_2O_3 layer to the cathode is detrimental – it settles as Cr_2O_3 and blocks the reactive sites. To avoid this, the alloy is often covered with a more stable Cr compound, like $LaCrO_3$ or a Cr spinel like $MnCr_2O_4$.

3.1.3 High temperature proton conducting electrolytes

Proton conducting hydrates, solid acids, and hydroxides may conduct by defects or disorder among their protons. However, they decompose at relatively low temperatures.

Oxides and other nominally water-free materials may still contain a certain concentration of protons in equilibrium with surrounding water vapour. With acceptor-doping the proton concentration may be further increased. Oxide ions are hosts for the protons, so that the protons can be seen as present as hydroxide groups occupying oxide ion lattice sites; $OH_O^{\bullet}$. When they migrate, the protons jump from oxide ion to oxide ion, and the defect is thus often also denoted as interstitial protons, $H_i^{\bullet}$. The protons are bonded rather strongly, so that the activation energy for the jump is quite high, and relatively high temperatures are required for

conductivity. The best high temperature proton conductors are perovskites with large and basic A-site cations, like $BaCeO_3$ and $BaZrO_3$ doped with a suitably small lower-valent cation like Y^{3+} on the B-site, which at very high temperatures and/or dry conditions are charge compensated by oxygen vacancies. Under operating conditions, the vacancies hydrate according to

$$H_2O(g)+v_O^{\bullet\bullet}+O_O^x=2OH_O^{\bullet}$$

Eq. 119

Proton conduction in these materials is thus a compromise at increasing temperature between sufficient proton mobility and loss of protons from dehydration. Most materials thus exhibit a maximum in proton conductivity with temperature, see Figure 3-7, left.

The proton conductivity in the best Ba-based perovskites is superior to the oxide ion conduction in ZrO_2-based materials at low and intermediate temperatures, but ends up lower by an order of magnitude, typically at 0.01 S/cm, at high temperatures due to the loss of protons and high grain boundary resistances. Proton ceramic fuel cells have the advantage of forming water as product on the cathode side, see Figure 3-7, right, so as not to dilute the fuel.

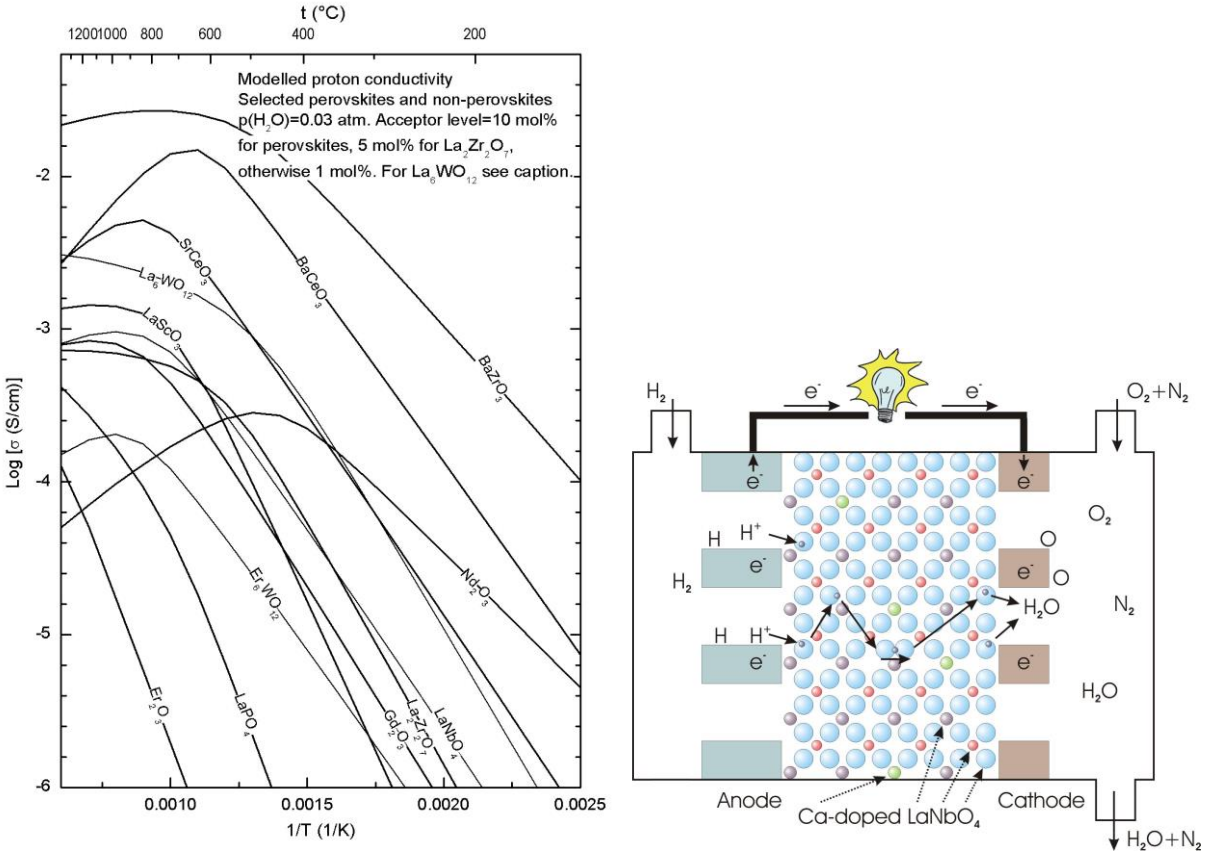

Figure 3-7. Left: Partial proton conductivities in wet atmospheres for a number of acceptor-doped perovskite and non-perovskite oxides (except "La_6WO_{12}", which is inherently defective) [11] Right: Proton conducting solid oxide fuel cell, based on Ca-doped $LaNbO_4$. Note how H_2 fuel can be utilized fully as no water is produced to dilute it on the anode side.

[11] T. Norby, in "Proton conductivity in perovskite oxides", in "Perovskite oxides for solid oxide fuel cells", T. Ishihara, ed., Springer, 2009, ISBN 978-0-387-77707-8.

Some of the best Ba- or Sr-based perovskites have the disadvantage of being reactive towards acidic gases, notably CO_2 to form $BaCO_3$ or $SrCO_3$. The reaction prevents use with reformed fossil or biological fuels and also in some cases with normal air. The formation of $BaCO_3$ markedly weakens grain boundaries and the overall mechanical properties. Alternative materials without the most basic alkali earths comprise acceptor-doped $LaScO_3$, $LaPO_4$, and $LaNbO_4$. The proton conductivity of these is an order of magnitude less than in the Ba-based perovskites, and thinner films, in the micrometer-range, would be needed. In addition, new sets of anode and cathode may need to be developed. These should be mixed electron proton conductors or permeable to hydrogen or water vapour. This is well taken care of for the anode by a cermet of e.g. Ni and the electrolyte, aided by the solubility and transport of atomic hydrogen in Ni. For the cathode, no material with good mixed proton and electron (electron hole) conduction is identified, and one resorts to ceramic-ceramic (cercer) composites of the electrolyte and an electronically conducting oxide. At UiO we presently work with $BaLnCo_2O_{6-ó}$ (Ln = La, Pr, Gd) based double perovskites – which display some hydration – for this purpose.[12]

3.1.4 SOFC geometries and assembly

The materials and ways of assembling them in SOFC concepts are many and challenging. As electrolyte is used Y- or Sc-doped ZrO_2, or other oxide ion conductors (based e.g. on CeO_2 or $LaGaO_3$). These must be sintered gastight, typically at 1400 °C, and in as thin layers as possible.

Ni-YSZ-cermet is used as anode. These are fabricated as a fine grained mixture of NiO and YSZ powders that is sintered onto the YSZ electrolyte at high temperature (typically 1400 °C). NiO is then reduced to Ni metal under the reducing conditions at the anode, at around 800 °C. Ni is a very good catalyst for reforming of methane and for electrochemical oxidation of hydrogen. Because the Ni metal has higher thermal expansion coefficient than YSZ it is a challenge to fabricate constructions of YSZ+Ni/YSZ that can be cycled in temperature without cracking.

$LaMnO_3$ and similar perovskites is used as cathode, doped with acceptors to give high electronic p-type conductivity. $LaMnO_3$ has a thermal expansion similar to that of YSZ.

SOFC, like other fuel cells, need interconnects to connect single cells in stacks and to separate the gases. $LaCrO_3$ doped with an acceptor is a perovskite material with a high electronic (p-type) conductivity from reducing to oxidising conditions and it has TEC similar to that of YSZ. The problem with it is the cost; it is expensive to sinter dense and to machine. It has limited stability and low heat conduction. One thus seeks to develop metallic interconnects for SOFCs: With that one can achieve better electrical and thermal conduction and the materials have in principle easier and cheaper machining. But the metals (except noble metals) that can

[12] R. Strandbakke, *et al.*, "Gd- and Pr-based double perovskite cobaltites as oxygen side electrodes for proton ceramic fuel cells and electrolyser cells", *Solid State Ionics*, **278** (2015) 120-32.

withstand 800-1000 °C without oxidising – and where the protective oxide layer is conducting – are Cr-rich Fe-Cr superalloys, which form Cr_2O_3 as protective layer. These are expensive and very hard. Moreover, chromium compounds evaporate and deposit on and poison the $LaMnO_3$-cathode. To solve the problem with the hardness one has to form the parts using powder metallurgy. To reduce evaporation one covers them with a layer of $LaCrO_3$. Today the temperature for SOFC is sought brought down to 600 °C. If that succeeds we can imagine using ordinary stainless steel qualities as interconnects. These then have sufficiently low corrosion rates, and are machineable and more affordable in every sense than the superalloys. The desire for lower temperatures (often referred to as intermediate temperature SOFCs) does however, put severe demands on the conductivity of electrolytes and the kinetics of electrodes.

SOFC-modules can be built along various design classes. The first with any success was the tubular design, introduced by Westinghouse (now Siemens-Westinghouse). Here, carrier tubes are made of a porous cathode material, closed in one end. Electrolyte is deposited as a thin layer by chemical vapour deposition (CVD), where after the anode is sprayed on as a slurry and sintered. A stripe is left without electrolyte and anode and instead covered with an interconnect. The tubes are stacked so that the cathode has contact to the next anode through the interconnect stripe. This makes the series connection that builds voltage. At the same time the tubes are placed in parallel to increase the current, se figure.

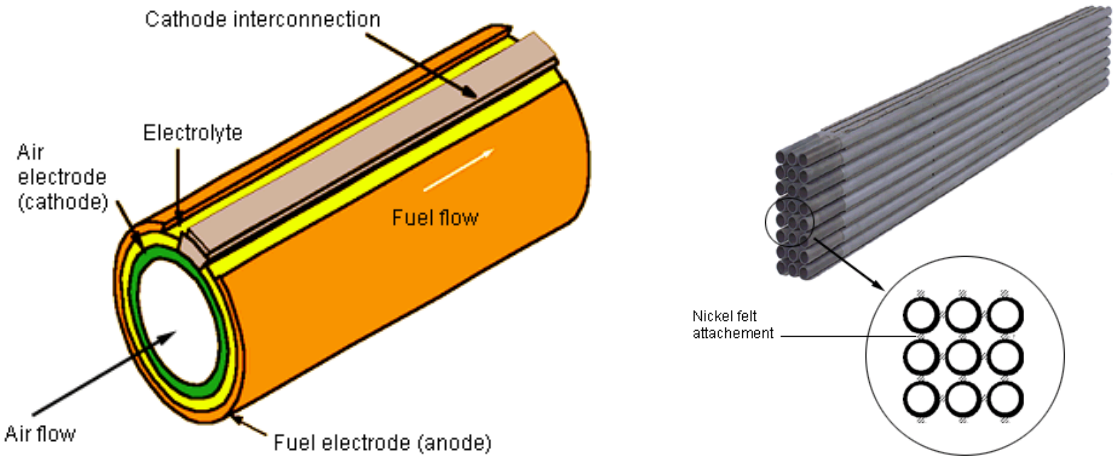

Figure 3-8. The construction of SOFC tube (left) and stacking (right) in series (upwards) and parallel (sideways). From Siemens-Westinghouse.

The figure below shows how a stack like this is operated. Notice how some used fuel is re-circulated for use in reforming of new fuel, and how rest air and rest fuel are mixed and burned after the fuel cell to provide heat to preheating of ingoing air and fuel. In the tubular design sealing and manifolding is relatively unproblematic, but the packing density of cells is poor.

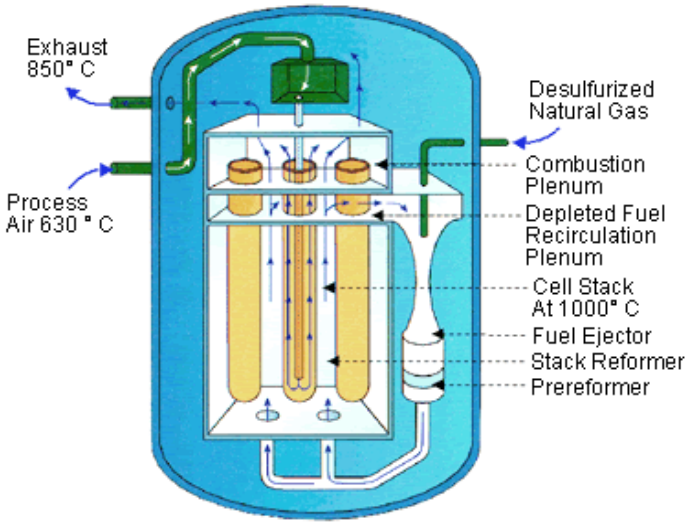

Figure 3-9. Schematic illustration of how a stack of tubular SOFC can be operated. From Siemens-Westinghouse.

Another tubular concept comprises series-connected cells on an inert porous support tube, see Figure 3-10, ensuring high voltage and low current per tube.

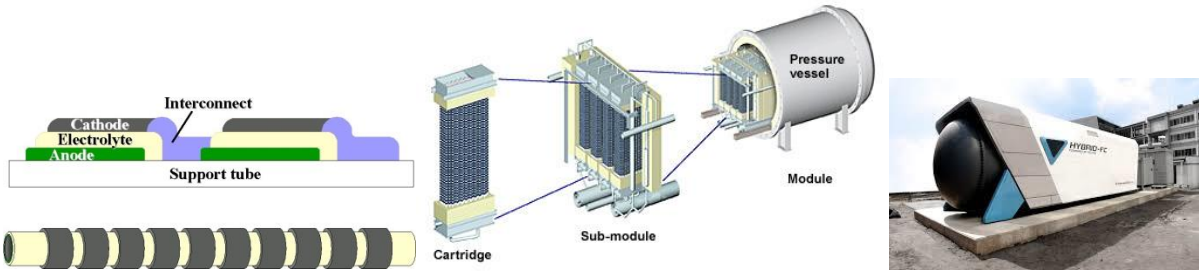

Figure 3-10. Segmented-in-series tubular SOFC technology from Mitsubishi Heavy Industries, Japan. Left: Schematic of layers deposited on the wall of the porous inert support tube, through which fuel flows inside and air on the outside. Middle: Tubes are mounted hanging in a cartridge, which are mounted in modules to form a system of natural-gas fuelled SOFC of 200 kW power, integrated with a 50 kW micro-gas turbine and generator to convert remaining fuel in the exhaust also to electricity. Right: System installed and operative at Kyushu University.

In the so-called *planar concept* thin plates of cathode-electrolyte-anode are stacked, connected and separated by bipolar interconnect plates, for instance in a cross-flow configuration, as shown in Figure 3-11. The packing density becomes very good, while the sealing between the layers is challenging. The sealing can be for instance glass, glass-ceramic, or mica. Most SOFC development projects and installations today use planar concepts.

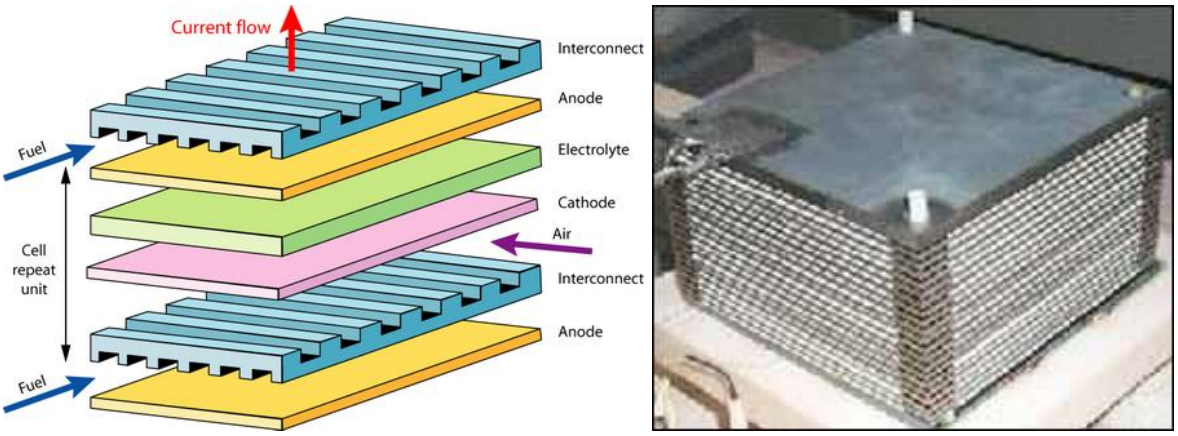

Figure 3-11. Left: Schematic principle of planar SOFC stack. Right: Planar SOFC stack.

4 Wagner analysis of transport in mixed conducting systems

Not presently included…

5 Mixed conducting gas separation membranes

Not yet included.

6 Reactivity of solids

Not yet included.

7 Creep, demixing, and kinetic decomposition

Not yet included.

8 Sintering

Not yet included.

9 Polymer Electrolyte Membrane Fuel Cells and Electrolyser Cells

Not yet included.

10 Batteries

10.1 Introduction

We have learned that a battery – like all electrochemical cells - involves a pair of redox reactions between which electrons and ions are transferred. In a battery, electrons are transferred via the electrodes through an external wire, while the ions are transferred through an electrolyte.

The path of the ions will vary depending on the type of battery that is produced. For primary batteries we don't really care about maintaining any structural integrity of the system, so several of these designs let the ions accumulate in the electrolyte. The battery may actually be visualised as if the cathode and the anode merely dissolves into the electrolyte while the electrons travel through the external wire. One example of such battery is the traditional alkaline battery:

Reduction: $MnO_2 + H_2O + e^- = MnOOH + OH^-$ | 2

Oxidation: $Zn + 4OH^- = [Zn(OH)_4]^{2-} + 2e^-$ | 1

Total reaction: $2MnO_2 + Zn + 2H_2O + 2OH^- = 2MnOOH + [Zn(OH)_4]^{2-}$

Eq. 120

Here, the Zn is effectively dissolved into the electrolyte as $[Zn(OH)_4]^{2-}$. If this battery were to be recharged then it would involve electroplating Zn at the anode and oxidation of MnOOH to MnO_2. The latter reaction would not be too troublesome since the MnOOH particles would likely be situated in the place where the MnO_2 particles were, but electroplating of Zn would most likely lead to a more dense Zn structure than in the original design of the battery, with the result of lowering its power. However, the most severe obstacle would be to prevent electrolysis of the water in the battery during charging, rather than electroplating Zn. With electrolysis of water, the internal resistance would increase since the electrolyte effectively would dry up, but most severely, its internal pressure of both H_2 and O_2 would increase with many possible dramatic outcomes. So, don't recharge primary batteries, they are not designed for it!

Another example of a battery chemistry that seemingly results in dissolution of the cathode and anode is the traditional lead acid battery:

Reduction: $PbO_2 + SO_4^{2-} + 4H^+ + 2e^- = PbSO_4 + 2H_2O$ | 1

Oxidation: $Pb + SO_4^{2-} = PbSO_4 + 2e^-$ | 1

Total reaction: $PbO_2 + Pb + 2\ SO_4^{2-} = 2PbSO_4 + 2H_2O$

During discharge, both the cathode and anode become converted into $PbSO_4$ while consuming the H_2SO_4 in the electrolyte. This battery can be recharged because the $PbSO_4$ formed on the cathode and the anode remains at the positions where the PbO_2 and Pb were. In such sense, nothing is dissolved into the electrolyte, it is rather the electrolyte that becomes dissolved into the cathode and anode during charging.

10.1.1 Exercises

a) Look up the chemistry for the *Nickel Cadmium* battery. Explain its chemistry in terms of reduction, oxidation and total reaction, and provide the electrochemical potentials. What is the electrolyte, and how does the composition of the electrolyte vary with charge/discharge? Is something transported through the electrolyte during charge/discharge, or is something dissolved into it? What was the main reason why these batteries failed to work? (Hint: consider what would happen during rapid charging.)

b) Look up the chemistry for the *Nickel metal hydride* battery. Explain its chemistry in terms of reduction, oxidation and total reaction, and provide the electrochemical potentials. What is actually oxidized at the anode during discharge? What is the electrolyte, and how does the composition of the electrolyte vary with charge/discharge? Is something transported through the electrolyte during charge/discharge, or is something dissolved into it?

Both these battery chemistries require some volume for the electrolyte, even though material is moved from the electrodes into the electrolyte, and vice versa. Would it not be better if the ionic charge could merely travel from within the anode into the cathode? Then the functionality of the electrolyte could be reduced to a simple ionic conductor.

The answer to this rhetorical question is of course – yes. However, in order to realise this, while also enabling the possibility to recharge the batteries, we need structure types that can allow for, not only transport of ions, but also variation of their content without collapsing into other structures.

10.2 Solid-state Li ion battery electrolytes

The original electrolytes for Li-ion batteries have been liquid, based on stable salts of Li^+ dissolved in non-aqueous solvents. The better packing and reliable separation offered by a solid electrolyte brings the development of composite polymer Li-ion conductors. Truly solid Li^+ ion conductors may offer the ultimate solution, but are difficult to realise in terms of all requirements (redox stability, mechanical stability, conductivity).

Lithium salts traditionally used comprise $LiPF_6$, $LiBF_4$, $LiClO_4$, and $LiCF_3SO_3$ (lithium triflate). They are dissolved in e.g. ethylene carbonate or dimethyl carbonate. Typical conductivities are 0.01 S/cm at room temperature, increasing somewhat by increasing temperature. The stability of organic solvents during charging is increased by its decomposition into a so-called solid electrolyte interphase (SEI) at the anode during the first charging. Many ionic liquids are under investigation for use in Li ion electrolytes with improved stability. Polymers like polyoxyethylene (POE) in a composite with the Li ion salt makes the electrolyte more solid (polymer Li-ion batteries).

Solid Li ion conductors comprise a range of glasses and crystalline compounds, like the layered perovskite-related $Li_{3x}La_{0.67-x}TiO_3$ where Li+ ions diffuse via vacancies on the partially filled A-site sublattice.

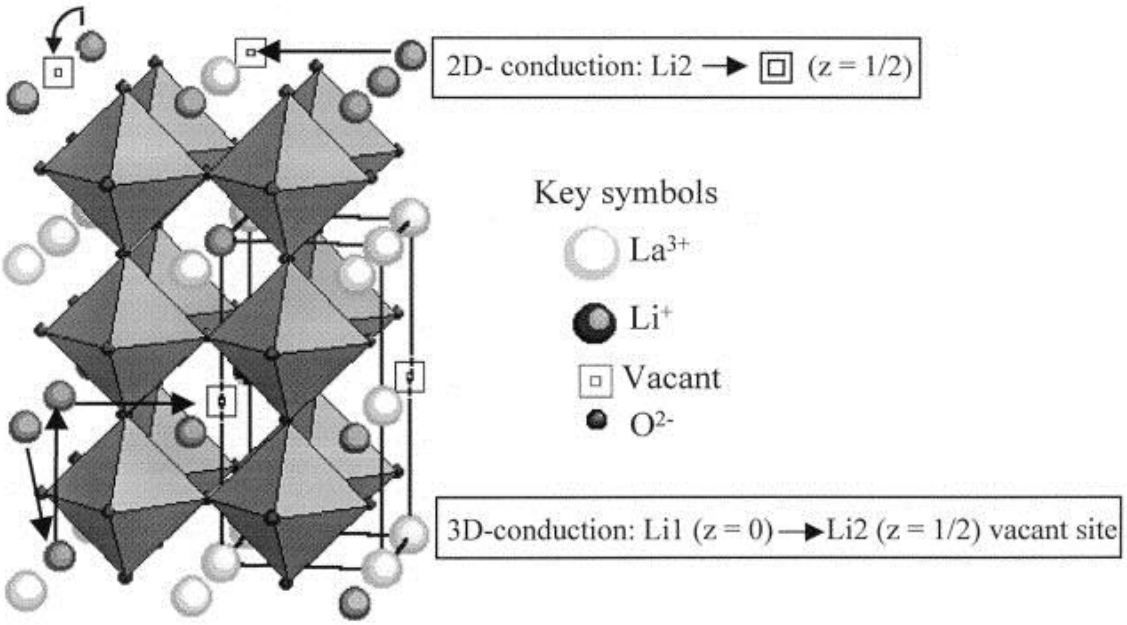

Figure 10-1. Conductivity pathways in $Li_{3x}La_{0.67-x}TiO_3$ [13]

As evident from the figure below, the conductivities at room temperature are considerably lower for this materials class than the 10^{-2} S/cm for the best liquid Li ion conductors.

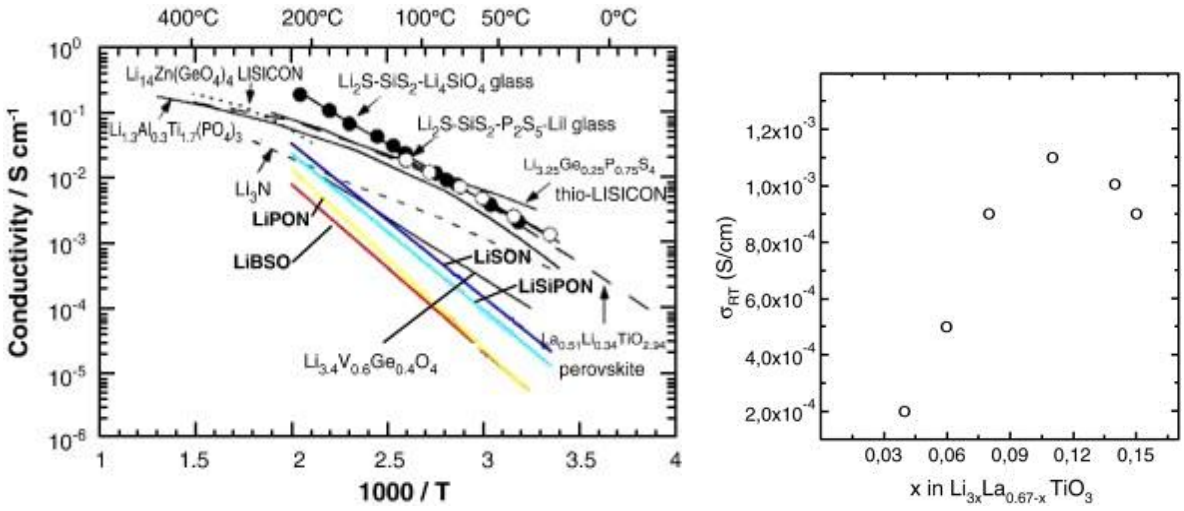

Figure 10-2. Left: Conductivity of some solid-state Li ion conductors vs 1/T. Right: Conductivity of $Li_{3x}La_{0.67-x}TiO_3$ vs x. [14]

10.3 Li ion battery electrodes

The first cathode material for Li ion batteries was TiS_2 which was charged with Li ions to become $LiTiS_2$. The anode was Li metal, making the battery dangerous in case of rupture. The first real commercial success for Li containing rechargeable batteries was with use of layered

[13] A.I. Ruiz et al., *Solid State Ionics*, 112 (1998) 291.

[14] Ph. Knauth, *Solid State Ionics*, 180 (2009) 911.

intercalating $LiCoO_2$ as cathode material, combined with a change of the anode material to Li-intercalated graphite Li_xC as anode. This made it much safer, and since now Li was passed from one intercalation phase to another during charge and back during discharge, *the rocking chair mechanism* was coined for this kind of batteries.

We will now first briefly describe carbon and related Li ion anodes, and then describe cathode materials in more detail.

10.3.1 Carbon-group Li ion anode materials: Li_xC and Li_xSi

Direct reaction of crystalline graphite and metallic Li will result in a compound with composition LiC_6, passing through compounds like LiC_{12} and LiC_{18} on its way, Figure 10-3. It is possible to intercalate Li up to LiC_2, however, this is an unstable compound that will decompose over time to LiC_6 and Li. The conclusion of these observations is that LiC_6 is a more stable compound than Li + C, with the implications that the anode potential is raised from Li/Li^+ with about 0.1-0.2 V to the LiC_6/Li^+, resulting in loss in overall capacity[15]. What is lost in electrochemical capacity is gained in safety. The major drawback when using metallic lithium as anode material is that lithium is electroplated during charging. Such plating processes are most prone to occur at those positions protruding the longest into the electrolyte. If these are not completely consumed during discharge, they will become the next suitable place for plating during next charge, and eventually lead to dendritic growth through the electrolyte that will sort circuit the battery with possible dramatic outcome.

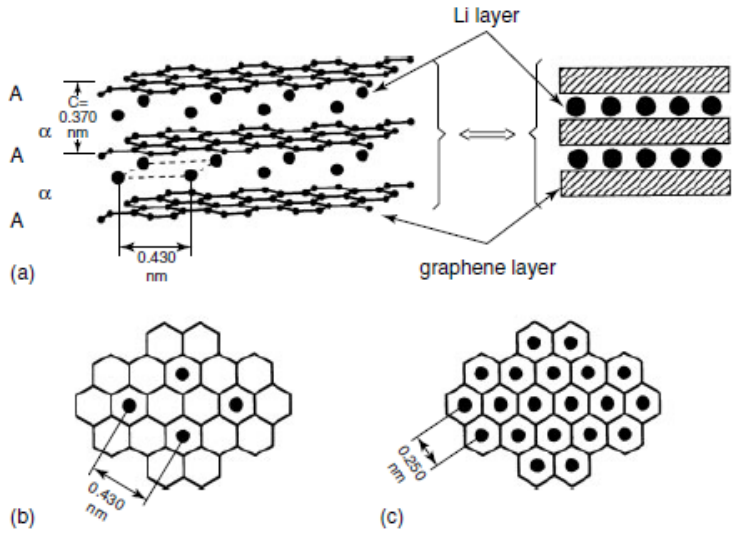

Figure 10-3. Structure of LiC_6 (a) Left: schematic drawing showing the AA layer stacking sequence and the αα inter-layer ordering of the intercalated lithium. Right: Simplified representation. (b) In-plane distribution of Li in LiC_6. (c) In-plane distribution of Li in LiC_2.

[15] **Consider:** Why does the overall capacity vary with potential? How do you calculate the energy capacity from potential and… something more…?

Potentiometric measurements of graphite as it is discharged are shown in Figure 10-4. Such potentiometric measurements give the potential of the material as compared to a reference electrode, as a function of number of electrons (mAh) running through the circuit. In the current configuration, the graphite is wired as the cathode material towards metallic Li as the anode. Whether your material is a cathode or anode, depends on the electrochemical potential of the material you wire it up to. Li metal is a most suitable reference material for non-aqueous systems. It is soft, hence easily shapeable, but highly reactive towards oxygen, moisture and nitrogen. Therefore, remember to work in pure argon atmosphere when working with metallic lithium.

The progression of the potentiometric graph shows clear steps as the content of Li is varied. This is clear evidence of staging of Li as different layers are filled up with Li towards the LiC_6 composition. The curve below (Figure 10-4) is shown as a discharge towards the Li^+/Li anode, hence the small potentials. The reverse progression would also appear during charging, and will also be part of the overall battery characteristics when such highly crystalline graphite is used as anode material towards other cathode materials.

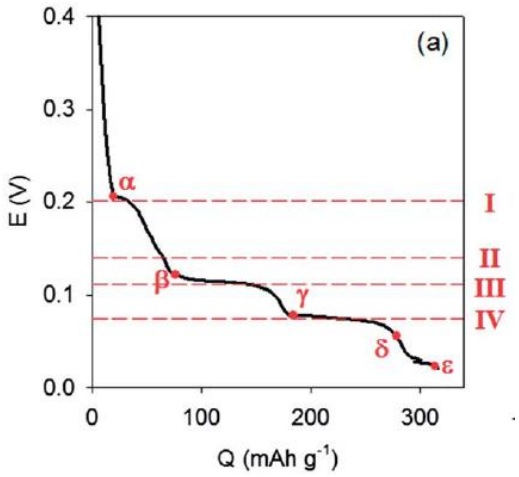

Figure 10-4. Potentiometric profile of lithiation of natural graphite at 0.05 C (Q = capacity; E = cell potential versus Li/Li+). (I) LiC_{72} + LiC_{36}, (II) LiC_{36} + LiC_{27} +LiC_{18}, (III) LiC_{18} + LiC_{12}, (IV) LiC_{12} + LiC_6.[16]

One question thus remains, is Li intercalated into graphite as Li^+ while simultaneously reducing the graphite host, or is Li intercalated as neutral metal? If lithium was intercalated as neutral atoms there would be limited reasons to maximise the inter Li-distance, as is the case for the LiC_6 structure, and even higher contents of Li would be expected to be stable. It is thus safe to assume that lithium intercalates as Li^+.

As host material, highly crystalline graphite raises the potential towards Li/Li^+ with the least amount amongst carbon based materials. Unfortunately, this is also the most expensive form of carbon (not counting diamond and exotic nanomaterials). Numerous other versions of economically viable amorphous to partly crystalline carbon are used in present batteries. What

[16] RSC Adv., 2014, 4, 16545

is gained in reduced expense is lost in energy by a higher potential towards Li/Li^+, typically in the range 0.4-1.2 V.

Other elements in the carbon group can also be used for intercalation of Li. Silicon anodes are thus under study and development. The volume expansion upon intercalation is substantial, but this is solved by using porous Si that has enough internal volume to take up the expansion internally. Recently there is interest also in tin, Sn, as anode material.

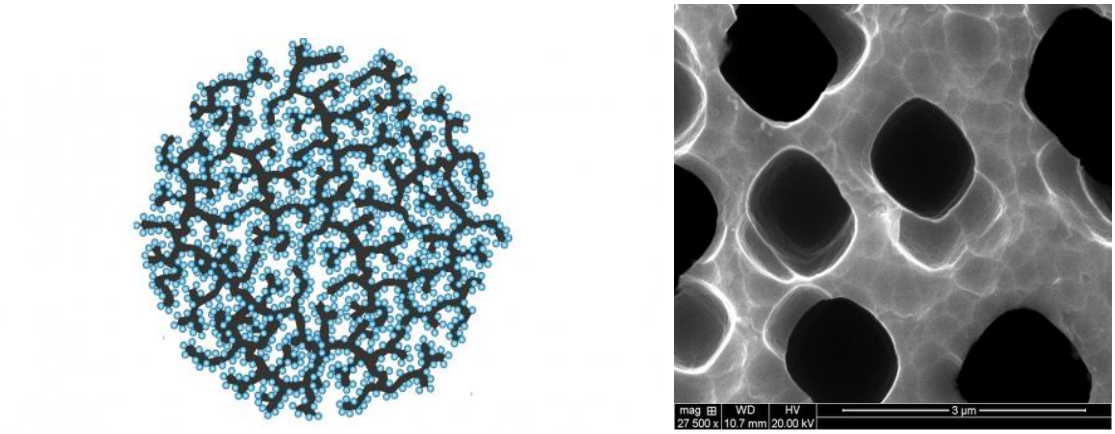

Figure 10-5. Left: Nanocomposite of Si backbone and C nanoparticles. Right: Porous Si structure.

10.3.1.1 Exercises

a) Why does the overall capacity vary with potential? How do you calculate the energy capacity from potential and… something more…?

b) What can be formed when Li reacts with O_2? With H_2O? With N_2?

c) Regard the different stages of intercalation in graphite and consider these as individual phases. Use the Gibbs phase rule to argue that you would expect to observe steps in the potentiometric diagram rather than a slope.

d) How would the potentiometric graph appear if the material shows complete solid solubility with respect to Li^+ content?

10.3.2 The first cathode material: TiS_2

TiS_2 was the first cathode material demonstrating the concept of secondary lithium batteries utilizing metallic Li as the anode material. The TiS_2 (and the other dichalcogenide structures) adopt a layered structure as shown in Figure 10-6.

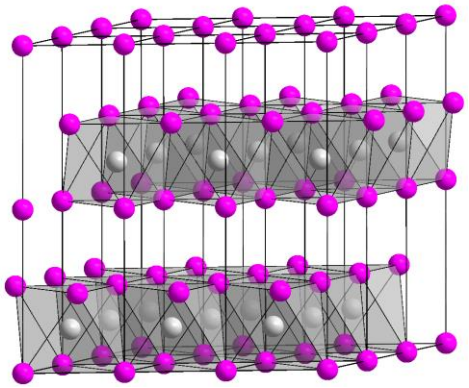

Figure 10-6. Illustration of the TiS_2 structure. The Ti atoms (grey) are situated in octahedral holes a layered structure of sulphur (purple). [Wikipedia: TiS_2]

TiS_2 adopts a hexagonal close packed structure where half of the octahedral holes are filled with Ti^{4+} in a layered manner. The layered structure of the TiS_2 is maintained during charge/discharge and function as hosts for Li^+ ions from the anode reaction ($Li = Li^+ + e^-$) where Li^+ enters empty octahedral sites between the TiS_2 layers. Intercalation of Li^+ ions compensate the overall charge reduction of the $Ti^{4+/3+}$ pairs during discharge, maintaining charge neutrality of the structure. On overall, Li is oxidized on the anode, transported through the electrolyte, and stored in the cathode material as Li^+ ions in a layered host matrix, where Ti is reduced from Ti^{4+} to Ti^{3+}. The compound also shows good electronic conductivity within the TiS_2 layers due to a small overlap between the conduction and valence band and the layered structure ensures good ionic conductivity. Overall, TiS_2 is an ideal cathode material. The electrochemical potential of the $Ti^{3+/4+}$ pair in this configuration is ca. 2 V versus Li/Li^+. This is somewhat limited based on the present status and numerous other metal chalcogenides that have been tested. However, most of these exhibited a low cell voltage of < 2.5 V versus a metallic lithium anode. This limitation in cell voltage is due to the overlap of the higher-valent M^{n+}:d band with the top of the nonmetal:p band. Figure 10-7, for example, illustrates the overlap of the Co^{3+}:3d band with the top of the S^{2-}:3p band in cobalt sulphide. Such an overlap results in an introduction of holes or removal of electrons from the S^{2-}:3p band and the formation of molecular ions such as S_2^{2-} with a potential collapse of the whole structure. This results in an inaccessibility of the higher oxidation states of the M^{n+} ions in a sulphide, leading to a limitation in cell voltage to <2.5 V.

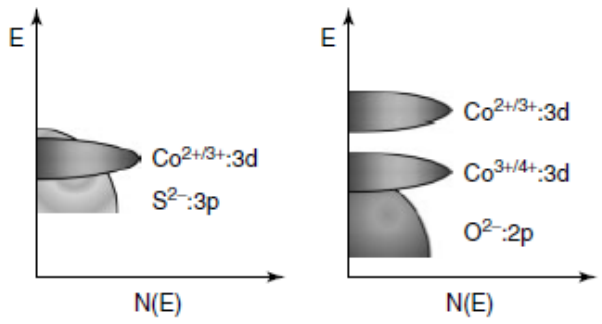

Figure 10-7. Relative energies of metal:d (e.g., Co:3d) and non-metal:p in a sulphide and an oxide.

The $LiTiS_2$ battery did not make a commercial success due to safety issues related to use of metallic lithium. Dendrites of Li would too easily be formed during rapid charging, eventually leading to short circuit and overheating.

10.3.2.1 Exercises

a) The *c*-axis of hexagonal TiS_2 and $LiTiS_2$ are c = 5.70 Å and c = 6.17 Å, respectively, and contains one open layer. The ionic radius of Li^+ is reported to be 0.90 Å. Does this add up? Explain why there is room for Li^+ in the structure.

b) TiS_2 is in fact a semimetal. What does it mean that a material is a semimetal? What is the difference between a semimetal and half-metal? Look it up!

10.3.3 $LiCoO_2$

Using chalcogenides as host materials resulted in limited availability of the higher oxidation states of the transition metals, since these would overlap with the S^{2-}:3p bands. Oxide materials have typically higher crystal energy than sulphides due to reduced interatomic distance, and more ionic bonding. This moves the O^{2-}:2p band lower in energy than the S^{2-}:3p and opens for higher valence states of the transition element. For example, while Co^{3+} can be readily stabilized in an oxide, it is difficult to stabilize Co^{3+} in a sulphide since the $Co^{2+/3+}$ redox couple lies within the S^{2-}:3p band, as seen in Figure 10-7.

In 1990, the Sony Corporation commercialized the combination of $LiCoO_2$ as cathode material together with the more safe LiC_6 anode material. This manifested the first real mass commercialisation of secondary Li-ion batteries, however, as we will see later, not entirely without safety concerns.

Reduction:	$Li_{1-x}CoO_2 + xe^- + xLi^+ = LiCoO_2$	$\| x$
Oxidation:	$LiC_6 = xLi^+ + xe^- + Li_{1-x}C_6$	$\| x$
Total reaction:	$Li_{1-x}CoO_2 + LiC_6 = LiCoO_2 + Li_{1-x}C_6$	

Eq. 121

The $LiCoO_2$ oxide is a member of the series of layered oxides with general formula $LiMO_2$ (M = V, Cr, Co, and Ni). Li^+ and M^{3+} occupy alternate (111) planes of the rock salt structure to give a layered sequence of –O–Li–O–M–O– along the stacking sequence. The Li^+ and M^{3+} ions occupy the octahedral interstitial sites of the cubic close-packed oxygen array as shown in Figure 10-8. This structure is also called the *O3 layered structure*, since the Li^+ ions occupy the octahedral sites (O referring to octahedral) and there are three MO_2 sheets per unit cell. This structure with covalently bonded MO_2 layers allows a reversible extraction/insertion of lithium ions from/into the lithium planes. The lithium-ion movement between the MO_2 layers provides fast two-dimensional lithium-ion diffusion, and the edge-shared MO_6 octahedral arrangement with a direct M-M interaction provides good electronic conductivity. As a result, the $LiMO_2$ oxides have become attractive cathode candidates for lithium-ion batteries.

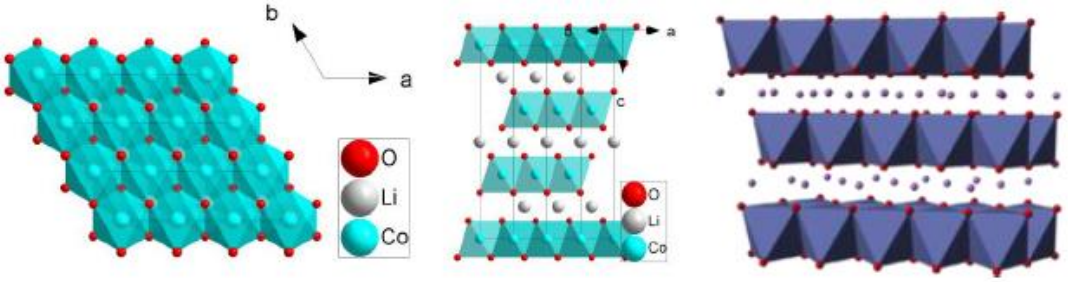

Figure 10-8. Crystal structure of $LiCoO_2$; (left) one layer showing AB stacking of oxygen atoms (red spheres) with Co in octahedral voids; (middle) AB… stacking of CoO_2 layers with Li cations in interlayer regions; note that the O-atoms are stacked ABCABC… along the c-axis; (right) perspective of the layered stacking.

$LiCoO_2$ is still a widely used transition metal oxide cathode in commercial lithium-ion batteries because of its high operating voltage (~4 V), ease of synthesis, and good cycle life. $LiCoO_2$, synthesized by conventional high temperature procedures at T >800 °C, adopts the O3 layered structure shown in Figure 10-8, with an excellent ordering of the Li^+ and Co^{3+} ions on the alternate (111) planes of the rock salt lattice. The ordering is due to the large charge and size differences between the Li^+ and Co^{3+} ions. The highly ordered structure exhibits good lithium-ion mobility and electrochemical performance. The direct Co-Co interaction with a partially filled t_{2g}^{6-x} band associated with the $Co^{3+/4+}$ couple leads to high electronic conductivity (metallic) for $Li_{1-x}CoO_2$ (10^{-3} S cm^{-1}). In addition, a strong preference of the low-spin Co^{3+} and Co^{4+} ions for the octahedral sites, as evident from the high octahedral-site stabilization energy (OSSE), as seen in Table 1 provides good structural stability. In contrast, synthesis at low temperatures (~400 °C) results in a considerable disordering of the Li^+ and Co^{3+} ions, leading to the formation of a lithiated spinel-like phase with a cation distribution of $[Li_2]_{16c}[Co_2]_{16d}O_4$, which exhibits poor electrochemical performance.

Even though one Li^+ ion per formula unit can be theoretically extracted from $LiCoO_2$ with a capacity of ~274 $mAhg^{-1}$, only 50% (~140 $mAhg^{-1}$) of its theoretical capacity can be utilized in practical lithium-ion cells because of structural and chemical instabilities at deep charge (x > 0.5 in $Li_{1-x}CoO_2$). Extraction of more than 0.5 Li^+ ions from $LiCoO_2$ leads to chemical instability due to the overlap of the $Co^{3+/4+}$:t_{2g} band with the top of the O^{2-}:2p band as shown in Figure 10-9.

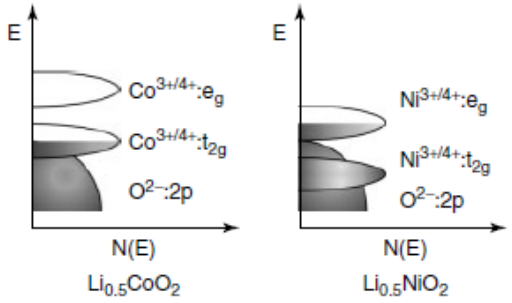

Figure 10-9. Comparison of the qualitative energy diagram of $Li_{0.5}CoO_2$ and $Li_{0.5}NiO_2$.

Removal of a significant amount of electron density from the O^{2-}:2p band will result in an oxidation of O^{2-} ions and a slow loss of oxygen and cobalt from the lattice during repeated cycling. Sometimes dramatic breakdown of the cathode material may occur during deep charging, with very high internal pressure build up and resulting safety hazards.

10.3.4 $LiNiO_2$

$LiNiO_2$ is isostructural with $LiCoO_2$ and offers a cell voltage of ~3.8V. Ni is less expensive and less toxic than Co. The operating voltage of the $Ni^{3+/4+}$ couple is slightly lower than that of the $Co^{3+/4+}$ couple in $LiCoO_2$, in spite of Ni being more electronegative than Co and lying to the right of Co in the Periodic Table. This is because while the redox reaction with Ni^{3+}:$t^2_{2g}e^1_g$ involves the upper-lying, σ-bonding e_g band, that with Co^{3+}:$t^2_{2g}e^0_g$ involves the lower-lying, π-bonding t_{2g} band. However, it is difficult to synthesize $LiNiO_2$ as a well-ordered stoichiometric material with all Ni^{3+} because of the difficulty of stabilizing Ni^{3+} at the high synthesis temperatures and the consequent volatilization of lithium. It invariably forms $Li_{1-x}Ni_{1+x}O_2$ with some excess Ni^{2+}, which results in a disordering of the cations in the lithium and nickel planes due to smaller charge and size differences between Li^+ and Ni^{2+} and consequently poor electrochemical performance. In addition, charged $Li_{1-x}NiO_2$ suffers from a migration of Ni^{3+} ions from the octahedral sites of the nickel plane to the octahedral sites of the lithium plane via the neighbouring tetrahedral sites, particularly at elevated temperatures. This is due to a lower OSSE associated with the low-spin Ni^{3+}:$t^2_{2g}e^1_g$ ions compared to that of the low-spin Co^{3+}:$t^2_{2g}e^0_g$ ions (Table 1). While a moderate OSSE allows the Ni^{3+} ions to migrate through the tetrahedral sites under mild heat, the stronger OSSE of Co^{3+} hinders such a migration. Moreover, $LiNiO_2$ also suffers from Jahn–Teller distortion (tetragonal structural distortion) associated with the low-spin Ni^{3+}:$3d^7$ ($t^2_{2g}e^1_g$) ion. Also, $Li_{1-x}NiO_2$ electrodes in their charged state are thermally less stable than the charged $Li_{1-x}CoO_2$ electrodes, an indication that Ni^{4+} ions are reduced more easily than Co^{4+} ions. As a result, $LiNiO_2$ is not a promising material for lithium-ion cells.

Table 1. Crystal field stabilization energies (CFSEs) and octahedral site stabilization energies (OSSE) of some 3d transition metal ions.

Ion	Octahedral coordination		Tetrahedral coordination		OSSE[d] (Dq)
	Configuration[a]	CFSE[b] (Dq)	Configuration[a]	CFSE[b,c] (Dq)	
V^{3+}:$3d^2$	$t^2_{2g}e^0_g$	−8	$e^2t^0_2$	−5.33	−2.67
Cr^{3+}:$3d^3$	$t^3_{2g}e^0_g$	−12	$e^2t^1_2$ (HS)	−3.56	−8.44
Mn^{3+}:$3d^4$	$t^3_{2g}e^1_g$ (HS)	−6	$e^2t^2_2$ (HS)	−1.78	−4.22
Fe^{3+}:$3d^5$	$t^3_{2g}e^2_g$ (HS)	0	$e^2t^3_2$ (HS)	0	0
Co^{3+}:$3d^6$	$t^6_{2g}e^0_g$ (LS)	−24	$e^3t^3_2$ (HS)	−2.67	−21.33
Ni^{3+}:$3d^7$	$t^6_{2g}e^1_g$ (LS)	−18	$e^4t^3_2$ (HS)	−5.33	−12.67

[a] LS and HS refer, respectively, to low-spin and high-spin configurations.
[b] Pairing energies are neglected for simplicity.
[c] Obtained by assuming $\Delta_t = 0.444\Delta_o$; Δ_t and Δ_o refer, respectively, to tetrahedral and octahedral splittings.
[d] Obtained by taking the difference between the CFSE values for octahedral and tetrahedral coordinations.

However, partial substitution of Co for Ni has been shown to suppress the cation disorder and Jahn–Teller distortion. For example, $LiNi_{0.85}Co_{0.15}O_2$ has been found to show a reversible capacity of ~180 $mAhg^{-1}$ with excellent cyclability. The increase in the capacity of $LiNi_{0.85}Co_{0.15}O_2$ compared to that of $LiCoO_2$ can be understood by considering the qualitative band diagrams for the $Li_{1-x}CoO_2$ and $Li_{1-x}NiO_2$ systems, as shown in Figure 10-9. With a low-spin Co^{3+}:$3d^6$ configuration, the t_{2g} band is completely filled and the e_g band is empty ($t^2_{2g}e^0_g$) in $LiCoO_2$. Since the t_{2g} band overlaps with the top of the O^{2-}:2p band, deep lithium extraction with $(1 - x) < 0.5$ in $Li_{1-x}CoO_2$ results in the removal of a significant amount of electron density from the O^{2-}:2p band and consequent chemical instability, limiting its practical capacity. In contrast, the $LiNiO_2$ system with a low-spin Ni^{3+}:$t^2_{2g}e^1_g$ configuration involves the removal of electrons only from the e_g band. Since the e_g band barely touches the top of the O^{2-}:2p band, $Li_{1-x}NiO_2$, and $LiNi_{1-y}Co_yO_2$ exhibit better chemical stability than $LiCoO_2$, resulting in higher capacity values.

Recent studies have shown that partial substitution of manganese in $LiNiO_2$ not only provides high capacities (~200 $mAhg^{-1}$), but also results in a significant improvement in thermal stability compared to $LiNiO_2$. The increase in capacity and thermal stability is associated with the substitution of chemically more stable Mn^{4+} ions for Ni^{3+}. Recently, the mixed layered oxide $LiMn_{1/3}Ni_{1/3}Co_{1/3}O_2$ has become an attractive cathode material because of its high capacity, better thermal stability, and stable cycle performance. In these mixed layered oxides, Ni, Mn, and Co exist as, respectively, Ni^{2+}, Mn^{4+}, and Co^{3+}. However, only $Li_{1-x}CoO_2$ becomes metallic on charging, because of the partially filled t_{2g} band, while $Li_{1-x}NiO_2$ and $Li_{1-x}MnO_2$ remain as semiconductors during charging as the e_g band is redox active and not the t_{2g} band in the edge-shared MO_6 lattice.

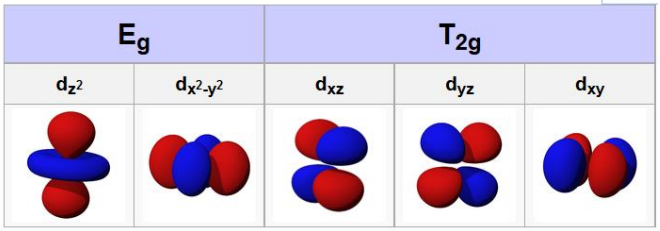

Figure 10-10. Illustration of the E_g and T_{2g} orbitals in octahedral environment.

10.3.5 Layered $LiMnO_2$

Layered $LiMnO_2$ is attractive from an economical and environmental point of view, since manganese is inexpensive and environmentally benign compared to cobalt and nickel. However, $LiMnO_2$ synthesized at high temperatures adopts an orthorhombic structure instead of the layered O3-type structure, resulting in poor electrochemical performance. The stability of the layered structure is also challenged by the Jahn–Teller distortion induced by the Mn^{3+} ions as well as the low OSSE value of Mn^{3+} ions and the consequent easy migration of the Mn^{3+} ions from the octahedral sites of the Mn planes to the octahedral sites of the Li planes via the neighbouring tetrahedral sites.

10.3.6 Other layered oxides

$LiVO_2$ is isostructural with $LiCoO_2$ and has the O3 layered structure. However, in de-lithiated $Li_{1-x}VO_2$ with $(1 - x) < 0.67$, the vanadium ions migrate from the octahedral sites of the vanadium layer into the octahedral sites of the lithium layer because of the low OSSE of the vanadium ions. Therefore, the kinetics of lithium transport and the electrochemical performance is very poor, making $LiVO_2$ an unattractive cathode material.

$LiCrO_2$ can also be prepared in the O3 structure, but it has been shown to be electrochemically inactive for lithium insertion/extraction.

Layered $LiFeO_2$, like $LiMnO_2$, is thermodynamically unstable at high temperatures and has to be prepared by an ion exchange of layered $NaFeO_2$ with Li^+. However, the O3-type $LiFeO_2$ also exhibits poor electrochemical performance due to structural instabilities since the high-spin Fe^{3+}:$3d^5$, with an OSSE value of zero, can readily migrate from the octahedral sites to the tetrahedral sites.

10.3.7 Spinel oxide cathodes

Oxides with the general formula LiM_2O_4 (M = Ti, V, and Mn) crystallize in the normal spinel structure, in which the Li^+ and the $M^{3+/4+}$ ions occupy, respectively, the 8a tetrahedral and 16d octahedral sites of the cubic close-packed oxygen array. A strong edge-shared octahedral $[M_2]O_4$ array permits reversible extraction of the Li^+ ions from the tetrahedral sites without collapsing the three-dimensional $[M_2]O_4$ spinel framework. While an edge-shared MO_6 octahedral arrangement with direct M–M interaction provides good hopping electrical conductivity, the interconnected interstitial (lithium) sites via the empty 16c octahedral sites in the three-dimensional structure provide good lithium-ion conductivity.

10.3.8 Spinel $LiMn_2O_4$

Spinel $LiMn_2O_4$ has become an attractive cathode, as Mn is inexpensive and environmentally benign compared to Co and Ni involved in the layered oxide cathodes. The extraction/insertion of lithium ions from/into the $LiMn_2O_4$ spinel framework occurs in two distinct steps. The lithium extraction/insertion from/into the 8a tetrahedral sites occurs around 4 V with the maintenance of the initial cubic symmetry, while that from/into the 16c octahedral sites occurs around 3 V by a two-phase mechanism involving the cubic spinel $LiMn_2O_4$ and the tetragonal lithiated spinel $Li_2Mn_2O_4$. A deep energy well for the 8a tetrahedral Li^+ ions and the high activation energy required for the Li^+ ions to move from one 8a tetrahedral site to another via an energetically unfavourable neighbouring 16c site lead to a higher voltage of 4 V. On the other hand, the insertion of an additional lithium into the empty 16c octahedral sites occurs at 3 V, Figure 10-12. Thus, there is a 1 V jump on going from tetrahedral-site lithium to octahedral-site lithium with the same $Mn^{3+/4+}$ redox couple, reflecting the contribution of site energy to the lithium chemical potential and the overall redox energy. The Jahn–Teller distortion associated with the single electron in the e_g orbitals of a high spin Mn^{3+}:$3d^4$ ($t^3_{2g}e^1_g$) ion results in the cubic-to-tetragonal transition (Figure 10-11) on going from $LiMn_2O_4$ to $Li_2Mn_2O_4$. The cubic-to-tetragonal transition is accompanied by a

6.5% increase in unit cell volume, which makes it difficult to maintain structural integrity during discharge–charge cycling and results in rapid capacity fade in the 3 V region.

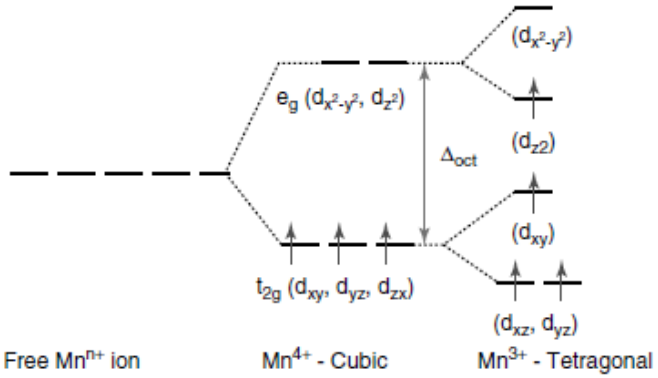

Figure 10-11. Illustration of Jahn-Teller distortion in manganese oxides.

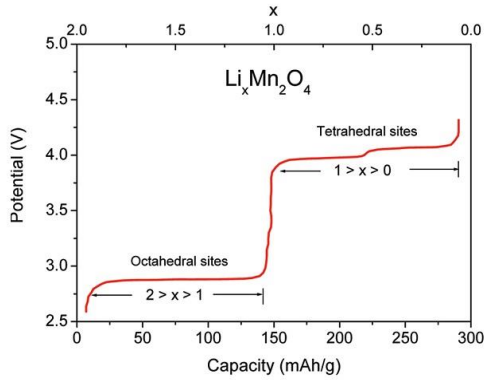

Figure 10-12. Potential vs. Li^+/Li profile of spinel $Li_xMn_2O_4$ for complete reversible lithium intercalation ($0 \leq x \leq 2$) [*Chem. Mater.*, 2010, 22, 587].

Therefore, $LiMn_2O_4$ can only be used in the 4 V region with a limited practical capacity of around 120 $mAhg^{-1}$, which corresponds to an extraction/insertion of 0.8 Li^+ ion per formula unit of $LiMn_2O_4$. However, $LiMn_2O_4$ tends to exhibit capacity fade even in the 4 V region as well, particularly at elevated temperatures (55 °C). Dissolution of manganese into the electrolyte is believed to be the main cause for this capacity fade, especially at elevated temperatures. Manganese dissolution is due to the disproportionation of Mn^{3+} into Mn^{4+} (remains in the solid) and Mn^{2+} (leaches out into the electrolyte) in the presence of trace amounts of HF that is produced by a reaction of trace amounts of water in the electrolyte with the $LiPF_6$ salt. The Mn disproportionation reaction is given below as

$$2Mn^{3+} = Mn^{2+} + Mn^{4+}$$ Eq. 122

10.3.9 5 V Spinel Oxides

Initially, cation-substituted $LiMn_{2-x}M_xO_4$ spinel oxides were studied to improve the capacity retention in the 4 V region. However, such substitutions to give $LiMn_{2-x}M_xO_4$ (M = Ni, Fe, Co, and Cr) lead to a 5 V plateau in addition to the 4 V plateau. The 4 V region in $LiMn_{2-x}M_xO_4$

corresponds to the oxidation of Mn^{3+} to Mn^{4+}, while the 5 V region corresponds to the oxidation of M^{3+} to M^{4+} or the oxidation of M^{2+} to M^{3+} and then to M^{4+}. It is interesting to note that while the M = $Co^{3+/4+}$ and $Ni^{3+/4+}$ couples offer around 4 V, corresponding to the extraction/insertion of lithium from/into the octahedral sites of the layered $LiMO_2$, they offer 5 V corresponding to the extraction/insertion of lithium from/into the tetrahedral sites of the spinel $LiMn_{2-x}M_xO_4$. The 1 V difference is due to the differences in the site energies between octahedral and tetrahedral sites, as discussed earlier.

With a higher operating voltage and theoretical capacities of around 145 $mAhg^{-1}$, $LiMn_{1.5}Ni_{0.5}O_4$ has emerged as an attractive cathode candidate. In comparison to $LiMn_2O_4$, here Mn predominantly remains in the +4 oxidation state during cycling, avoiding the normal Jahn–Teller distortions of Mn^{3+} ions, while Ni^{2+} first oxidizes to Ni^{3+} and then to Ni^{4+}.

One major concern with the spinel $LiMn_{1.5}Ni_{0.5}O_4$ cathode is the chemical stability in contact with the electrolyte at the higher operating voltage of 4.7 V.

10.3.10 Polyanion-containing Cathodes

Although simple oxides such as $LiCoO_2$, $LiNiO_2$, and $LiMn_2O_4$ with highly oxidized redox couples ($Co^{3+/4+}$, $Ni^{3+/4+}$, $Mn^{3+/4+}$, respectively) were able to offer high cell voltages of ~4 V in lithium-ion cells, they are prone to release oxygen from the lattice in the charged state at elevated temperatures because of the chemical instability of highly oxidized species such as Co^{4+} and Ni^{4+}. One way to overcome this problem is to work with lower-valent redox couples like $Fe^{2+/3+}$. However, a decrease in the oxidation state raises the redox energy of the cathode and lowers the cell voltage. Recognizing this, and to keep the cost low, oxides containing polyanions such as XO_4^{2-} (X = S, Mo, and W) were proposed as lithium insertion hosts in the 1980s by Manthiram and Goodenough. Although the $Fe^{2+/3+}$ couple in a simple oxide like Fe_2O_3 would normally operate at a voltage of <2.5 V vs Li/Li^+, surprisingly the polyanion-containing $Fe_2(SO_4)_3$ host was found to exhibit 3.6 V vs Li/Li^+, while both $Fe_2(MoO_4)_3$ and $Fe_2(WO_4)_3$ were found to operate at 3.0 V vs Li/Li^+ (Figure 10-13). The remarkable increase in cell voltage on going from a simple oxide such as Fe_2O_3 to polyanion hosts like $Fe_2(XO_4)_3$, all operating with the same $Fe^{2+/3+}$ couple, were attributed to a shift in the bonding type between oxygen and iron and consequent differences in the location of the $Fe^{2+/3+}$ redox levels, as seen in Figure 10-13.

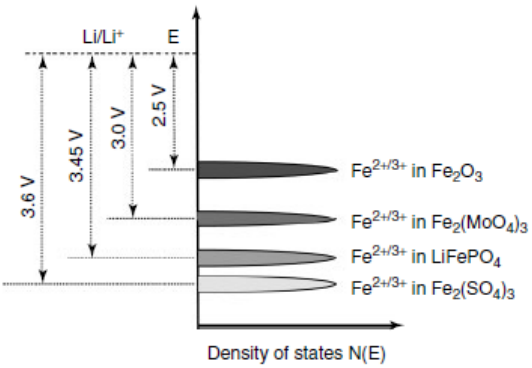

Figure 10-13. Positions of the $Fe^{2+/3+}$ redox energies relative to that of Li/Li^+ in various Fe-containing lithium insertion hosts and consequent changes in cell voltages, illustrating the role of polyanions.

In the $Fe_2(SO_4)_3$ and $Fe_2(MoO_4)_3$ hosts with corner-shared FeO_6 octahedra, XO_4 tetrahedra, and Fe–O–*X*–O–Fe (*X* = S, Mo, or W) linkages, the strength of the *X*–O bond can influence the Fe–O covalence and thereby the relative position of the $Fe^{2+/3+}$ redox energy. The stronger the *X*–O bonding, the weaker the Fe–O bonding, and consequently the lower the $Fe^{2+/3+}$ redox energy relative to that in a simple oxide like Fe_2O_3. Another way of representing this situation is to consider the ionic strength of the polyanions. The more electronegative the centre in the polyanion is, the more ionic the bond towards iron becomes, and the lower in energy level its redox states fall. The net result is a higher cell voltage on going from Fe_2O_3 to $Fe_2(MoO_4)_3$ or $Fe_2(SO_4)_3$. Comparing $Fe_2(MoO_4)_3$ and $Fe_2(SO_4)_3$, the S–O covalent bonding in $Fe_2(SO_4)_3$ is stronger compared to the Mo–O bonding in $Fe_2(MoO_4)_3$, leading to a weaker Fe–O covalence in $Fe_2(SO_4)_3$ than that in $Fe_2(MoO_4)_3$, resulting in a lowering of the $Fe^{2+/3+}$ redox energy in $Fe_2(SO_4)_3$ compared to that in $Fe_2(MoO_4)_3$ and a consequent increase in cell voltage by 0.6 V. Thus, the replacement of simple O^{2-} ions by XO_4^{n-} polyanions was recognized as a viable approach to tune the position of redox levels in solids and consequently to realize higher cell voltages with chemically more stable, lower-valent redox couples like $Fe^{2+/3+}$.

10.3.10.1 Exercises

a) Look at the shape of the potential curve in Figure 10-12, what does the steps in this potential curve tell about the evolution of different phases in this material during charging?
b) What kind of shape would you expect for the potential curve during charging or discharging of $LiMn_{1.5}Ni_{0.5}O_4$ where the Ni atoms are oxidized in steps? How would the curves be affected if the transition elements are perfectly ordered, or if a complete disorder prevails?
c) Identify different types of polyanions and try to group them according to their overall electronegative character for the transition element.
d) How can you modify polyanions to become even more electronegative? (Hint: think partial or full substitution of the elements in the polyanion).

10.3.11 Phospho-olivine $LiMPO_4$

In 1997, Goodenough's group identified $LiFePO_4$ as well as $LiMPO_4$ (M = Mn, Co, and Ni) crystallizing in the olivine structure, as a facile lithium extraction/insertion host that could be combined with a carbon anode in lithium-ion cells.

In the initial work, fewer than 0.7 lithium ions were extracted per formula unit of $LiFePO_4$ even at very low current densities, which corresponds to a reversible capacity of <120 $mAhg^{-1}$. The lithium extraction/insertion occurred via a two-phase mechanism with $LiFePO_4$ and $FePO_4$ as end members without much solid solubility. The limitation in capacity was attributed to the diffusion-limited transfer of lithium across the two-phase interface and poor electronic conductivity due to the corner-shared FeO_6 octahedra. $LiFePO_4$ is a one-dimensional lithium-ion conductor with the lithium-ion diffusion occurring along edge-shared LiO_6 chains (*b* axis), Figure 10-14. Intimate mixture with conductive carbon and particle size

minimization are therefore necessary to optimize the electrochemical performance. Consequently, with a reduction in particle size and coating with conductive carbon, reversible capacity values of ~160 $mAhg^{-1}$ were realized.

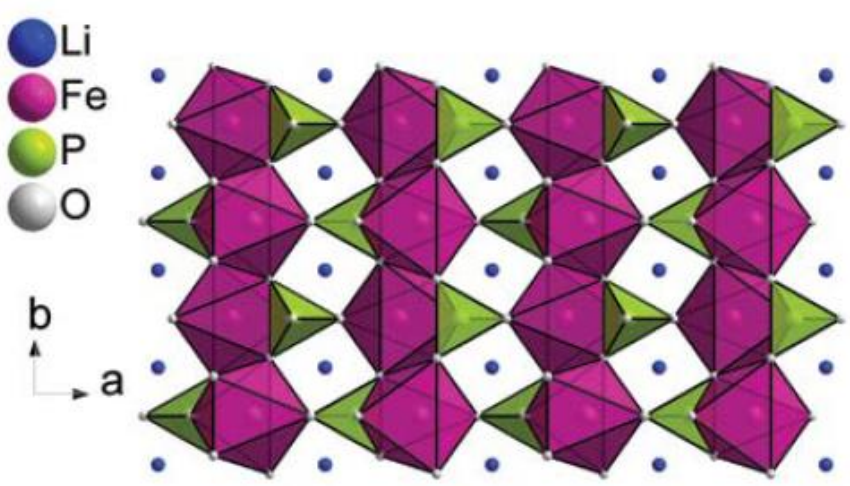

Figure 10-14. Crystal structure of olivine $LiFePO_4$ with one-dimensional lithium diffusion channels.

Replacing the transition-metal ion Fe^{2+} by Mn^{2+}, Co^{2+}, and Ni^{2+} increases the redox potential significantly from 3.45 V in $LiFePO_4$ to 4.1, 4.8, and 5.1 V, respectively, in $LiMnPO_4$, $LiCoPO_4$, and $LiNiPO_4$ because of the changes in the positions of the various redox couples (Figure 10-15). As we have seen earlier, the electronegativity of *X* and the strength of the *X*–O bond play a role in controlling the redox energies of metal ions in polyanion-containing samples. However, in the case of $LiMPO_4$ cathodes, the polyanion PO_4 is fixed, so the shifts in the redox potential can only be associated with the changes in the M^{2+} cations. It is well known that the redox energies of transition metal $M^{2+/3+}$ couples decrease as we go from left to right in the periodic table because of the increase in the nuclear charge, the extra electrons being added to the same principal quantum number (e.g., 3d in the case of first row transition metals). However, $LiFePO_4$ exhibits a lower voltage (3.43 V) than $LiMnPO_4$ (4.13 V) despite Fe being to the right of Mn in the periodic table as the upper-lying t_{2g} of Fe^{2+}:$t^4_{2g}e^2_g$ is the redox-active band (due to the pairing of the sixth electron in the t_{2g} orbital) compared to the lower-lying e_g of Mn^{2+}:$t^3_{2g}e^2_g$ (Figure 10-15). In addition, a systematic shift in the redox potential (open-circuit voltage) of the $M^{2+/3+}$ couples has been observed in the $LiM_{1-y}M_yPO_4$ (Mn, Fe, and Co) solid solutions compared to those of the pristine $LiMPO_4$. The potential of the lower-voltage couple increases, while that of the higher-voltage couple decreases in the $LiM_{1-y}M_yPO_4$ solid solutions compared to that of the pristine $LiMPO_4$. The shifts in the redox potentials have been explained by the changes in the *M*–O covalence (inductive effect) caused by the changes in the electronegativity of *M* or *M*–O bond length as well as by the influence of the *M*–O–*M* interactions in the solid solutions.

$LiMnPO_4$ is of particular interest because of the environmentally benign manganese and the favourable position of the $Mn^{2+/3+}$ redox couple at 4.1 V vs Li/Li^+, which is compatible with

most of the electrolytes. However, it has been shown to offer low practical capacity even at low currents due to the wide band gap of ~2 eV and low electronic conductivity of $\sim 10^{-14}$ S cm^{-1} compared to $LiFePO_4$, which has an electronic conductivity of $\sim 10^{-9}$ S cm^{-1} and a band gap of ~0.3 eV.

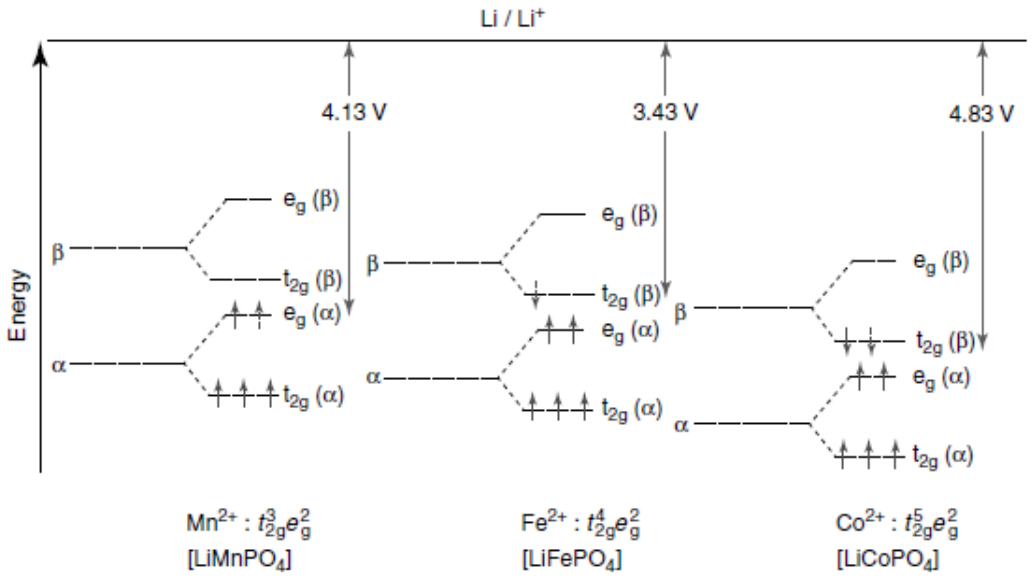

Figure 10-15. Crystal field splitting and 3d-orbital energy level diagram for the high-spin Mn^{2+}, Fe^{2+}, and Co^{2+} ions in olivine Li*M*PO_4. The electron involved in the redox reaction is shown with a dashed line. The α and β representation of the d orbitals represents the energy involved in pairing spins.

10.3.12 Summary – Li ion battery electrode materials

It is now time to try to summarize the items we have covered that affect the properties of battery materials, with reference to Li ion batteries:

- The cathode and anode material need to have a stable structure that can accommodate large variations in Li^+ content.
- The Li^+ that enters the structure may accommodate octahedral or tetrahedral positons, however, Li^+ is more energetically favoured in tetrahedral sites than in octahedral sites, which can raise the electrochemical potential of the cathode material by 1 V.
- In order to keep a stable cathode material, the transition element needs a high stabilisation energy (CFSE) for the site where it is supposed to be (mostly octahedral sites). Otherwise, the transition element may diffuse into the sites that are meant to be for Li^+. This may block easy transportation of Li^+ ion the structure and remove the transition element from being electrochemically active. Co^{3+} likes octahedral positions, while Fe^{3+} does not care.
- The electrochemical potential of the cathode material will mostly be determined by the redox chemistry of the transition element. The redox energy for higher oxidation states are lower in energy (higher potential towards Li/Li^+) than the redox energy for the lower oxidation states.
- The redox chemistry of the transition elements will be affected by the strength of the bonds to the host lattice (S^{2+}, O^{2-}, polyanion). The weaker the covalent character of the

bonds to the host lattice becomes, the lower in energy (higher potential towards Li/Li^+) the redox energy will be.
- The practical limitations for choice of active redox chemistry is oxidation of the host lattice (S^{2-}, O^{2-}). If this happens, the host structure typically collapses and formation of S_2, O_2 will result. The latter with possible dramatic consequences.
- Application of polyanionic host lattice will typically reduce energy level of the oxygen p-band, and open for exploitation of lower energy levels of the transition element.
- The cathode and anode material need to be both electronic and ionic conducting in order to be suitable as electrode material.

10.4 Performance metrics of batteries

We have now visited a number of different cathode chemistries, and one popular anode chemistry. On overall, we have mostly referred to its theoretical or practical electrochemical potential, and its overall capacity. For the next session, we will dwell a bit deeper into the characteristics of batteries from the measurement point of view. What are the characteristics we seek in batteries, and how does this relate to the chemistries already mention?

10.4.1 Different kinds of voltages

Let us repeat some terms related to voltages of electrochemical cells, and introduce a couple of new ones specially related to batteries. We have already treated the **equilibrium potential** defined for batteries as the electrochemical potential at open circuit, based on the activities (almost the same as concentrations) of the different species as placed in the Nernst equation. The **overpotential** is the potential difference (voltage) between that expected from thermodynamics and what is experimentally observed. This is directly related to a cell's efficiency.

When characterising batteries, we can add an additional set of potentials to our vocabulary. With reference to Figure 10-16 for visual explanations, some of these are: **Open circuit voltage (OCV)**: This is the potential measured when the battery is not connected to an external load. In practice you have to connect a voltmeter to measure it, but make sure this has a very high internal resistance so that the current drawn is small. This potential can be taken to be *the same as the equilibrium potential.*[17] **Closed circuit potential**: This is the opposite of the open circuit potential and rather the measurement under a load. The load should in principle be given, but is mostly forgotten, in such cases it can be taken for granted that it is the internal resistance of the battery that dictates the overall resistance. **Mid-point potential**: The potential of the battery when it is discharged to 50% of its capacity. **Cut off voltages**: The voltages measured when the discharge, or charge, is stopped. This is a potential set by the user (or producer) in order to ensure that the chemistry that is used during cycling is the desired one. When reporting practical capacities of batteries, one should always also report within which potential ranges one has cycled the batteries – in other words the upper and lower cut off voltages.

[17] However, remember that another definition of equilibrium would be that the battery is fully discharged so that by that definition the equilibrium potential would be zero.

10.4.2 State of discharge

State of discharge (SOD) is defined as 1.0 when the battery is fully discharged, and 0.0 when it is fully charged. State of charge (SOC) is SOD-1.

Below is an example for a $LiNi_{1/3}Co_{1/3}Mn_{1/3}O_2$ cathode material with respect to a Li-metal anode.

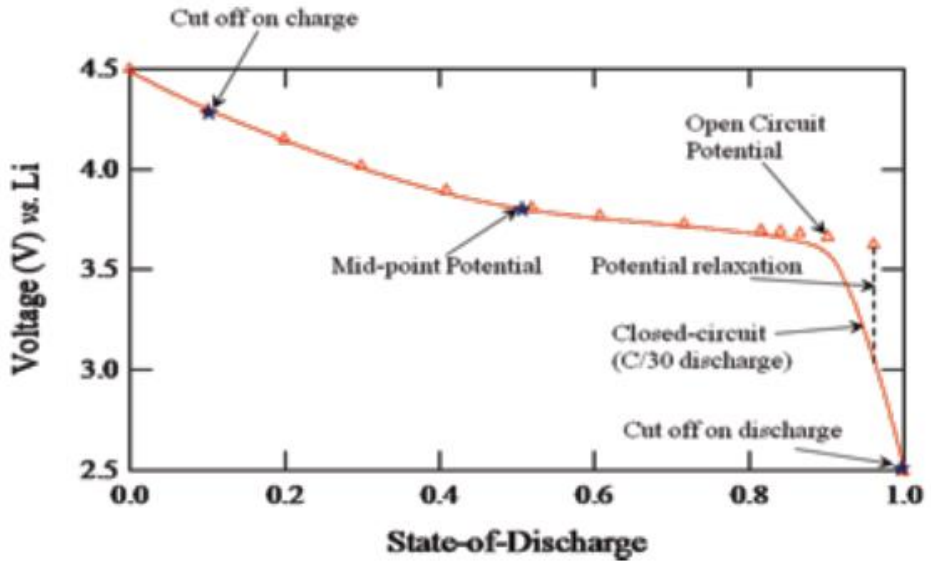

Figure 10-16. Example profile of potential of a battery as function of its discharge state.

The open circuit potential above was measured by first discharging the battery at C/30 to a specified State of discharge and then performing an open circuit. The potential relaxes from the closed circuit to the open circuit (the time constant can range from minutes to days depending on the system). The vertical dotted line close to state of discharge of 1.0 shows the potential relaxing from the closed circuit to the open circuit. In the measurement above, the battery was charged above the cut-off potential. In other words, the battery was overcharged. When the potential of the cell is increased beyond the cut-off potential, other reactions (or side reactions) become thermodynamically more favourable. Typically, side reactions tend to be detrimental to battery performance.

The rate of charge or discharge is given as C-values, like C/30 as stated above. A C value of 1 means that it takes 1 hour to fully charge or discharge the battery by monitoring the number of electrons (ampere × time) and comparing this with the specific capacity of the battery. The C-values are given inversely with time, so that a C-value of 10 C refers to $1/10^{th}$ of an hour, i.e., 6 minutes, while a C value of C/10 or 0.1C refers to 10 hours, i.e., 600 minutes.

In order to give proper C-values, one have to be able to calculate the theoretical capacity of the battery. There are numerous different types of capacities that can be reported, but one intrinsic capacity that is practical when comparing battery chemistries is to count the number of electrons that can be accessible per gram of material. This is given by:

$$q = nF/(3600*M) \text{ mAh/g}$$ Eq. 123

where n = number of electrons available per formula unit of material, F = Faraday's constant, M = molecular weight of the chosen formula unit.

This means that one also has to identify the redox chemistry involved when reporting the capacity. Specific capacities are reported per material, and not per battery system, so if you are calculating for a cathode material you don't have to consider what type of anode it will be used against, this will come later when calculating the specific energy.

The specific capacity for $LiFePO_4$ can be calculated assuming that all the Li can take part in the reaction, n = 1. What should be used for molecular weight? The condition in the charged state ($FePO_4$) or discharged state ($LiFePO_4$)? The overall mass variation in this case is not large (150.8 vs. 157.7 g/mol), but will make a difference when comparing various chemistries. The correct manner is to report for the most mass-intensive case ($LiFePO_4$), but sadly, you can frequently find cases in the literature where different states are compared. One of the most adverse effects is when the capacity of Li and $Li_{22}Si_5$ are compared in different states, almost proving that it is possible to store more Li in $Li_{22}Si_5$ than in Li.

The practical capacity obtainable from a battery relates to the current drawn through the battery. This will have to be measured by passing a constant current while monitoring the closed circuit voltage until it reaches its cut-off value. The practical specific capacity can then be reported as the area under the graph in the figure below. The x-axis is linearly proportional to the amount of electrons passed through the battery and calculated by monitoring the current, multiplying with time and dividing with the mass of the cathode material.

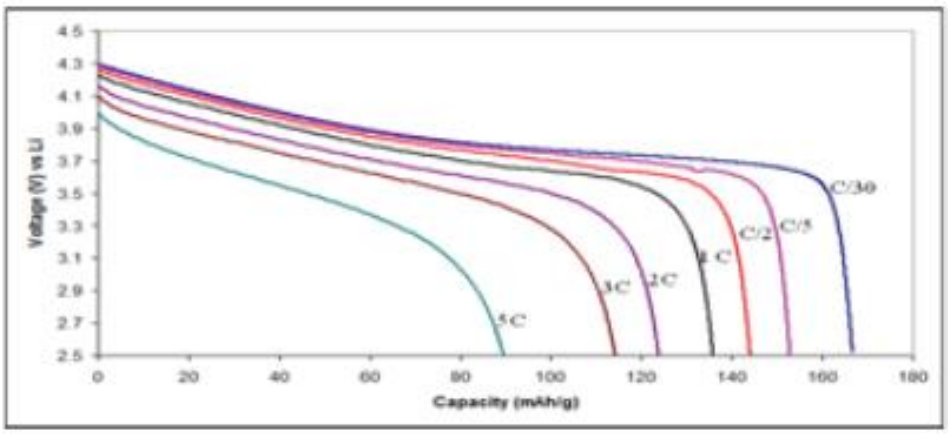

Figure 10-17. Potentiostatic discharge of $LiNi_{1/3}Co_{1/3}Mn_{1/3}O_2$ at different discharge rates.

The example above is for the cathode material $LiNi_{1/3}Co_{1/3}Mn_{1/3}O_2$ that should have a theoretical capacity of 277.8 mAh/g provided that all the Li is electrochemically active. The practical capacity is measured to 165 mAh/g for a discharge rate of C/30, which proves that all the Li is not accessible.

The remaining Li above the cut-off potential chosen here is not accessible for electrochemical work. If a higher cut-off potential had been chosen, a higher capacity could have been reached,

however, it is more likely that the electrolyte or the cathode material itself would decompose under such high potentials.

10.4.2.1 Exercises

a) Verify that the specific capacity for $LiFePO_4$ is 170 mAh/g.
b) Calculate the amount of Li that is available for electrochemical reaction in $LiNi_{1/3}Co_{1/3}Mn_{1/3}O_2$.

11 Selected Additional Topics in Solid-State Electrochemistry

Not yet included.

11.1 Computational techniques

Here…

11.1.1 Atomistic simulations

Here…

11.1.2 Numerical techniques

Here…

11.2 Charge separation and role of space charge layers at interfaces

Here…

11.3 Electrochemical sensors

Here…